

Title	Studies on the Oxidative Leaching of Chalcopyrite(Dissertation_全文)
Author(s)	Hirato, Tetsuji
Citation	Kyoto University (京都大学)
Issue Date	1987-05-23
URL	http://dx.doi.org/10.14989/doctor.k3806
Right	
Type	Thesis or Dissertation
Textversion	author

新 制
工
696
京大附図

Studies on the Oxidative Leaching of Chalcopyrite

Tetsuji Hirato

1986

Studies on the Oxidative Leaching of Chalcopyrite

by

Tetsuji Hirato

1986

Submitted to Kyoto University

in Partial Fulfilment of the Requirements
for the Degree of Doctor of Engineering

Abstract

The present work was undertaken to obtain a fuller understanding of the mechanism of the oxidative leaching of chalcopyrite with ferric chloride, ferric sulfate or cupric chloride. The leaching was investigated chemically, electrochemically and morphologically, by using a massive chalcopyrite crystal of museum grade. Also, the correlation between the chemical leaching and the electrochemical leaching of chalcopyrite was examined.

The leaching of natural chalcopyrite crystal with ferric chloride was studied kinetically. The morphology of the leached chalcopyrite was also investigated. It was found that the elemental sulfur layer formed on the chalcopyrite surface after leaching in a ferric chloride solution was porous and not a barrier to further leaching. The leaching rate of chalcopyrite in a ferric sulfate solution was approximately one order smaller than that in a ferric chloride solution. This suggests that ferric chloride is a more reactive leachant for chalcopyrite. The leaching rate of several chalcopyrite specimens varied significantly, even though the chalcopyrite crystals originated from the same deposit of the same mine. The leaching rate cannot be reproduced if repeat leaching tests utilize the same specimen which is polished by Emery paper prior to each experiment. A new experimental technique has been developed to obtain reliable kinetic data. Using this technique, the effect

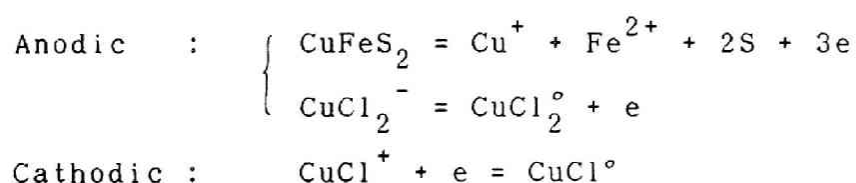
of several factors on the leaching was investigated. The leaching rate of chalcopyrite is of a half order with respect to ferric chloride concentration. The effect of ferrous chloride on the leaching of chalcopyrite in a ferric chloride solution was found to be almost insignificant. The leaching rate of chalcopyrite increases with an increase in sodium chloride concentration. The apparent activation energy for chalcopyrite leaching in a ferric chloride solution was found to be 69.0 kJ mol^{-1} . This amount of activation energy suggests that the leaching of chalcopyrite in a ferric chloride solution should be chemically controlled. Also a comparative study of electrochemical leaching and chemical leaching of chalcopyrite was done to elucidate the leaching mechanism of chalcopyrite in ferric chloride media. It was found that the mixed potential of chalcopyrite in a ferric chloride solution is determined by a combination of the following anodic and cathodic reactions:



The dependency of the mixed potential upon ferric chloride concentration was found to be $72 \text{ mV decade}^{-1}$ at 343 K , showing a satisfactory agreement with the theoretical value. By displaying the leaching rates of chalcopyrite in ferric chloride on a Tafel plot, a straight line, whose slope was $140 \text{ mV decade}^{-1}$ was obtained. This finding suggests that the leaching kinetics are controlled by a one electron transfer mechanism. The dependency of E upon $\log i$ for chemical leaching of chalcopyrite in ferric chloride well agrees with that for electrochemical

leaching. This finding strongly supports the electrochemical mechanism of ferric chloride leaching of chalcopyrite. Cupric chloride, the resultant product of leaching, may play an important role in the later stages of leaching as an oxidizing agent, since cupric chloride is thought to be a more reactive reagent than ferric chloride.

The electrochemical leaching and chemical leaching of chalcopyrite were compared to elucidate the leaching mechanism of chalcopyrite with cupric chloride. Also the morphology of the surface of leached chalcopyrite was studied using a chalcopyrite crystal. It was observed that the elemental sulfur layer formed on the chalcopyrite surface during the leaching in acidic cupric chloride solutions was porous and not a barrier to further leaching. The leaching of chalcopyrite with cupric chloride shows linear kinetics and its leaching rate is of a half order with respect to cupric chloride concentration, whereas it is an inverse half order with respect to cuprous chloride concentration. The mixed potential of chalcopyrite exhibits a $66 \text{ mV decade}^{-1}$ dependency upon cupric chloride concentration, and $-69 \text{ mV decade}^{-1}$ upon cuprous chloride concentration. These dependencies are in good agreement with the theoretical values expected from the mixed potential determined by a combination of the following anodic and cathodic reactions on the chalcopyrite surface:



Furthermore, the dependencies of leaching rate upon the concentrations of cupric chloride and cuprous chloride were explained by the application of a Butler-Volmer equation to each anodic or cathodic reaction. The plots of mixed potential against the logarithm of the current density calculated from the leaching rate of chalcopyrite in acidic cupric chloride solutions and in acidic cuprous chloride solutions containing 0.1 mol dm^{-3} CuCl_2 and 3 mol dm^{-3} NaCl both gave straight lines, whose slopes were $121 \text{ mV decade}^{-1}$ and $135 \text{ mV decade}^{-1}$, respectively. These findings suggest the validity of the leaching kinetics controlled by a one electron transfer mechanism. The dependency of $121 \text{ mV decade}^{-1}$ and $135 \text{ mV decade}^{-1}$ mentioned above for the chemical leaching of chalcopyrite both agree fairly well with the dependency of $130 \text{ mV decade}^{-1}$ for the electrochemical leaching. This strongly supports the electrochemical mechanism of chalcopyrite leaching with cupric chloride. The activation energy obtained for the chemical leaching was fairly close to that obtained for electrochemical leaching, this again supports an electrochemical mechanism.

The leaching of natural chalcopyrite crystals with ferric sulfate was studied kinetically. The morphology of the leached chalcopyrite and the electrochemical properties of the chalcopyrite electrode were also investigated. It was found that the leaching of chalcopyrite obeyed a parabolic rate law at the initial stage, then a linear kinetics over the extended period. At the initial stage, a dense sulfur layer was formed on the chalcopyrite surface. The growth of the layer caused it

to peel off from the surface, leaving a roughened surface. At the linear stage, no thick sulfur layer was observed. The apparent activation energy for chalcopyrite leaching in a ferric sulfate solution was found to be 76.8 to 87.7 kJ mol⁻¹. The amount of activation energy determined suggests that the leaching of chalcopyrite in a ferric sulfate solution is chemically controlled. The leaching rate of chalcopyrite increased with the increase in ferric sulfate concentration up to 0.1 mol dm⁻³ Fe(SO₄)_{1.5}, but at a higher ferric sulfate concentration, the leaching rate was only marginally dependent on the concentration of ferric sulfate. The dependency of the mixed potential upon ferric sulfate concentration was found to be 79 mV decade⁻¹ from 0.01 mol dm⁻³ to 1 mol dm⁻³ Fe(SO₄)_{1.5} at 343 K. Both the leaching rate and the mixed potential decreased with the increase in the concentration of ferrous sulfate. The anodic current of Fe(II) oxidation on the chalcopyrite surface in a sulfate medium was larger than that in a chloride medium.

Contents

	page
Abstract	i
Contents	vi
Acknowledgements	x
Chapter 1 Introduction	1
1.1 General	1
1.2 Literature Survey	4
1.2.1 Ferric Chloride Leaching	4
1.2.2 Ferric Sulfate Leaching	7
1.2.3 Cupric Chloride Leaching	12
1.2.4 Other Oxidants	14
1.2.5 Electrochemical Studies on Chalcopyrite	15
1.3 Problems Remaining in Previous Studies and Purposes of This Study	21
References	25
Chapter 2 The Leaching of Chalcopyrite with Ferric Chloride	29
2.1 Introduction	29
2.2 Experimental Procedures	31
2.2.1 Sample and Chemicals	31
2.2.2 Leaching Experiments	32
2.2.3 Electrochemical Measurements	34
2.2.4 Morphological Observations	36
2.3 Experimental Results	37

2.3.1	Comparison of Leaching Reactions of Chalcopyrite with Ferric Chloride and Those with Ferric Sulfate	37
2.3.2	Morphology of Surface of Chalcopyrite Leached with Ferric Chloride	41
2.3.3	Determination of Leaching Rate	47
2.3.4	Effect of the Concentration of Ferric Chloride .	50
2.3.5	Effect of the Concentration of Ferrous Chloride	56
2.3.6	Effect of the Concentration of Cupric Chloride on the Mixed Potential	63
2.3.7	Effect of Temperature	64
2.3.8	Effect of Addition of Sodium Chloride	69
2.3.9	Correlation of the Leaching Rates of Chalcopyrite Chemically Leached and Those Electrochemically Leached	73
2.4	Discussion	77
2.4.1	Complex Formation	77
2.4.2	Leaching Mechanism of Chalcopyrite in Ferric Chloride Solutions	80
2.5	Conclusions	91
	Reference	94
Chapter 3	The Leaching of Chalcopyrite with Cupric Chloride	97
3.1	Introduction	97
3.2	Experimental Procedures	98
3.2.1	Sample and Chemicals	98
3.2.2	Leaching Experiments	98

3.2.3	Electrochemical Measurements	100
3.2.4	Morphological Observations	101
3.3	Experimental Results	101
3.3.1	Leaching Rate Curve	101
3.3.2	Morphology	101
3.3.3	Effect of the Concentration of Cupric Chloride and Cuprous Chloride	104
3.3.4	Effect of the Concentration of Sodium Chloride .	113
3.3.5	Effect of Temperature	116
3.4	Discussion	116
3.4.1	Speciation of Aqueous Solution System of HCl- CuCl ₂ -CuCl-NaCl	116
3.4.2	Leaching Mechanism of Chalcopyrite in Cupric Chloride Solutions	123
3.4.3	Correlation of the Leaching Rate and Electro- chemical Dissolution Rate of Chalcopyrite	129
3.5	Conclusions	132
	References	134
Chapter 4	The Leaching of Chalcopyrite with Ferric Sulfate	135
4.1	Introduction	135
4.2	Experimental Procedures	136
4.2.1	Sample and Chemicals	136
4.2.2	Leaching Experiments	136
4.2.3	Electrochemical Measurements	137
4.2.4	Morphological Observations	137
4.3	Results and Discussion	138

4.3.1	Leaching Rate Curve	138
4.3.2	Morphology	140
4.3.3	Effect of Temperature	145
4.3.4	Effect of the Concentration of Ferric Sulfate ..	148
4.3.5	Effect of the Concentration of Ferrous Sulfate .	155
4.4	Conclusions	160
	References	162
Chapter 5	Conclusions	163

Acknowledgements

The author is very grateful to his thesis supervisor, Professor H. Majima, for his encouragement and counsel given throughout the course of this work.

The author is also thankful to Dr. Awakura for his invaluable suggestions during this study, and to Dr. Matsuda for his thoughtful advice and encouragement. Thanks are also extended to Professors E. Ichise and K. Ono for their fruitful discussions..

He extended his hearty thanks to Mr. Tokuji Tanaka (Kyoto University), Mr. S. Fukui (Mitsubishi Metal Corp.), Mr. Toshihiko Tanaka (Kansai Electric Power Corp. Inc.), Mr. M. Kinoshita (Mitsubishi Metal Corp.) and K. Takahara (Hachinohe Seiren K.K.) for their earnest assistance in the experimental works for this study, and to Mr. H. Ueshima (Nippon Denso K.K.), Mr. K. Sato (Hitachi Metal Corp.) and Mr. M. Mashima (Graduate Student, Kyoto University) for their kindness to drive him home whenever he hoped.

Chapter 1

Introduction

1.1 General

Hydrometallurgical processes are playing an increasingly important role in the development of new technology for processing copper sulfide concentrates. Conventionally, these concentrates are processed by smelting and converting methods which, while achieving high recoveries of copper and precious metals, also produce large quantities of sulfur dioxide gas. Venting of this off-gas to the atmosphere represents a potential ecological hazard and has resulted in processing constraints on domestic copper producers in the form of costly pollution abatement equipment. These restrictions, in conjunction with the high costs of fuel and the necessity to process low grade ores that cannot be economically upgraded by conventional milling, concentration and smelting, have opened the door to the development of hydrometallurgical alternatives to compete with the traditional methods of copper production. Hydrometallurgy offers several possible alternative processes for producing copper from sulfide concentrate without producing sulfur dioxide and frequently offers the possibility of direct recovery of most of the sulfur in the solid state.

Chalcopyrite (CuFeS_2) is the most important copper mineral in the world today. However, chalcopyrite is quite refractory to hydrometallurgical processing and only fairly potent solutions will dissolve it. On the other hand, ferric chloride, ferric

sulfate and cupric chloride are recognized as the most important leaching reagents for chalcopyrite. Many attempts to use these reagents on an industrial scale have been reported. The United States Bureau of Mines developed a ferric chloride leaching process¹ which was able to extract over 99 % of the copper in a chalcopyrite concentrate during 2 hr of leaching at 379 K. As originally conceived, the Cymet Process² combined ferric chloride leaching together with anodic dissolution of chalcopyrite concentrates. With recent improvements on this process³ the leach-anodic dissolution step has been replaced by a more conventional two stage leaching operation employing ferric chloride-cupric chloride. Cominco Limited⁴ has also advanced a process based on ferric chloride leaching of chalcopyrite concentrates. Elkem-Spigerverket⁵ has piloted a ferric chloride leaching process which is based on the dissolution of chalcopyrite in $3 \text{ mol dm}^{-3} \text{ FeCl}_3$ at about 383 K. The Duval Corporation has developed^{6,7} a process whereby chalcopyrite concentrates are dissolved in a cupric chloride-ferric chloride solution at the boiling point (380 K).

Although none of the above processes is currently operating on a commercial scale, several are being evaluated at the pilot plant or demonstration unit level. Ferric chloride leaching may soon be practically applied for the treatment of chalcopyrite concentrates. The processes described above differ in their methods of handling the pregnant solutions and, especially, in their metal recovery operations, but are all based on the reaction of chalcopyrite with chloride media. Although ferric

sulfate is not used for the leaching of copper sulfide on an industrial scale, it is important as the active agent in dump leaching and recently has received more attention. Low cost, minimal corrosion problems, and the ability to regenerate sulfuric acid during electrowinning of copper are the main reasons for the interest in sulfuric acid systems.

For such processes it is important to have a sound understanding of the mechanisms of the reactions occurring during the dissolution step. A number of investigations have been conducted to elucidate the reaction kinetics and to delineate the important leaching variables in these systems. Although relevant work has been reported by Jones and Peters^{8,9}, Dutrizac et al.¹⁰⁻¹³, Palmer et al.¹⁴, Wadsworth and his co-workers^{15,16}, and other investigators, some ambiguities still remain. Particularly in ferric chloride or cupric chloride leaching of chalcopyrite, many researchers postulated that the leaching occurs electrochemically. However, no direct experimental evidence has been given to support the electrochemical mechanism, although some important studies are available on the electrochemical behaviour of chalcopyrite.

The observations on leached surfaces should provide useful information on the understanding of the leaching mechanism. However, at present, only a limited amount of knowledge about the morphological aspect of chalcopyrite leaching is available.

In this study, the leaching experiments were conducted chemically and electrochemically using a massive chalcopyrite crystal of museum grade to obtain a fuller understanding of the

mechanism of the oxidative leaching of chalcopyrite. Also the morphology of leached surface was studied. The correlation between the chemical leaching and the electrochemical leaching of chalcopyrite was mainly investigated.

1.2 Literature Survey

1.2.1 Ferric Chloride Leaching

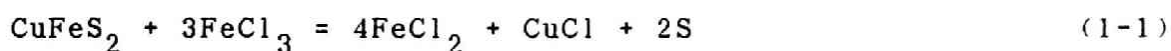
A number of studies have been published on the leaching of chalcopyrite with ferric chloride.

In 1933, Sullivan¹⁷ reported that concentrated Fe(III) solutions were beneficial, but this was not true for ferric sulfate leaching. Fine grinding and high temperatures also increased the rate of extraction, as expected.

More recently, Ermilov, Tkachenko and Tseft¹⁸ investigated the kinetics of dissolution of chalcopyrite in ferric chloride solutions over the temperature interval 333 to 379 K. The rate increased moderately rapidly with increasing temperature: the apparent activation energy was about 50 kJ mol^{-1} . The rate increased directly with the ferric ion concentration for initial ferric chloride concentrations between 50 and 100 g dm^{-3} . The sulfur formed during dissolution did not interfere with the dissolution kinetics.

A more complete examination of the leaching reaction was undertaken by Haver and Wong¹; they reported excellent dissolution rates (essentially 100 % extraction in one hour) on finely ground material with strong Fe(III) solutions at reflex temperatures (379 K). The stoichiometry of the reaction was

found to be



Jones and Peters⁸ and Jones⁹ studied the dissolution of chalcopyrite in both ferric chloride and ferric sulfate media: ferric chloride solutions were found to be the more effective lixiviant at 363 K, and this is in agreement with the earlier study of Sullivan¹⁷. For ferric chloride solutions, linear kinetics were observed to about 90 % dissolution and this suggests that the elemental sulfur reaction product is not impeding the reaction in the chloride system. As would be expected, the rate increased as the particle size decreased. The apparent activation energy reported was 72.4 kJ mol^{-1} . Increasing ferric chloride concentrations (0.1 and 1.0 mol dm^{-3}) increased the leaching rate, but the presence of the Fe(II) reaction product was found to have little effect. From mixed potential studies, they suggested that this phenomenon was due to the catalysis of the reaction by cuprous and cupric ions, so that ferric chloride leaching was in reality cupric chloride leaching. The ferric ion served to suppress the concentration of cuprous ions, and raise the potential of the Cu(II)/Cu(I) couple which exhibited a high degree of reversibility on the chalcopyrite surface.

Dutrizac¹¹ studied the kinetics of dissolution of synthetic chalcopyrite in both ferric chloride and ferric sulfate media, using the rotating disk technique. For ferric chloride solutions, linear kinetics were observed. The apparent activation energy was about 46.0 kJ mol^{-1} . The rate increased

with increasing ferric chloride concentrations but was insensitive to the concentrations of hydrochloric acid, the ferrous chloride reaction product and "inert" magnesium or lithium chlorides. Cupric chloride substantially accelerated the rate. Small amounts of sulfate in an otherwise all chloride system greatly reduce the chalcopyrite leaching rate.

Dutrizac¹² surveyed the literature on the ferric ion leaching and also carried out experimental studies to elucidate points still in dispute. He found that the leaching rate were more rapid in chloride media than in ferric sulfate solutions, and the activation energy of ferric chloride leaching was about 42 kJ mol⁻¹. The rate was essentially independent of acid concentration and degree of agitation. Increasing ferric ion concentration increased the leaching rate.

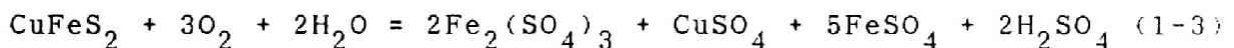
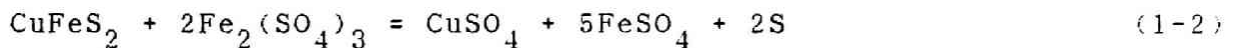
Palmer et al.¹⁴ studied the rate of dissolution of monosize chalcopyrite in the lixiviants containing ferric chloride, sodium chloride and hydrochloric acid. Linear kinetics were observed which is indicative of control by surface phenomena. Rate exhibited one-half power dependence on total ferric iron concentration. Additionally, the rate of dissolution increased with chloride ion concentration for values up to one molar but became independent of this parameter for higher concentrations. Based on these observations, they proposed a mechanism involving mixed electrochemical control. The anodic reaction involves the oxidation of chalcopyrite to cupric ion, ferrous ion and elemental sulfur. Four cathodic reactions occur in parallel, and these are the reduction of uncomplexed ferric ion and

reduction of the first, second and third chloro complexes of trivalent iron.

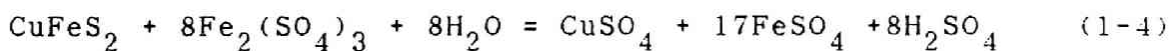
Dutrizac¹³ studied the leaching rate of eleven chalcopyrites from different localities in both ferric chloride and ferric sulfate media and found that similar leaching rate ($\pm 50\%$) were observed for all the chalcopyrite under all leaching conditions, when the rates were corrected for the amount of chalcopyrite. The activation energy was found to be 70 kJ mol^{-1} in chloride media.

1.2.2 Ferric Sulfate Leaching

Sullivan¹⁷, who showed that hot solutions dissolved appreciable amounts of copper from finely divided material, but the rate appeared to decrease rapidly with time. A significant amount of sulfur was oxidized to sulfate, and two equations for the leaching reaction were given:



A number of investigators have observed only the reaction (1-2),, i.e, no sulfate formation. Exceptionally, Jones and Peters⁸ reported 18 % sulfur was oxidized to sulfate after approximately 17 days. However, they considered the following reaction instead of reaction (1-3).



Dutrizac et al.¹⁰ also studied the reaction of chalcopyrite with ferric sulfate. To avoid the complications of impurities and an indefinite surface area, they used synthetic chalcopyrite

which was pressed into disks. They found the leaching rate to decrease with time, t , according to a parabolic rate law:

$$\text{Cu dissolved} = k\sqrt{t} \quad (1-5)$$

This result was attributed to a thickening film of elemental sulfur on the surface, which retarded the reaction. The reaction was found to be independent of pH, rotation speed and Fe(III) concentration above a very low level ($0.005 \text{ mol dm}^{-3}$) but sharply dependent on Fe(II) concentration. It was concluded that the rate determining step was the diffusion of Fe^{2+} ions away from the surface through the sulfur film. An activation energy of 72.4 kJ mol^{-1} was determined. This interpretation has been criticized by Roman and Benner who concluded that such a high activation energy must be due to chemical control, and Peters¹⁹ who suggested that the parabolic dissolution rate could be due to the diffusion of solid state defects out to the surface of the mineral.

Dutrizac et al.¹⁰ also found that natural massive chalcopyrite leached about 15 times slower than synthetic material. They claimed that the same parabolic rate law applied however, but the data appear to be insufficient to verify this. The slower leaching rate was attributed to the reduced porosity of the natural material. This postulate has been affirmed in another publication by the same authors²⁰ in which natural chalcopyrite was crushed and then pressed into a disk like the synthetic mineral. The results showed that the pressed disk of natural mineral also reacted rapidly.

Lowe²¹ also examined the kinetics of ferric sulfate leaching

of chalcopyrite and found the reaction to be independent of pH and Fe(III) concentration, and therefore concluded that the rate-controlling step was a surface electrode reaction involving chemisorbed ferric ions. An activation energy of 74.5 kJ mol^{-1} was calculated. The experimental data for these calculations consisted only of Fe(III) consumption; the stoichiometry was assumed to be that of reaction (1-2).

Jones and Peters⁸ studied the leaching of chalcopyrite with ferric sulfate using both massive specimen and particulate sample and measured the mixed potential of the mineral during leaching. The kinetics were linear over an extended period with using a massive chalcopyrite. The chalcopyrite leaching rate was independent of particle sizes below 100 mesh. In regard to this, the morphology of chalcopyrite leached with ferric sulfate showed a selective attack on grain boundaries or fissures. It was suggested that if the rate of leaching in ferric sulfate depends on the total grain boundary area exposed to the solution, then further size reduction will not be beneficial once all the grains are broken up and exposed. The increase in Fe(III) concentration was not beneficial, but increasing Fe(II) concentration was sharply detrimental to the Cu extraction. A linear relationship of mixed potential vs $\log C(\text{Fe(III)})$ was obtained ($0.005\text{-}1 \text{ mol dm}^{-3} \text{ Fe(III)}$). On the other hand, the addition of Fe(II) had little effect up to $0.05 \text{ mol dm}^{-3} \text{ Fe(II)}$, but thereafter a substantial drop in potential was observed. It was suggested that the rate determining step was the electrochemical surface reaction.

Beckstead et al.¹⁵ studied acid ferric sulfate leaching of attritor-ground chalcopyrite concentrate. The kinetics were parabolic. The activation energy was 83.7 kJ mol^{-1} . The leaching rate was found to be independent of the concentration of Fe(III), Fe(II), Cu(II) and sulfuric acid. Except for temperature, particle size was the only controllable variable which has a significant effect on the rate of the leaching. Attrition grinding was found to be the most effective.

Munoz et al.¹⁶ also obtained almost the same results reported by Beckstead et al.¹⁵ and through a further research on the effect of particle size, they found that the leaching rate had an inverse second order dependence on the initial particle diameter. The data analysis, using the Wagner theory of oxidation, suggests that the rate limiting process may be the transport of electrons through the elemental sulfur layer. Predicted reaction rate calculated from first principles using the physicochemical properties of the system (conductivity of elemental sulfur and the free energy change for the reaction) agree satisfactorily with experimentally determined rates. Further evidence which supports this analysis includes an experimental activation energy of 83.7 kJ mol^{-1} which is approximately the same as the apparent activation energy for the transfer of electrons through elemental sulfur (96.3 kJ mol^{-1}) calculated from both conductivity and electron mobility measurements reported in the literature.

Dutrizac¹¹ studied the leaching rate of disks of synthetic chalcopyrite and reported "non linear" kinetics. Initial leaching rate was evaluated by fitting the various data to an

equation of the form:

$$\text{dissolved Cu (mg cm}^{-2}\text{)} = bt + ct^2 \quad (1-6)$$

and then calculating the slope at $t = 0$. Using the initial leaching rates, the activation energy was found to be 38 kJ mol^{-1} .

Dutrizac¹² also surveyed the literature on the ferric ion leaching of chalcopyrite and undertook experimental work to resolve points still in dispute. In the paper, initial slopes as determined by fitting the data to a parabolic equation:

$$\text{dissolved Cu (mg)} = a + bt + ct^2 \quad (1-7)$$

instead of Eq. (1-6). The rate was essentially independent of acid concentration and degree of agitation. However, the rate increased as the mean particle size was decreased below 100 mesh, in contrast to Jones and Peters, proportionally to the inverse of the mean particle size. Sulfate concentrations, especially ferrous sulfate concentrations, decrease the leaching rate substantially; furthermore, cupric sulfate did not promote leaching in the sulfate system. Chloride additions to sulfate solutions accelerated slightly the dissolution rates at elevated temperatures. Leaching in the ferric sulfate system was nearly independent of the concentration of Fe(III).

As mentioned in Section 1.2.1, Dutrizac¹³ studied the leaching rate of eleven chalcopyrites from different localities in both ferric chloride and ferric sulfate. In chloride solution, all the chalcopyrite seemed to leach at a similar rate ($\pm 50\%$). The average activation energy in sulfate system was about 65 kJ mol^{-1} .

The chalcopyrite leaching in ferric sulfate solution, however,

more fundamental ambiguities still remain than in ferric chloride leaching, for example; kinetics or a method to deduce leaching rates.

1.2.3 Cupric Chloride Leaching

Cathro²² reported a hydrometallurgical process for the recovery of copper from chalcopyrite concentrates by means of a cupric chloride leaching. The concentrate had first been "activated" by heating it with sulfur at a temperature near 673 K. This activation process converts most of the iron of the chalcopyrite to pyrite, which is insoluble in the cupric chloride leachant. The copper is converted to the mineral idaite, which dissolves readily in hot cupric chloride: at 379 K, 98 % of the copper was extracted in a three-stage countercurrent leach, the leaching time being 1 hr per stage.

Demarthe et al.²³ reported that a double leach by cupric chloride at 363 K could dissolve more than 98 % of the copper and iron in the chalcopyrite within 6 hr. No pressure vessels are requested, since the oxidation of Cu(I) into Cu(II) by air is a fast reaction and hence leach liquor regeneration can be achieved at atmospheric pressure. This concept had been suggested at the end of the 19th century but no development followed, mainly because of corrosion problems.

Wilson and Fisher²⁴ investigated the leaching of chalcopyrite in cupric chloride solutions containing high concentrations of sodium chloride and reviewed the thermodynamic and kinetic factors important in the system. Linear kinetics were observed

and were attributed to the anodic dissolution of chalcopyrite. An experimental activation energy of $134.7 \text{ kJ mol}^{-1}$ was observed. The rate was found to be directly proportional to mineral surface area and independent of Cu(II) and Cl^- concentration. They mentioned that the dissolution rate was probably controlled by a step in anodic reaction of chalcopyrite.

Bonan et al.²⁵ also investigated the chalcopyrite leaching by cupric chloride in strong sodium chloride solutions. Leaching rate were high above 358 K and the kinetics followed a shrinking core diffusion model. High copper recovery can be obtained provided that high $\text{Cu(II)}/\text{Cu(I)}$ ratios are maintained. Elemental sulfur was obtained with no sulfate formation. The combination of the influences of the ratio of concentrations of $\text{Cu(II)}/\text{Cu(I)}$ and the concentration of Cl^- was nearly the same on the solution potential and the leaching rate, explaining the action of the concentration of chloride ion in chalcopyrite leaching. They concluded that cupric chloride leaching in terms of kinetic models did not seem to be as well defined and clearly required additional research.

McDonald et al.²⁶ studied the equilibria associated with cupric chloride leaching chalcopyrite concentrate. The precipitate from a refluxing slurry of elemental sulfur and aqueous cuprous and ferrous chlorides contained predominantly covellite (CuS) and a small amount of pyrite (FeS_2). Mössbauer spectra indicate that there was no chalcopyrite formation. Cupric chloride leaching experiments on both chalcopyrite concentrate and cupric sulfide indicated that the extent of

cuprous ion formation in these aqueous cupric chloride solution is controlled by the thermodynamics of the equilibrium:



1.2.4 Other Oxidants

Several other oxidizing agents have been extensively studied, but those studies are not directly related to the present work. Therefore, here only the brief descriptions are given in this thesis.

Linge²⁷ studied the leaching of chalcopyrite in acidic ferric nitrate solution and found the leaching followed the parabolic kinetics.

At sufficiently high temperatures and pressures, oxygen will dissolve chalcopyrite at practical rates. In strongly acid solutions, iron and copper both go into solution, and the yield of elemental sulfur is high²⁸. At higher pH, iron is hydrolyzed and sulfur is largely oxidized to sulfate²⁹. In ammoniacal solutions, intermediate sulfur species, particularly thiosulfate, $\text{S}_2\text{O}_3^{2-}$, are formed. Sherritt-Gordon utilizes the $\text{NH}_3\text{-O}_2$ system to dissolve chalcopyrite-pentlandite concentrates³⁰ and the new Arbiter process³¹ also uses $\text{NH}_3\text{-O}_2$.

Beckstead and Miller³² studied the ammonia oxidation leaching of chalcopyrite and reported that a catalytic electrochemical surface reaction was shown to control the reaction kinetics.

Murr and Hiskey³³, using shock loaded chalcopyrite, examined the influence of dislocation density upon the rate of dissolution in acid dichromate solutions. It was found that before and

after shock loading, in the presence of dichromate, the kinetics were surface controlled following a linear rate law. The shock loaded sample demonstrates a modest increase in rate of approximately 12 % even though the dislocation density increased by several orders of magnitude. The linear rate constant was observed to increase up to 333 K, with an activation energy of 50 kJ mol⁻¹. Above 333 K the rate was found to diminish with increasing temperature. This was attributed to the adsorption of Cr(VI) ion. Marked decrease in rate was noticed above 363 K due to the formation of a tightly adherent sulfur coating.

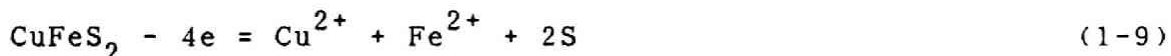
Nitric acid is an effective oxidizing agent for chalcopyrite³⁴⁻³⁶ but the chemistry of the dissolution reaction is complex. In addition to the possibility of sulfate formation, there is a complicated dependence on nitric acid concentration. Both NO₂ and NO may be produced in the reaction, but NO₂ can further react with the sulfide, or react with water to form more nitric acid and NO. At high acid strengths, NO₂ is lost by evolution and elemental sulfur is oxidized to sulfate; thus the efficiency of the reaction, in terms of copper extracted, is decreased although the rate of reaction is increased. In dilute acid the NO and NO₂ may be trapped within the solution, and re-oxidized by O₂, the nitric acid thus acting as a catalyst.

1.2.5 Electrochemical Studies on Chalcopyrite

Springer³⁷ examined the semiconducting properties of chalcopyrite by measuring the anodic polarization up to 10 mA cm⁻² and found no saturation current, as expected for an n-type

semiconductor³⁸. Zevgolis³⁹ also measured anodic polarizations, at much higher voltages, and found a saturation current at about 50 mA cm⁻² above 3.244 V vs SHE. He concluded that the hole density in chalcopyrite determines the value of the limiting anodic current. This conclusion was supported by an illumination experiment which increased the current, presumably due to the increased concentration of holes³⁸. However, the 200 W illuminator used shone directly on the mineral specimen, and raised the bath temperature by 4 K. The resulting heat effect was not corrected for.

Zevgolis also examined the stoichiometry of the anodic dissolution reaction (in 1.5 mol dm⁻³ H₂SO₄ at 303 K) and claimed 100 % current efficiency for the reaction:



However, Jones⁹ claimed that Zevgolis apparently made an error in calculating current efficiency, and that only 50 % of the current was actually accounted for by reaction (1-9).

Oki and co-workers^{40,41} have studied the anodic reactions of covellite (CuS) and chalcopyrite at high current densities. The CuS electrode suffered a very large potential (40 V) increase after a certain time, which was attributed to cupric sulfate precipitation in agreement with Etienne⁴². However, up to this point the reaction went smoothly, producing elemental sulfur:



as noted before. The chalcopyrite electrode potential (in 1 mol dm⁻³ H₂SO₄, 298 K) was shown to be dependent on the concentration of Fe(II), Cu(II) and Fe(III) in dilute solutions of these ions

(10^{-3} - 10^{-2} mol dm $^{-3}$).

Anodic polarizations of chalcopyrite were carried out at 10 - 100 mA cm $^{-2}$, resulting mainly in the reaction



Seventy-five percent current efficiency was reported for this reaction, independent of current density. The concentration of Fe(II) was low compared to that of Fe(III).

Jones and Peters⁴³ studied the anodic behaviour of chalcopyrite in 0.1 mol dm $^{-3}$ HClO $_4$ and 0.1 mol dm $^{-3}$ H $_2$ SO $_4$ at 280 - 448 K at potential below 5V vs SHE. The polarization curves in the two acids were very similar, but at higher temperature the reactivity of chalcopyrite suddenly drops in sulfuric acid whereas in perchloric acid it continues to increase steadily with temperature.

Jones⁹ studied the anodic dissolution of chalcopyrite in chloride and sulfate solutions from 293 K to 448 K. In chloride the yield of elemental sulfur is nearly 100 %, whereas in sulfate solutions it is 75 % or less, the remainder being oxidized. The anodic polarization of chalcopyrite displays two important regions: first a diffusion region in which the current is highly time-dependent, but potential independent and second a higher current region, in which the current largely time independent but is linearly dependent on potential. At low temperatures chloride solutions and sulfate solutions give similar polarization curves but at 363 K and above, the higher current region in chloride solutions starts at much lower potentials (500 mV vs SHE) whereas in sulfate solutions it does not. Sulfuric

acid solutions passivate the mineral at high temperatures and potentials.

Ammou-Chokroum and his co-workers⁴⁴⁻⁴⁷ studied the electro-oxidation of chalcopyrite in acid chloride solution and proposed a mechanism involving the formation of CuS to explain the decrease in rate of electro-dissolution. The formation of CuS was thought to be responsible for the superficial enrichment of the solid surface in copper as well as for the retardation of the Fe(II) solubilization rate. Ammou-Chokroum concluded that CuS covered the chalcopyrite-electrolyte interface by accumulating in the porous sulfur layer network which formed a gradually thickening layer at surface. The CuS gradually blocked the pores of the sulfur network resulting in a decrease in the reaction area and hence in the dissolution rate. The next step in the dissolution sequence is the oxidation of interstitial CuS at the solid-solution interface that controls the overall long reaction rate.

Biegler and Swift⁴⁸ studied the anodic behaviour of chalcopyrite in $1 \text{ mol dm}^{-3} \text{ H}_2\text{SO}_4$ and $1 \text{ mol dm}^{-3} \text{ HCl}$ solutions by linear sweep voltammetry and potentiostatic methods. Voltammograms showed a small prewave, attributed to a surface oxidation process, followed by a region of active dissolution. Current-voltage and potentiostatic current-time curves were interpreted in terms of the kinetics of nucleation, growth and overlap of these discrete corrosion centers.

Bertram and Illi⁴⁹ studied anodic dissolution of chalcopyrite in acidic solution, the chalcopyrite electrode surface was

attacked and carried off, whereupon a yellowish green sulfur layer remains on it. Leaching experiments with constant overvoltages yield a constant current over several hours. At above 333 K, a considerable decline in current results.

Bertram and Greulich⁵⁰ studied the anodic dissolution of chalcopyrite in sulfuric acid solution and reported that the steeply rising current in cyclic voltammograms at 800 mV vs SCE due to activation of the ore surface. At higher electrode potential, the electrode was coated with oxides, leading to a drop in current density.

Price⁵¹ investigated the electroleaching of bornite and chalcopyrite and reported the optimum conditions for maximum current and energy efficiencies.

The current-time dependence at constant potential observed by Parker et al.⁵² indicated that the rate of chalcopyrite dissolution was being retarded by diffusion of products through a slowly thickening layer. Based on the results of ring-disk experiments they concluded that the passivating layer consisted of a copper polysulfide (CuS_x , where $x > 2$).

Parker et al.⁵³ also studied the electrolysis of reductants and oxidants in acidic solutions. On corroding chalcopyrite Fe(III)/Fe(II) is much less reversible than are Cu(II)/Cu(I) , I_3^-/I^- and $\text{Fe(CN)}_6^{3-}/\text{Fe(CN)}_6^{4-}$ salts.

McMillan et al.⁵⁴ studied the anodic dissolution of chalcopyrite in both acidic sulfate and acidic chloride media under conditions relevant to chemical leaching, i.e., at temperature above 343 K and over the potential region 0.2 -0.6 V

vs SHE. Double potential pulse chronoamperometry was used to probe the surface of the chalcopyrite anodes to determine the activation currents at various applied overpotentials. McMillan et al. suggested the formation of a surface layer which slows the rate of electron transfer. The electron transfer between various redox couples, including Cu(II)/Cu(I), Fe(III)/Fe(II) and I_3^-/I^- on chalcopyrite was compared using cyclic voltammetry. In the potential region of interest, the Fe(III)/Fe(II) couple is much less reversible on chalcopyrite than are the Cu(II)/Cu(I) and I_3^-/I^- redox couples.

Warren et al.⁵⁵ studied the electrochemical oxidation of chalcopyrite in sulfuric acid solutions using electrodes made from massive samples. Electrochemical characterization of chalcopyrite from various locations was performed in 1 mol dm⁻³ H₂SO₄ which showed significant differences in their behaviour. All sample exhibited passive-like response during anodic polarization. The current density in this passive region was reproducible and showed difference of up to two orders of magnitude between sample from different sources which has been attributed mainly to the presence of impurities in some of the samples. During anodic polarization chalcopyrite was found to be sensitive to pH at higher potential, but insensitive at low potential in sulfate solution. In addition, current decay measurements at constant potential in the low potential-passive region were found to follow the Sato-Cohen (logarithmic) model for solid film formation. Based on current and mass balance measurements, two intermediate sulfide phases appeared to form in

the sequence $\text{CuFeS}_2 \rightarrow \text{S}_1 \rightarrow \text{S}_2$. At higher potentials, in the transpassive region, the observed increase in current is compatible with the decomposition of water to form chemisorbed oxygen which releases copper and forms sulfate ions.

1.3 Problems Remaining in Previous Studies and Purposes of This Study

The leaching of chalcopyrite with ferric chloride has been studied by a number of investigators. Most of them reported that the leaching reaction follows linear kinetics and that the activation energies ranged from 40.6 to 82 kJ mol^{-1} , and concluded that the leaching was controlled by a surface reaction. Some researchers postulated that the leaching occurs electrochemically. The papers reported by Jones and Peters⁸ or Palmer et al.¹⁴ are typical examples. On the other hand, a number of investigators studied the electrochemical behaviour of chalcopyrite.

However, no direct experimental support has been provided to the electrochemical mechanism of the leaching of chalcopyrite. The kinetics at the initial stage of chalcopyrite dissolution has been examined by using electrochemical techniques such as a linear sweep voltammetric method, the results of which are useful to understand the transient phase change of the chalcopyrite surface.

As recently pointed out by Wadsworth¹⁹, the results obtained at the initial stage of chalcopyrite dissolution may not in fact be important for high fractional reaction. Therefore, it is

necessary to study the electrochemical behaviour of chalcopyrite dissolution under a steady state condition, which could be directly related to the oxidative dissolution of chalcopyrite by chemical oxidants for its high fractional reaction.

Although relevant work concerning the leaching of chalcopyrite with ferric sulfate has been reported by Munoz et al.¹⁶, Jones and Peters⁸ Dutrizac et al.¹⁰⁻¹³, and other investigators, some ambiguities still remain.

Dutrizac et al.¹⁰ studied the leaching of sintered disks of synthetic chalcopyrite with ferric sulfate and found that the leaching follows a parabolic rate law. In contrast, Jones and Peters⁸ studied the leaching of a massive sample of natural chalcopyrite and found that the leaching curve is linear over an extended leaching period. The leaching rate of particulate chalcopyrite, however, is hard to determine. Munoz et al.¹⁶ determined the parabolic rate constant, k_p , according to the equation: $1 - \frac{2}{3}\alpha - (1-\alpha)^{2/3} = k_p t$, where α is fraction reacted and t is leaching time. Dutrizac¹¹⁻¹³ evaluated the initial leaching rate by fitting the data to a parabolic equation and then calculating the initial slope. Jones and Peters⁸ presented leaching curves but not the leaching rate.

On the other hand, the morphological observations of the leached surface should provide useful information to improve the understanding of the leaching mechanism. At present, only a limited amount of knowledge about the morphological aspect of chalcopyrite leaching is available. Jones and Peters⁸ reported a formation of elemental sulfur only in certain fissures or grain

boundaries, leaving the greatest part unchanged in appearance. In contrast, Beckstead et al.¹⁵ and Munoz et al.¹⁶ found a formation of a dense elemental sulfur layer on a chalcopyrite particle.

These are some examples of the problems in the leaching of chalcopyrite with ferric sulfate which require further investigation.

There is only limited amount of information available on the kinetics of the leaching of chalcopyrite with cupric chloride. The electrochemical mechanism for the leaching was proposed by Wilson and Fisher²³ or Bonan et al.²⁴. However, no direct experimental support has been given in these studies.

The present study was conducted to obtain a fundamental understanding of the reaction kinetics of chalcopyrite leaching with ferric chloride, ferric sulfate or cupric chloride, particularly to give direct evidence for the electrochemical mechanism of chalcopyrite leaching. For this purpose, the leaching of chalcopyrite crystals of museum grade was investigated kinetically. To date, no investigation has been made to obtain kinetic data systematically using a massive sample. Electrochemical properties of chalcopyrite were measured under steady state conditions, which could be directly related to the chemical leaching with oxidants. The correlation between the chemical leaching of chalcopyrite and the electrochemical leaching was studied to verify the appropriateness of electrochemical mechanism. Furthermore, the morphologies of chalcopyrite leached chemically and electrochemically was investigated.

In Chapter 2, the leaching of natural chalcopyrite crystals with ferric chloride was studied. The morphology of the leached chalcopyrite was also investigated. A new experimental technique was developed to obtain reliable kinetics data. Using this technique, the kinetic data of the leaching of chalcopyrite with ferric chloride was obtained. Also the leaching of chalcopyrite with ferric chloride was studied electrochemically and the correlation between the chemical leaching and the electrochemical leaching was examined. On the basis of these results, an electrochemical mechanism of the leaching of chalcopyrite with ferric chloride was proposed.

In Chapter 3, the leaching of chalcopyrite with cupric chloride was studied kinetically, electrochemically and morphologically. Based on the results obtained and the speciation of the leaching solutions, an electrochemical mechanism of the leaching of chalcopyrite with cupric chloride was proposed.

Chapter 4 covers the leaching of chalcopyrite with ferric sulfate. The elemental sulfur formed on the leached chalcopyrite was found to play an important role in the leaching. The results of a kinetic study and an electrochemical study were discussed.

Conclusions are described in Chapter 5.

References

1. F.P. Haver and M.M. Wong: *J. Metals*, 1971, vol. 23(2), p. 59.
2. P.R. Kruesi: *Mining Congr. J.*, 1974, vol. 60(9), P. 22.
3. P.R. Kruesi and D.N. Goens: U.S. Patent 3901776, August 26, 1975.
4. E.F.G. Miller, E. Peters, G.M. Swinkels and A.I. Vizolyi: U.S. Patent 3798026, March 19, 1974.
5. J.M. Skeaff: CAMMET Report CF 77-26(FT), Dept. Energy, Mines and Resources, Ottawa, Canada KIAOGI, 1977.
6. G.E. Atwood and C.H. Curtis: U.S. Patent 3785944, January 15, 1974.
7. G.E. Atwood and C.H. Curtis: U.S. Patent 3879272, April 22, 1975.
8. D.L. Jones and E. Peters: "Extractive Metallurgy of Copper", J.C. Yannopoulos and J.D. Agarwal, eds., AIME, New York, NY, 1976, vol. 2, p. 633.
9. D.L. Jones: Ph.D. Thesis, Univ. British Columbia, Vancouver, B.C., 1974.
10. J.E. Dutrizac, R.J.C. MacDonald and T.R. Ingraham: *Trans. TMS-AIME*, 1969, vol. 245, p. 955.
11. J.E. Dutrizac: *Metall. Trans. B*, 1978, vol. 9B, p. 431.
12. J.E. Dutrizac: *Metall. Trans. B*, 1981, vol. 12B, p. 371.
13. J.E. Dutrizac: *Metall. Trans. B*, 1982, vol. 13B, p. 5.
14. B.R. Palmer, C.O. Nebo, M.F. Rau and M.C. Fuerstenau: *Metall. Trans. B*, 1981, vol. 12B, p. 595.
15. L.W. Beckstead, P.B. Munoz, J.L. Sepulveda, J.A. Herbst, J.D.

- Miller, F.A. Olson and M.E. Wadsworth: "Extractive Metallurgy of Copper", J.C. Yannopoulos and J.C. Agarwal eds., AIME, New York, NY, 1976, vol. 2, p. 611.
16. P.B. Munoz, J.D. Miller and M.E. Wadsworth: Metall. Trans. B, 1979, vol. 10B, p. 149.
 17. J.D. Sullivan: Trans. AIME, 1933, vol. 106, p. 515.
 18. V.V. Ermilov, O.B. Tkachenko and A.L. Tseft: Tr. Inst. Met., Obogashch, Alma Acta, 1969, vol. 30, p. 3.
 19. E. Peters: "The Physical Chemistry of Hydrometallurgy", AIME Int. Symposium on Hydrometallurgy, Chicago, 1973.
 20. J.E. Dutrizac and R.J.C. MacDonald: Can. Met. Quart., 1973, vol. 12, p. 409.
 21. Lowe: Ph.D. Thesis, Univ. Arizona, 1970.
 22. K.J. Cathro: "Extractive Metallurgy of Copper", J.C. Yannopoulos and J.D. Agarwal, eds., AIME, New York, NY, 1976, vol. 2, p. 776.
 23. J.M. Demarthe, L. Gandon and A. Georgeaux: "Extractive Metallurgy of Copper", J.C. Yannopoulos and J.D. Agarwal, eds., AIME, New York, NY, 1976, vol. 2, p. 825.
 24. J.P. Wilson and W.W. Fisher: J. Metals, 1981, vol. 33(2), p. 52.
 25. M. Bonan, J.M. Demarthe, H. Renon and F. Baratin: Metall. Trans. B, 1981, vol. 12B, p. 269.
 26. G.W. McDonald, T.J. Udovic, J.A. Dumesic and S.H. Langer: Hydrometallurgy, 1984, vol. 13, P. 125.
 27. H.G. Linge: Hydrometallurgy, 1976-77, vol. 2, p. 219.
 28. A.I. Vizsolyi: J. Metals, 1967, vol. 19, p. 52.
 29. P.H. Yu: Ph.D. Thesis, Univ. Utah, 1972.

30. F. Forward: J. Metals, 1955, vol. 7, p. 457.
31. M. Kuhn: paper presented at 3rd C.I.M. Hydrometallurgy Conference, Edmonton, 1973.
32. L.W. Beckstead and J.D. Miller: Metall. Trans. B, 1977, vol. 8B, p. 31.
33. L.E. Murr and B.J. Hiskey: Metall. Trans. B, 1981, vol. 12B, p. 255.
34. J.D. Porter, P.B. Queneau and T.J. Hudson: paper presented at AIME Annual Meeting, San Francisco, 1972.
35. F. Habashi, Trans. S.M.E.-AIME, 1973, vol. 254, P. 244.
36. G. Bjorling and G.A. Kolta: Proc. Intern. Mineral Processing Cong. 7th, New York, 1965.
37. G. Springer: Trans. Inst. Min. Met., C11, 1970.
38. W.H. Brattain and C.G.B. Garrett: Bell System Techn. Journal, 1955, vol. 34, p. 129.
39. E.N. Zevgolis: Ph.D Thesis, Univ. Minnesota, 1970.
40. T. Kato and T. Oki: Japan Inst. Metals. Journal, 1972, vol. 36, p. 947.
41. T. Oki and S. Ono: Japan Inst. Min. Met. Journal, 1967, vol 83, p.1159.
42. A. Etienne: Ph.D. Thesis, Univ. Brit. Col., 1970.
43. D.L. Jones and E. Peters: Int. Corros. Conf. Ser. 1973 (Pub.1976), NACE-4, p. 433.
44. M. Ammou-Chokroum, D. Steinmetz and A. Malve: Bull. Mineral, 1978, vol. 101(1), p. 26.
45. M .Ammou-Chokroum, P.K. Sen, and F. Fouques: Mem. Sci. Revue Metallurgie, 1979, vol.76, p.271.

46. M.Ammou-Chokroum, P.K.Sen, and F.Fouques: Mem. Sci. Revue Metallurgie, 1979, vol.76, p.333.
47. M.Ammou-Chokroum, P.K.Sen, and F.Fouques: Proc. XIII Intern. Mineral Proc. Cong., Warsaw, Poland, 1979. vol. 1, p. 527.
48. T. Biegler and D.A. Swift: J. Appl. Electrochem., 1979. vol. 9, p. 545.
49. R. Bertram and H. Illi: Chem.-Ing.-Tech., 1976, vol. 48, p.141.
50. R. Bertram and H. Greulich: Erzmetall, 1980. vol. 33, p. 509.
51. D.C. Price and J.P. Chilton: Hydrometallurgy, 1980, vol. 5, p. 381.
52. A.J. Parker, R.L. Paul and G.P. Power: Aust. J. Chem., 1981, vol. 34, p. 13.
53. A.J. Parker, R.L. Paul and G.P. Power: J. Electroanal. Chem., 1981, vol. 118, p. 305.
54. R.S. McMillan, D.J. MacKinnon and J.E. Dutrizac: J. Applied Electrochem., 1982, vol. 12, p. 743.
55. G.W.Warren, M.E.Wadsworth, and S.M.El-Raghy: Metall. Trans.B, 1982, vol. 13B, p. 571.

Chapter 2

The Leaching of Chalcopyrite with Ferric Chloride^{1,2}

2.1 Introduction

The dissolution of chalcopyrite in acidic ferric chloride solution has been studied by many researchers³⁻¹⁵. Some of those researchers postulated that dissolution occurs electrochemically. Papers reported by Jones and Peters⁹ and Palmer et al.¹³ are typical examples.

On the other hand, the anodic behavior of chalcopyrite in chloride media was investigated by Ammou-Chokroum et al.^{15,16}. They studied the dissolution of chalcopyrite in acidic solutions and postulated that the initial stage of dissolution involves the formation of hydrogen sulfide, ferrous ions and covellite. Furthermore they postulated that the ohmic potential drop across the precipitated chalcocite plays an important role in establishing the electrochemical behavior of chalcopyrite.

Jones¹⁷ studied the electrochemistry of chalcopyrite dissolution and found that for relatively low applied potentials, activation polarization is observed. For higher potentials, the transport of cuprous ions through the mineral lattice was thought to be rate controlling. Jones' data indicate that under those conditions involved in ferric chloride leaching where the potential applied to the anodic site is relatively low, activation polarization assumes importance.

Parker et al.^{18,19} studied potentiostatic oxidation of chalcopyrite and found the current-time dependence which

indicated that the rate of chalcopyrite dissolution was being retarded by diffusion of products through a slowly thickening layer. They concluded that the passivation layer consisted of a copper-bearing species and suggested a copper polysulfide.

McMillan et al.²⁰ studied anodic dissolution of chalcopyrite in both acidic sulfate and acidic chloride media and suggested the formation of a surface layer which slows the rate of electron transfer.

Biegler and Horne²¹ studied the electrochemistry of surface oxidation of chalcopyrite in acid solution and found the formation of a passivating film stable at 298 K.

Relating to the electrochemistry of chalcopyrite, the anodic behavior of chalcopyrite in sulfate-bearing solutions was examined by Warren²², Warren et al.²³ and in ammoniacal solutions by Warren and Wadsworth²⁴.

Recently Wadsworth pointed out the importance of the use of electrochemical measurements, either anodic or cathodic, in understanding dissolution kinetics²⁵. The following points made by him seem to be very important: The experimental methods used are sufficiently sensitive to see transient phase changes that may or may not be of major importance during the gross or massive leaching of sulfide concentrates. The characterization of initial kinetics which is possible by electrochemical measurements may not in fact be important for high fractional reactions. It may be that the products of reaction passivate late in the reaction because of the increasing quantities of reaction products formed. The direct use of electrochemical

measurements to identify important parameters in commercial leaching may be misleading especially if solid intermediate phases are formed. Caution is necessary in using mechanistic determinations solely from electrochemical measurements. Such measurements should be coupled with bulk measurements under conditions related to actual leaching systems if the identification of the important parameters for commercial application are to be identified.

Although some important studies are available on the electrochemical behavior of chalcopyrite, no direct experimental support has been provided for an electrochemical mechanism of chalcopyrite leaching in acidic ferric chloride solution. Under such circumstances, only the accumulation of experimental observation can lead to the appropriate conclusions.

This study was done to obtain a better understanding of the reaction kinetics of chalcopyrite leaching in ferric chloride solution. For this purpose, particular attention was paid to obtaining a reliable leaching rate. Also the correlation between the chemical leaching of chalcopyrite in ferric chloride solution and the electrochemical leaching of chalcopyrite in acidic chloride media was studied to verify the appropriateness of the electrochemical mechanism proposed by previous researchers.

2.2 Experimental Procedures

2.2.1 Sample and Chemicals

Chalcopyrite crystals of museum grade supplied from Shakanai

Mine, Akita prefecture, Japan, were used in leaching experiments in this work. Their copper, iron, and sulfur contents were 34.8 %, 30.4 %, and 34.8 %, respectively. The mineral crystals were not associated with any gangue minerals and the purity of the specimens appeared to be good. Disk specimen was prepared by cementing a chalcopyrite crystal in an epoxy resin such that one surface ($0.3-0.5 \text{ cm}^2$) was exposed to the leaching solution. Moreover, electrical contact was made by soldering copper wire with silver paste on the rear face of each specimen for electrochemical measurements (Fig. 2-1). After fine wet grinding with Emery paper, the specimen was subjected to experiments. The exposed surface area was measured prior to each experiment by using a planimeter on an enlarged photograph.

Deionized water whose specific resistivity was $5 \times 10^6 \text{ } \Omega\text{cm}$ and reagent grade chemicals were used to prepare all electrolyte solutions.

2.2.2 Leaching Experiments

A 0.5 dm^3 glass separable flask was used as a leaching reactor. The solution were agitated at constant speed of 300 r min^{-1} with a magnetic stirrer. Temperature of the solution ranged from 328 to 363 K and ferric chloride concentrations ranged from 0.01 to 1 mol dm^{-3} . The pH of the solution was adjusted to less than 1 by using hydrochloric acid. The specimen was subjected to wet polishing with Emery paper before only first leaching and the same specimen without further polishing was used in successive leaching experiments. The rate curve was

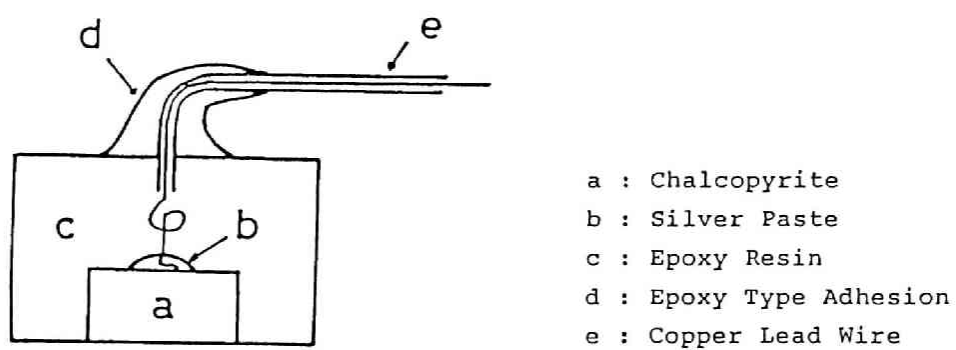


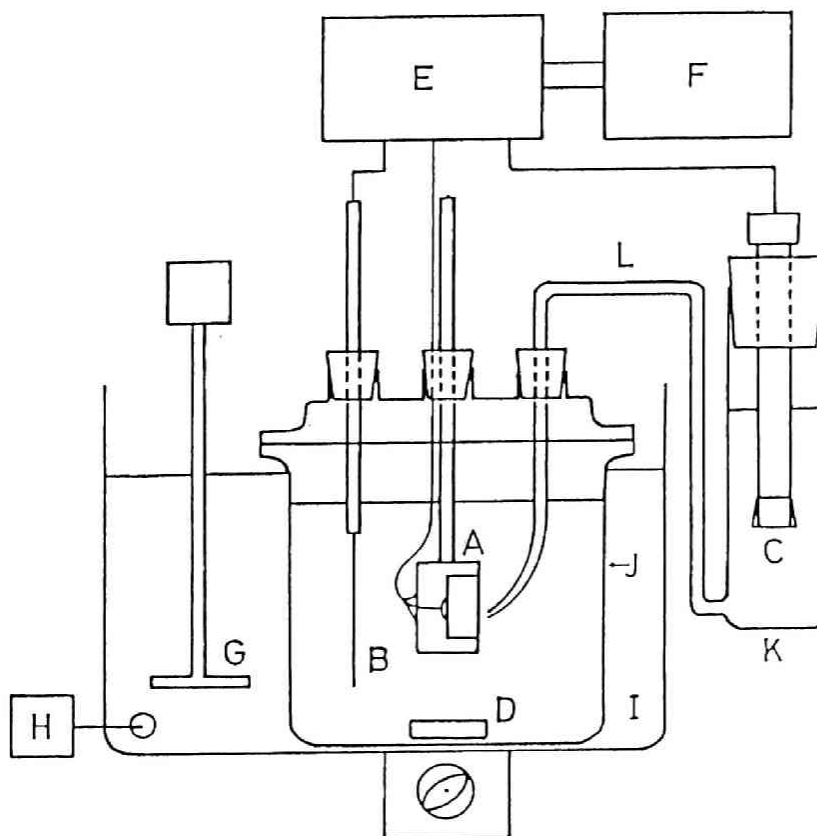
Fig. 2-1 Schematic illustration of chalcopyrite electrode.

determined by analyzing the total copper content in the aliquots which were periodically sampled from the leach solution. Copper analysis of the sample solution was done with an atomic absorption spectrophotometer (Jarell-Ash, Type AA-1). When the effect of ferrous chloride was studied, deoxygenated nitrogen gas was bubbled in a test solution throughout the experiment.

2.2.3 Electrochemical Measurements

The experimental set-up used for electrochemical measurements is schematically shown in Fig. 2-2. The measurement was conducted using a typical three electrode system, consisting of chalcopyrite working electrode, platinum counter electrode and 3.3 mol dm^{-3} KCl AgCl-Ag reference electrode, with a potentiostat (Nikko keisoku Model DPGS-10). The data were recorded on an X-Y recorder. Agitation was accomplished with a magnetic stirrer, keeping the working electrode stationary. Potential measurements between the working electrode and reference electrode were made through a Luggin capillary which was placed 1 cm away from the surface of chalcopyrite. This is possible because of extremely small electric currents involved and the good conductivity of the electrolyte. All potentials in this study are presented with respect to the standard hydrogen electrode (SHE) instead of the 3.3 mol dm^{-3} KCl AgCl-Ag electrode.

Two types of experiments were performed: constant potential experiments and mixed potential measurements in hydrochloric acid solution containing oxidizing or reducing reagents. During the



- | | |
|-------------------------|--|
| A : Working Electrode | H : Heater |
| B : Counter Electrode | I : Water Bath for Temperature Control |
| C : Reference Electrode | J : Separable Flask |
| D : Magnetic Stirrer | K : Glass Vessel |
| E : Potentiostat | L : Liquid Junction |
| F : X-Y Recorder | |
| G : Stirrer | |

Fig. 2-2 Schematic illustration of experimental set-up used for electrochemical measurements.

former experiments the current was measured as a function of time. The volume of solution used in the electrochemical measurements was 0.2 dm^3 and the cell was maintained in a thermostatted water bath to keep a constant temperature at 343 K unless otherwise stated.

When the effect of ferrous chloride concentration was studied, the following method was employed: A chalcopyrite electrode immersed in a 0.2 dm^3 of 0.2 mol dm^{-3} HCl solution containing 2 mol dm^{-3} NaCl charged in a separable glass flask was potentiostatically anodized at 706 mV vs SHE to measure the electric current. After the stable current was established, 1 mol dm^{-3} FeCl_2 solution containing 0.2 mol dm^{-3} HCl and 2 mol dm^{-3} NaCl was added in stages. The preparation of the ferrous sulfate solution was made by dissolving ferrous sulfate into water just before each experiment. Deoxygenated nitrogen gas was bubbled in a test solution kept at 343 K throughout the experiment.

2.2.4 Morphological Observations

Observation of the leached surface of chalcopyrite was done for two kinds of specimens: 1) a surface of chalcopyrite leached after fine wet grinding and a cross section of the chalcopyrite prepared by breaking it into two with a knife, and 2) a grain sized crystal of chalcopyrite leached without wet grinding. In both cases the product of the leaching reaction was observed by using a scanning electron microscope (SEM) and an electron probe micro analyzer (EPMA) (both Hitachi, Type X-650) and an electron spectroscopy of chemical analysis (ESCA) (Shimadzu 650-B).

2.3 Experimental Results

2.3.1 Comparison of the Leaching Reactions of Chalcopyrite with Ferric Chloride and Those with Ferric Sulfate

Figure 2-3 illustrates typical leaching rate curves of chalcopyrite in ferric chloride and ferric sulfate solutions. The leaching rate of chalcopyrite in ferric sulfate solution was approximately one order smaller than that in ferric chloride. The leaching curves are linear in the ferric chloride solution for approximately 100 hr after the initiation of process and parabolic in the ferric sulfate solution for the same period, respectively*. They are both followed by an accelerating phase. The morphology of the leached surface of chalcopyrite was examined by means of a SEM. Plate 2-1 shows the morphology of the chalcopyrite surface after 120 hr leaching in (a) 1.0 mol dm^{-3} ferric chloride solution and (b) 1.0 mol dm^{-3} ferric sulfate solution. It is obvious that elemental sulfur formation was distinctly observed on the surface leached in ferric chloride, while the surface leached in ferric sulfate is similar to the original surface (c).

The ESCA analysis of the sulfur on the chalcopyrite surfaces leached by the two solutions is shown in Fig. 2-4. The energy spectra of original surface exhibits two peaks at 161 eV and 162 eV. The energy spectra of the surface leached by ferric sulfate is not so distinct, with an energy peak remaining at 161 eV,

* The leaching of chalcopyrite with ferric sulfate was described in detail in Chapter 4.

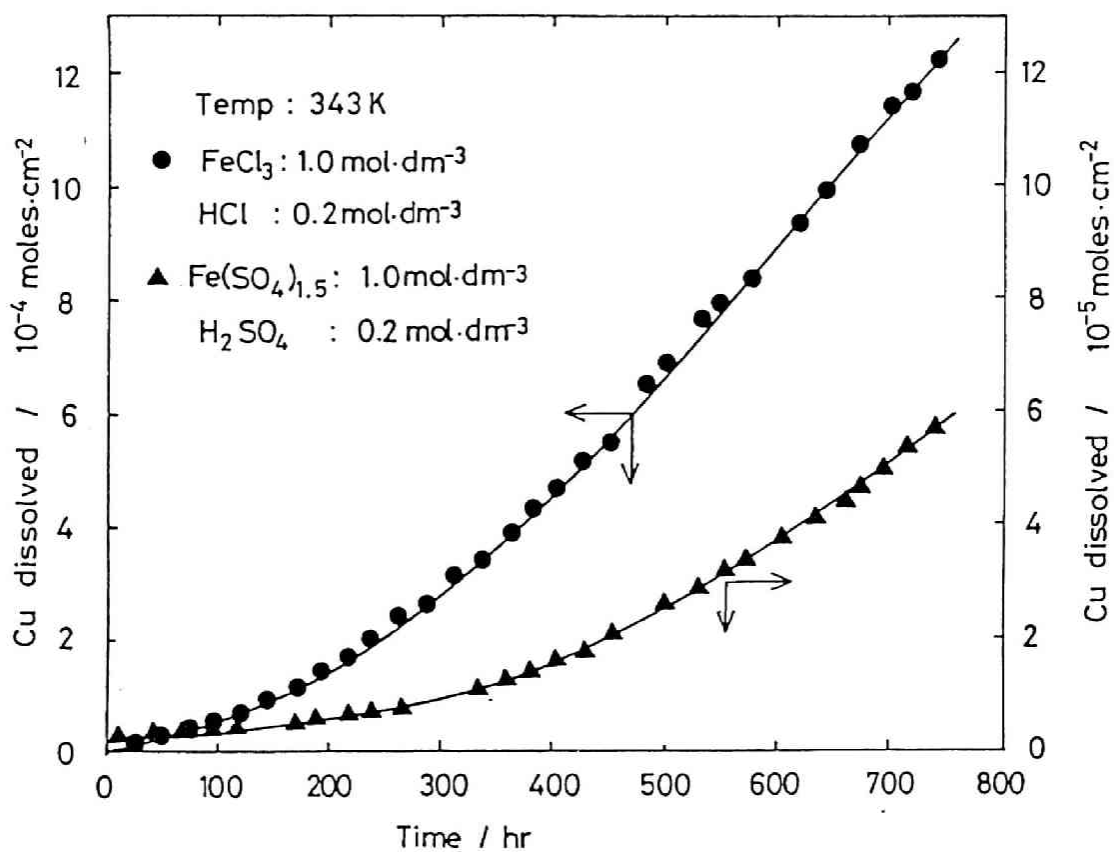


Fig. 2-3 Leaching rate curve of chalcopyrite crystal with ferric chloride or ferric sulfate. (Disk specimens were used in these experiments.)

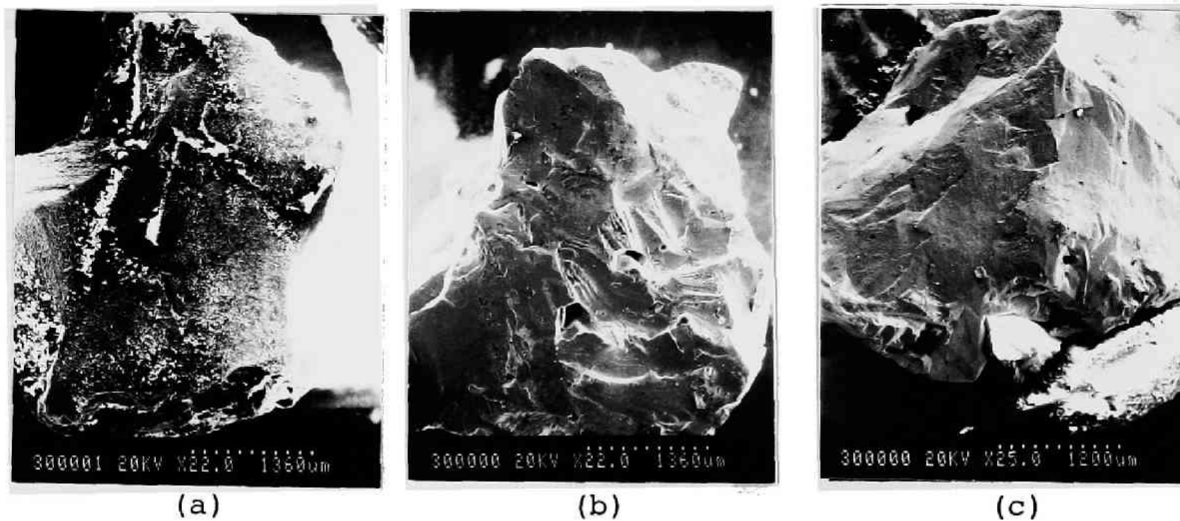


Plate 2-1 A comparison of the surface appearance of chalcopyrite.

(a) after 120 hr leaching in $1.0 \text{ mol dm}^{-3} \text{ FeCl}_3$ -
 $0.2 \text{ mol dm}^{-3} \text{ HCl}$ at 363 K.

(b) after 120 hr leaching in $1.0 \text{ mol dm}^{-3} \text{ Fe(SO}_4\text{)}_{1.5}$ -
 $0.2 \text{ mol dm}^{-3} \text{ H}_2\text{SO}_4$ at 363 K.

(c) fresh chalcopyrite.

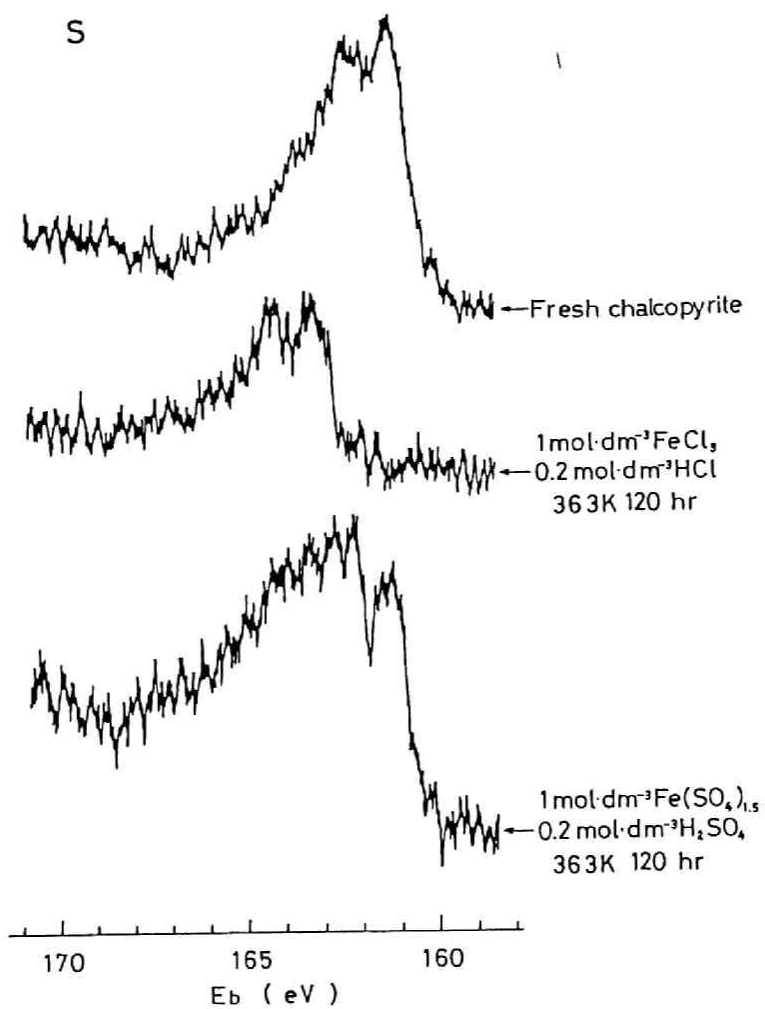


Fig. 2-4 Sulfur analysis of chalcopyrite surfaces by an ESCA.

whereas the ferric chloride one exhibits peaks at 163 and 164 eV. This finding suggests that the oxidation of sulfide sulfur occurred with ferric chloride. These results support the observation shown in Fig. 2-3 as well as Plate 2-1, suggesting that ferric chloride is more effective oxidant for the leaching of chalcopyrite than ferric sulfate.

2.3.2 Morphology of Surface of Chalcopyrite Leached with Ferric Chloride

Plate 2-2 shows the morphology of the chalcopyrite surface leached in 1.0 mol dm^{-3} of ferric chloride solution at different periods. X-ray analysis indicates that the layer on the leached surface is elemental sulfur, as is shown in Plate 2-2(f). After 24 hr of leaching, a plate-like structure was observed on the chalcopyrite crystal surface as shown in Plate 2-2(a). X-ray analysis of this revealed that elemental sulfur was formed at the fringe of each plate with unreacted chalcopyrite in the center. This indicates that the surface of chalcopyrite was not reacted homogeneously, and it was preferentially leached under the influence of a certain substrate structure. After 168 hr leaching (Plate 2-2(c)), it can be seen that the process has continued simultaneously at the edge of the plate-like structure and at the unreacted centre, with the formation of pits. After 240 hr the formation of a porous layer of elemental sulfur is evident over the entire surface as shown in Plate 2-2(d). The formation of elemental sulfur in this study is similar to that reported by Jones and Peters⁷, though they didn't mention the

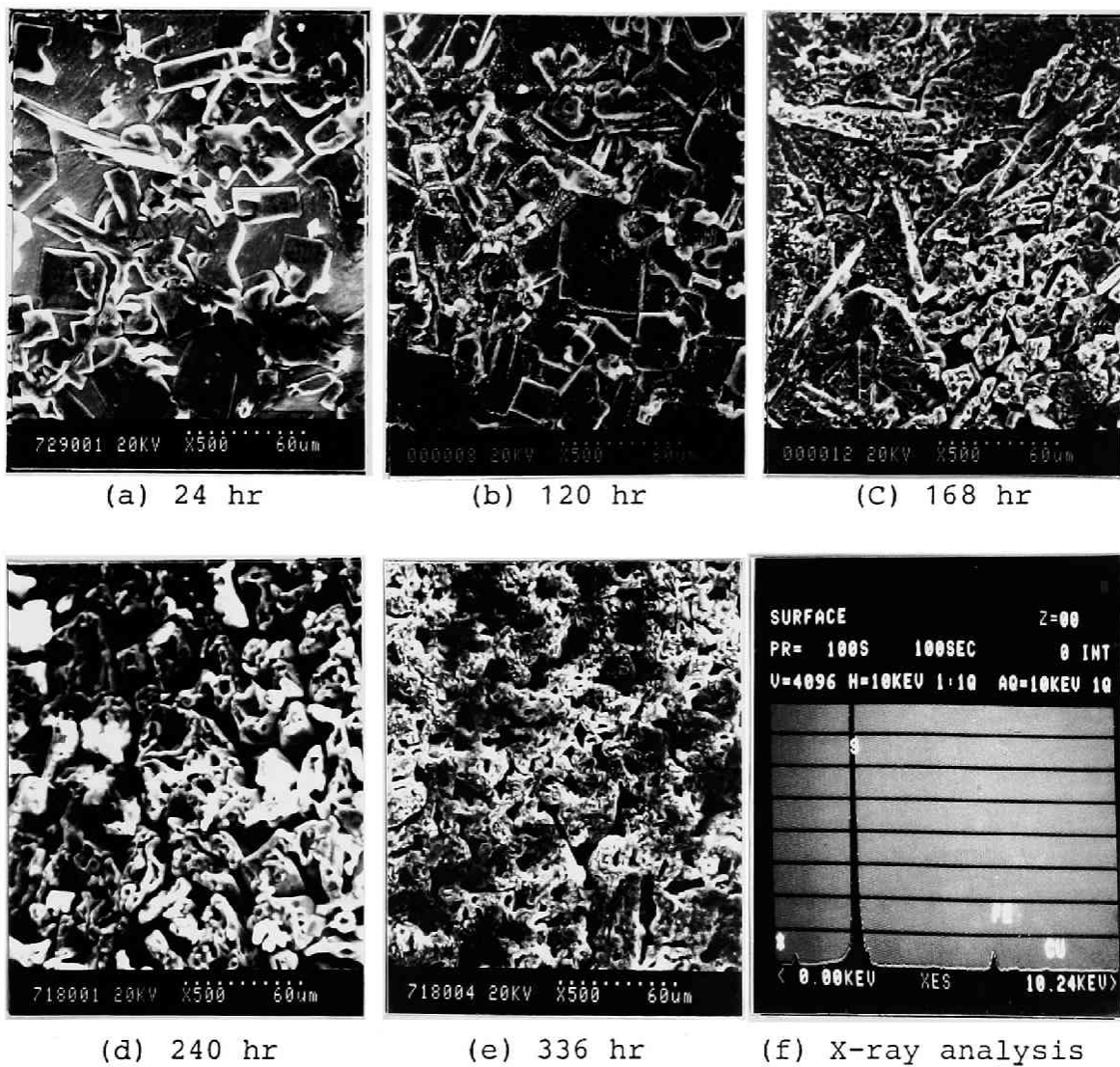


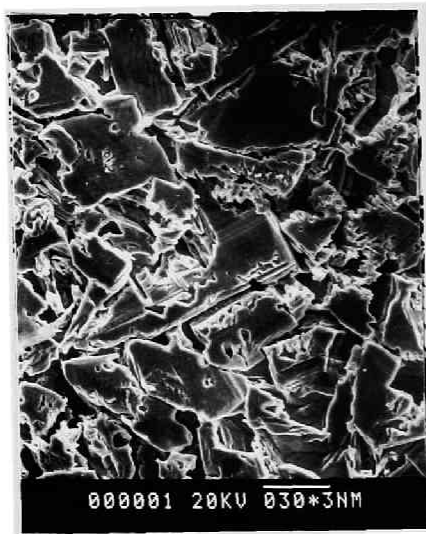
Plate 2-2 Morphological changes on the chalcopyrite surface leached with ferric chloride. ($1.0 \text{ mol dm}^{-3} \text{ FeCl}_3$ - $0.2 \text{ mol dm}^{-3} \text{ HCl}$ at 363 K)

formation of plate-like structure at the initial stage of leaching, shown in Plate 2-2(a).

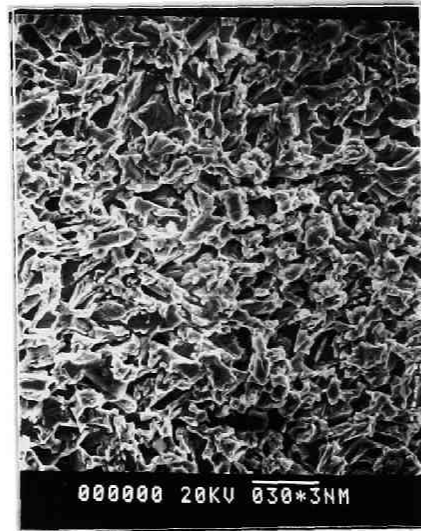
The leached chalcopyrite samples were soaked for 100 hr in carbon disulfide and refluxed for 24 hr in a Soxhlet extractor to remove elemental sulfur formed on the samples. Plate 2-3 shows the morphology of the surface of leached chalcopyrite after the elemental sulfur was removed. As is shown in this plate, the surface of unreacted chalcopyrite was roughened after an extended leaching period (Plate 2-3(b) or (c)) which is indicative of an increase in effective surface area. It was demonstrated in Fig. 2-3 that the leaching of chalcopyrite with ferric chloride was accelerated after prolonged leaching. This result was attributable to the increase in effective surface area of chalcopyrite during its leaching.

The cross sections of leached chalcopyrite are shown in Plate 2-4. The layer precipitated on the surface of chalcopyrite leached for 550 hr was identified to be elemental sulfur by X-ray analysis (Plate 2-4(e)). It is clearly seen in these photos that the sulfur layer became thicker and more porous with an increase in leaching time. These photos also show that the surface of unreacted chalcopyrite was roughened after an extended leaching period (Plate 2-4(c) or (d)) until it reached to a steady state.

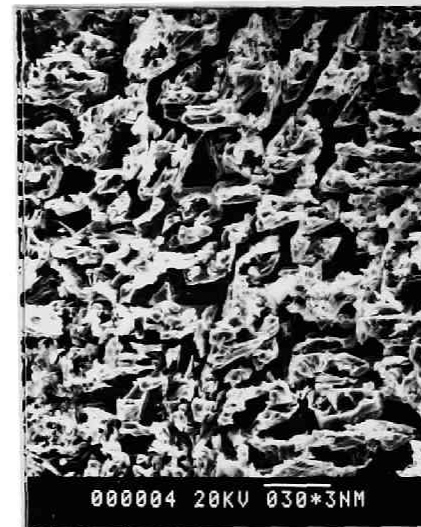
Plate 2-5 depicts an interesting observation of the inside cavity of a specimen leached for 336 hr. The formation of elemental sulfur was observed in a fissure which originally existed in the chalcopyrite crystal, as well as inside the



(a) 120 hr



(b) 240 hr



(c) 336 hr

Plate 2-3 Observation of the surface of leached chalcopyrite after the elemental sulfur formed on the surface was removed.

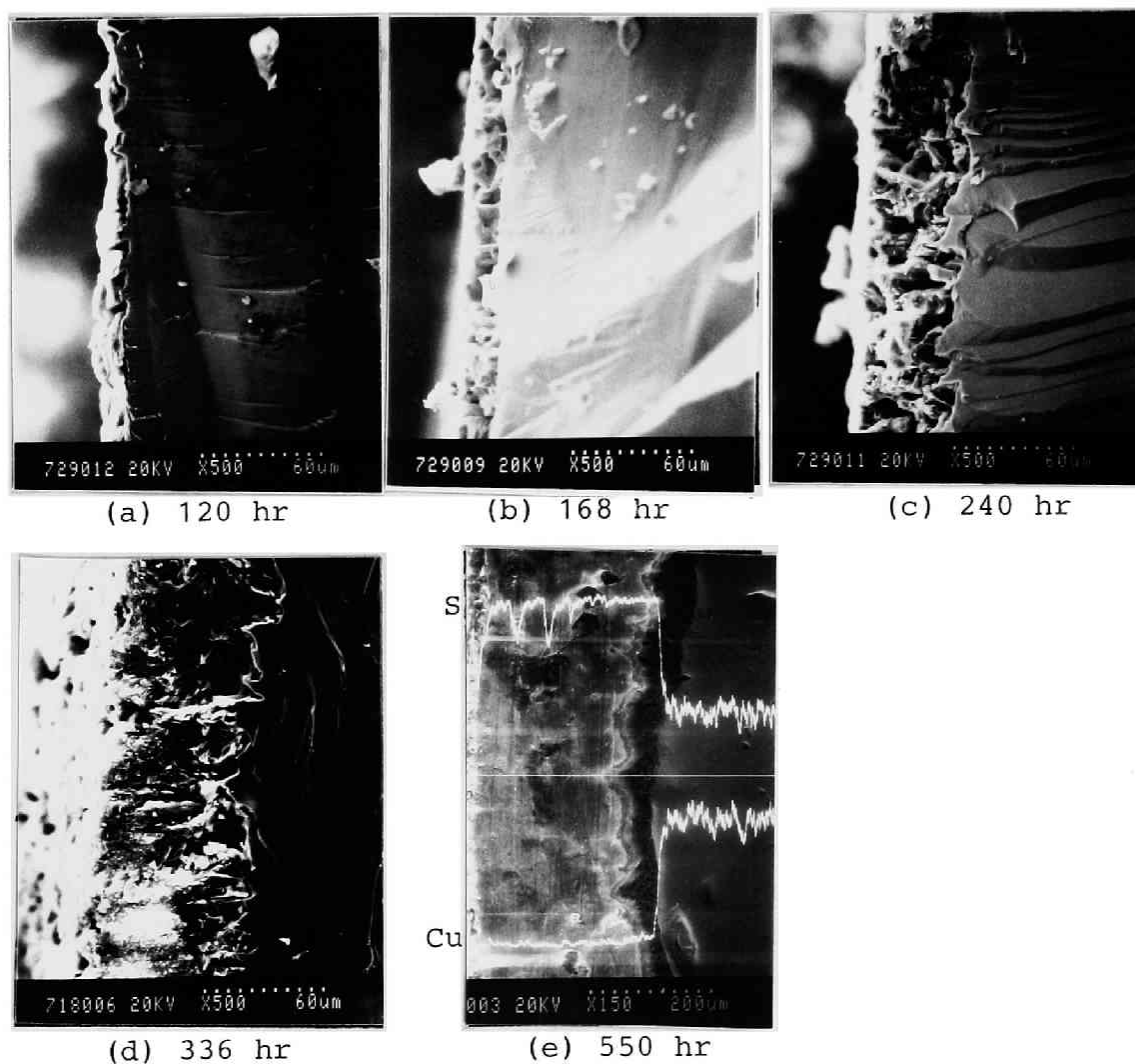


Plate 2-4 Observation of the cross section of chalcopyrite leached with ferric chloride. (Leaching conditions were the same as described in Plate 2-2.)

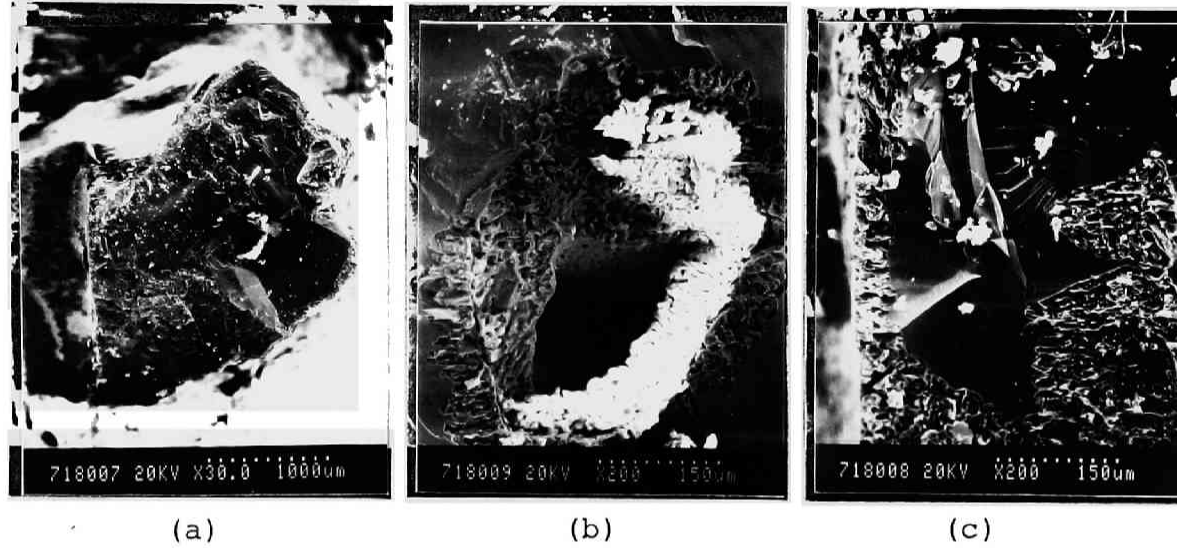


Plate 2-5 Elemental sulfur formed inside a cavity in chalcopyrite crystal. (Leaching conditions were the same as described in Plate 2-2(e).)

cavity. This indicates that the leachant migrated through the porous elemental sulfur as well as the narrow fissures originally present in the crystal, forming an elemental sulfur layer in the cavity.

It can be concluded that the elemental sulfur layer formed on the surface of chalcopyrite is porous and not a barrier to further leaching when ferric chloride is used as an oxidative leachant.

2.3.3 Determination of Leaching Rate

As shown in Fig. 2-3, the amount of copper dissolved from chalcopyrite in a ferric chloride solution increases linearly for approximately 100 hr until the amount of the dissolved copper is approximately 1×10^{-4} moles cm^{-2} . The leaching rates determined from different specimens of the same crystal were compared. A typical range of these rate curves is shown in Fig. 2-5. The leaching rate was found to vary by a factor of three. It must be noted that the leaching rate of chalcopyrite specimens may be significantly different even if the crystals originate from the same deposit of the same mine.

In addition, it was observed that the same leaching rate cannot be obtained by repeat leaching tests on the same specimen polished by Emery paper prior to each leaching experiment as shown in Fig. 2-6.

From these observations, it can be concluded that the preparation of a reliable leaching surface of chalcopyrite by this polishing technique is difficult. Many examples from

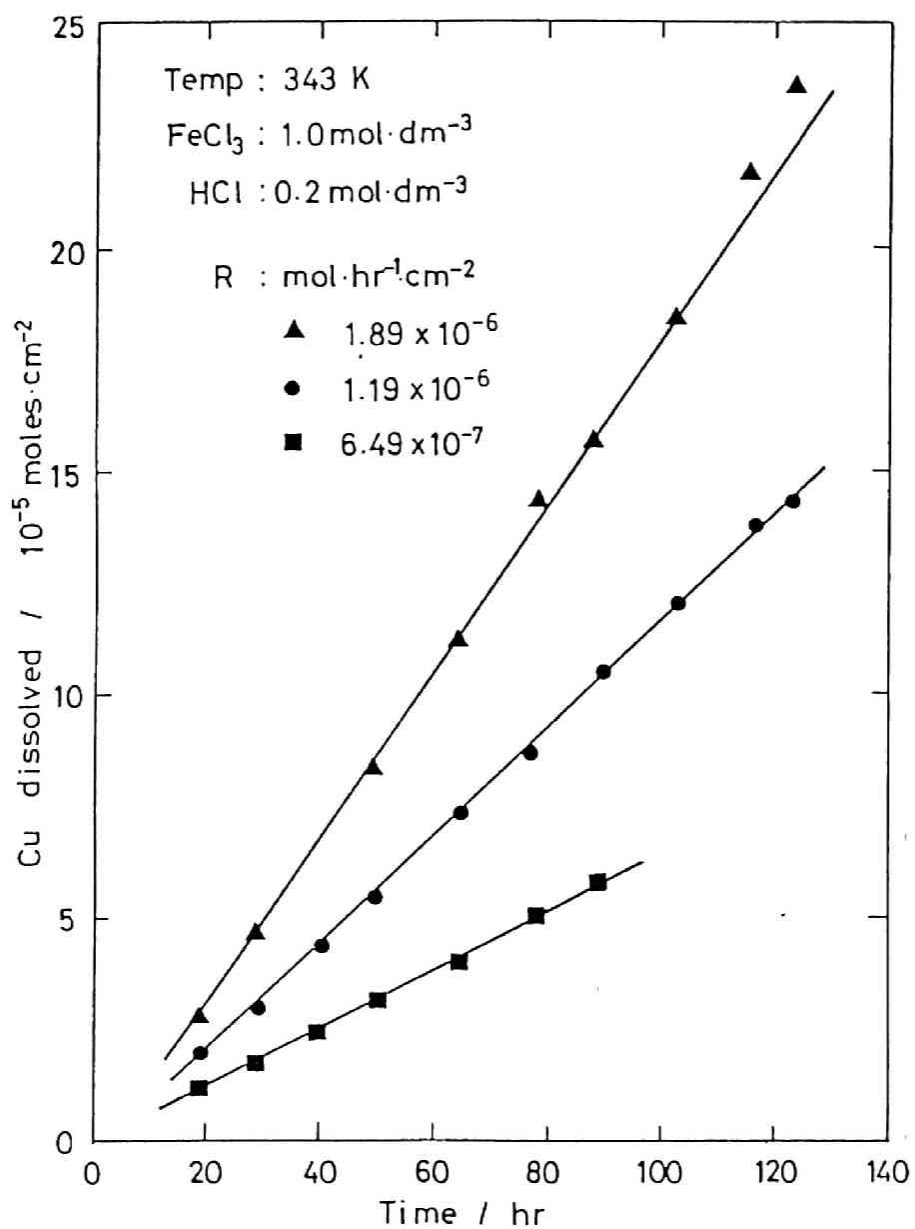


Fig. 2-5 Leaching rate curves for different chalcopyrite specimens with ferric chloride.

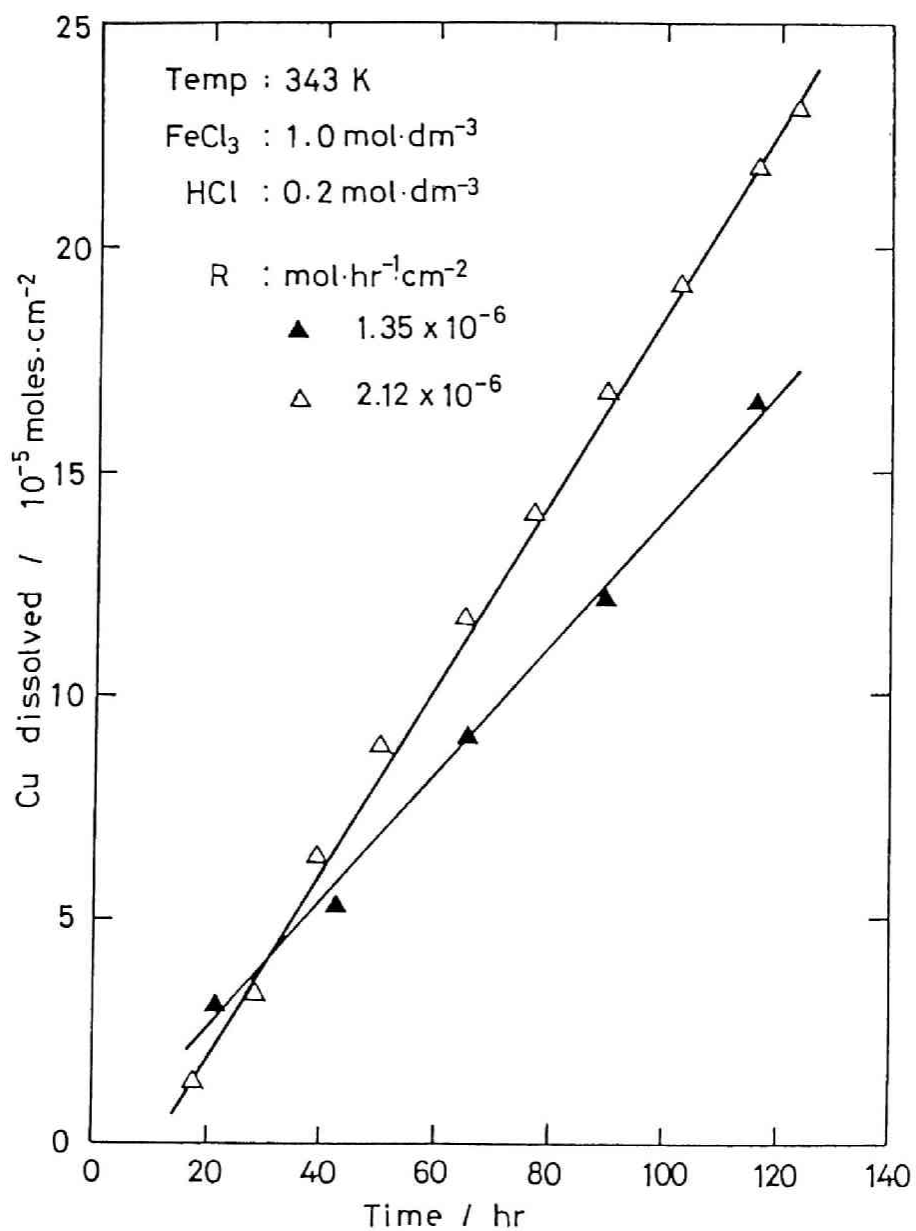


Fig. 2-6 Repeated leaching of polished chalcopyrite using the same specimen.

previous reports can be quoted in which the leaching rate varies considerably^{10,12}. This suggests that a new method is necessary for obtaining reliable kinetic data concerning the oxidative leaching of chalcopyrite with ferric chloride. After examining various methods, the following method was developed; the specimen was subjected to wet polishing with Emery paper before only first leaching and the same specimen without further polishing was used in successive leaching. According to this method, leaching experiments should be designed to keep the total dissolved copper to less than 1×10^{-4} moles cm^{-2} .

2.3.4 Effect of the Concentrations of Ferric Chloride

(a) Leaching Rate

The leaching experiments were carried out in the ferric chloride solutions whose concentrations were 1.0, 0.5, 0.1, 0.2, 0.05 and 0.01 mol dm^{-3} , respectively. The sequence of the concentration described above indicates the order of the leaching experiments. Figure 2-7 illustrates the leaching rate curves obtained at 343 K in solutions containing various initial concentrations of ferric chloride. The leaching curves of all ferric chloride concentrations are essentially linear and the rate increases with the concentration of ferric chloride. Figure 2-8 shows the relationship between $\log R$ and $\log C(\text{FeCl}_3)$. The two straight lines shown in this figure correspond to two series of leaching experiments with different specimens.

Although a distinct difference in leaching rates was observed with two specimens of the same ferric chloride concentration, a

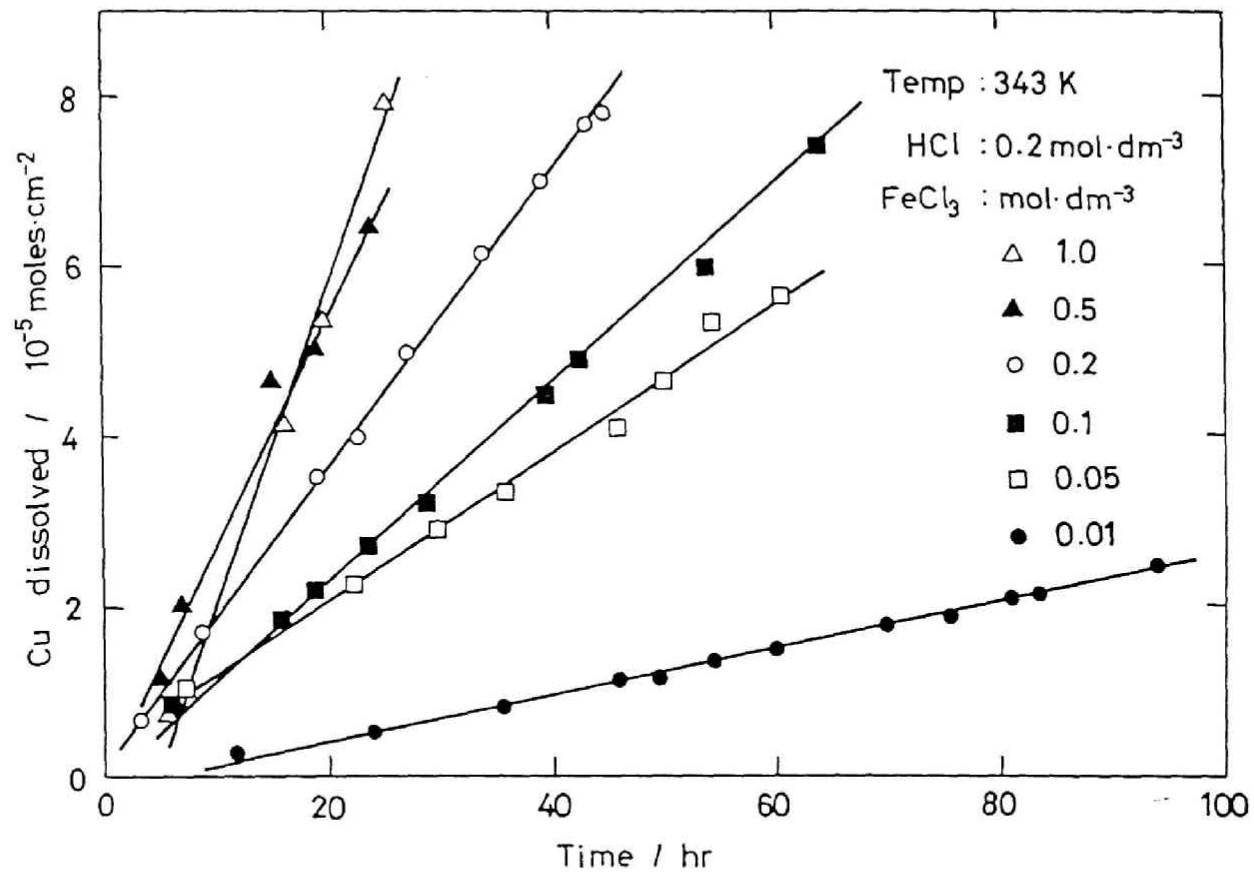


Fig. 2-7 Leaching rate curves of chalcopyrite with ferric chloride.

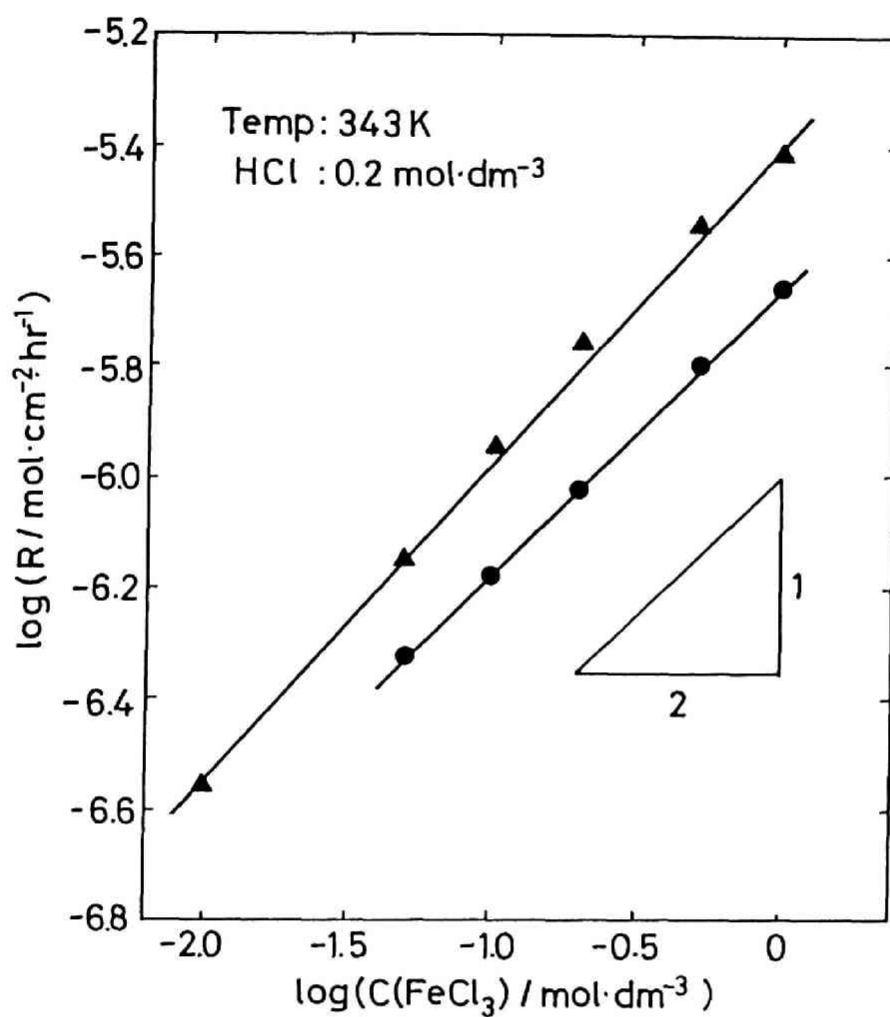


Fig. 2-8 Effect of ferric chloride concentration on the leaching rate of chalcopyrite. (Two different specimens were used.)

good linear relationship was observed between $\log R$ and $\log C(\text{FeCl}_3)$ over the concentration range of 0.01 to 1.0 mol dm⁻³, the slope of the graph being 0.5. Despite the reversion of the leaching experiment with 0.1 and 0.2 mol dm⁻³ FeCl₃, the leaching rate is on the same straight line as is shown in Fig. 2-8. This indicates that the leaching rate of chalcopyrite is of a half order with respect to ferric chloride concentration. This results agrees with the work by Palmer et al.¹³.

On the other hand, Ermilov et al.²⁶ reported that the leaching rate of chalcopyrite shows a first power dependence on the concentration of ferric chloride. Other workers have reported a less sensitive dependency. Jones and Peters⁹ studied the chemical leaching of monosized particulate chalcopyrite and observed that an increase in ferric chloride concentration from 0.1 to 1.0 mol dm⁻³ resulted in the a doubling of the rate. Dutrizac reported an 0.8 power dependency when using disks of synthetic chalcopyrite¹⁰ and an 0.3 power dependency with natural chalcopyrite concentrates¹². Ammou-Chokroum et al.²⁷ observed an 0.3 power dependence for ferric chloride concentration when using synthetic chalcopyrite.

In the experimental work of Dutrizac on synthetic chalcopyrite disks¹⁰, it was found that the amount of copper dissolved increased almost linearly with time. Therefore, it may be easy to determine the leaching rate. However, the amount of dissolved copper in the leaching of natural chalcopyrite increases in a complicated way. In the evaluation of leaching rates, initial rate constants derived from a second order polynomial equation

were used viz. $Cu(mg)=a+bt+ct^2$ (where t is the leaching time in hr) and by calculating the slope at $t=0$. The graphs showing the relationship between leaching rates determined by this method and ferric ion concentration vary tremendously, suggesting that this method is unreliable. In contrast, Palmer et al.¹³ studied the relationship between leaching rates and ferric chloride concentration by using monosized particles of natural chalcopyrite. They analyzed the kinetic data with McKewan's plot method and obtained a satisfactory linear relationship. They also elucidated the dependency of leaching rate on particle size and their results are thus sufficiently reliable. From these considerations, it can be concluded that the leaching rate of chalcopyrite with ferric chloride has a half order dependence on the ferric ion concentration. Palmer et al.¹³ assumed that a mixed electrochemical control occurs in this system. They applied the Butler-Volmer equation to the oxidative leaching of chalcopyrite thus assuming that single electron transfer occurs and that the value of the transfer coefficient is one-half. They proposed a mechanism which is attributable to a one-half order dependency of the leaching rate on the ferric ion concentration.

(b) Mixed Potential

Figure 2-9 illustrates the effect of the ferric chloride concentration on the mixed potential of a chalcopyrite specimen. Starting with a solution of $0.2 \text{ mol dm}^{-3} \text{ HCl}-0.01 \text{ mol dm}^{-3} \text{ FeCl}_3$ the ferric concentration was increased in stages to 1.0 mol dm^{-3} .

As can be seen in Fig. 2-9 a linear relationship of potential

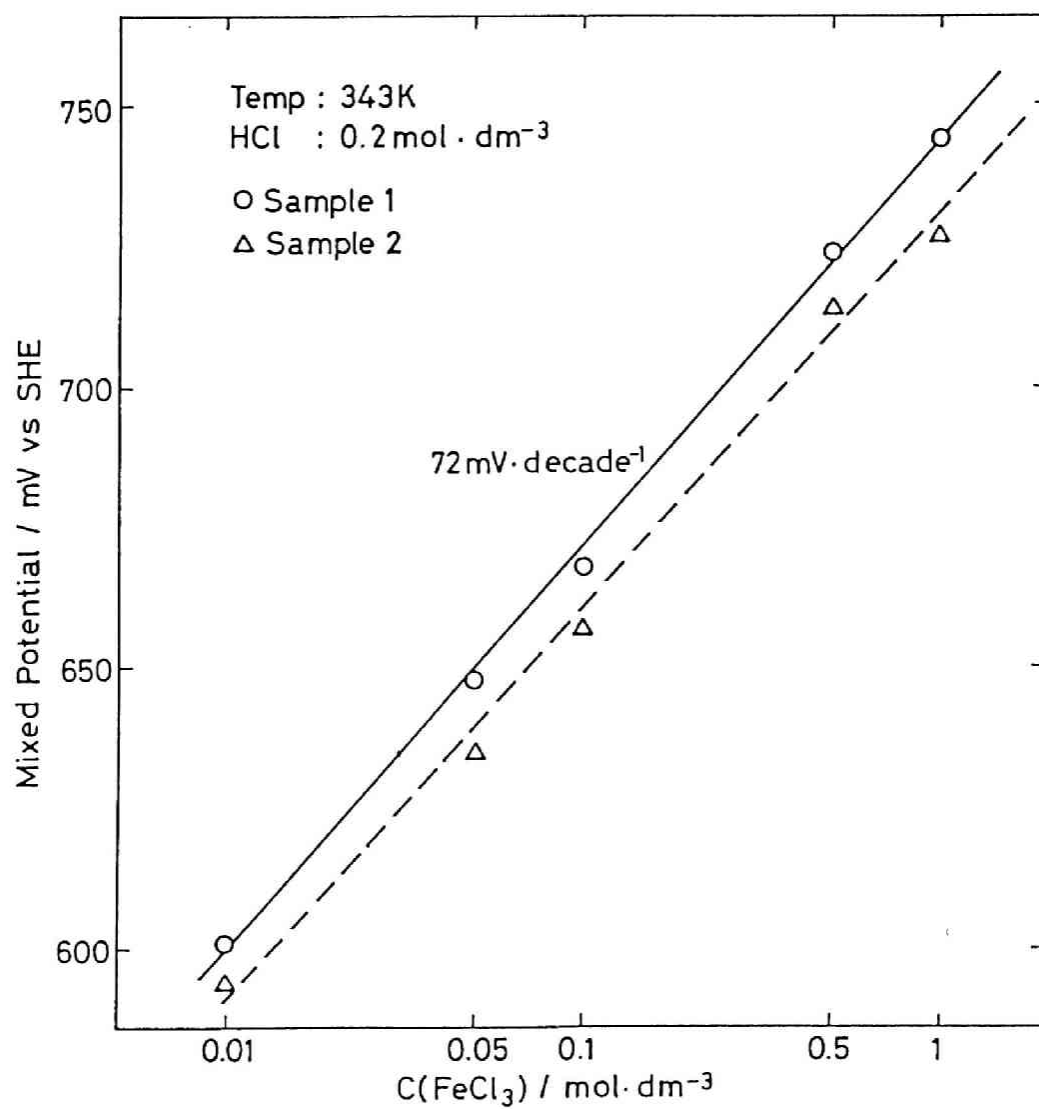


Fig. 2-9 Effect of ferric chloride concentration on the mixed potential of chalcopyrite.

vs $\log C(\text{FeCl}_3)$ was obtained. The two electrodes were approximately 10 mV apart. The slope of the line was found to be 72 mV decade⁻¹ at 343 K.

2.3.5 Effect of the Concentration of Ferrous Chloride

(a) Leaching Rate

When chalcopyrite is leached in ferric chloride-hydrochloric acid solutions, both ferrous chloride and cuprous chloride are produced as reaction products. Cuprous chloride thus formed readily oxidized to cupric state in the presence of dissolved molecular oxygen. It is important to know the effect of these products on the chalcopyrite leaching rate as both will be present in substantial amount in an actual leaching process. If the leaching reaction proceeds electrochemically, the change in redox potential of the ferric chloride solution should also affect leaching rates.

In order to examine the effect of the ferrous chloride concentration on leaching rate, a series of experiments was done at 343 K in an aqueous solution containing 0.2 mol dm⁻³ HCl-0.1 mol dm⁻³ FeCl₃, in which the ferrous chloride concentrations were changed from 0 to 0.9 mol dm⁻³. Since the leaching rate was found to be fairly sensitive to the chloride concentration (as will be described later), the total chloride concentration of the leaching solution was kept constant at 2.3 mol dm⁻³, by adding sodium chloride. Throughout the experiment, nitrogen gas was bubbled into the solution to avoid the oxidation of ferrous ions during the experiment. The leaching results illustrated in

Fig. 2-10 indicate that no significant effect was observed with an increase in the concentration of ferrous chloride. This finding supports the results obtained by Dutrizac et al.¹⁰ and Jones and Peters⁹.

(b) Mixed Potential

The effect of ferrous chloride concentration on the mixed potential of chalcopyrite was also examined in 0.2 mol dm^{-3} HCl solution containing 0.1 mol dm^{-3} FeCl_3 . The results obtained are shown in Fig. 2-11. For the reference, the effect of ferric chloride concentration is superimposed on the same figure. As is obvious in this figure, the mixed potential of chalcopyrite is almost independent of the ferrous chloride concentration in the range 0.01 to 1 mol dm^{-3} . The effect of ferrous chloride concentration on chemical leaching rate of chalcopyrite appeared similar to that of mixed potential.

(c) Oxidation of Ferrous Chloride on the Surface of a
Chalcopyrite Electrode

The presence of ferrous chloride does not affect the mixed potential of chalcopyrite. From this finding, it is supposed that the oxidation of ferrous chloride, which is the resultant product of the reduction of the leachant, is extremely slow on the chalcopyrite surface.

In order to examine the oxidation rate of ferrous chloride on a chalcopyrite surface, the stable current densities of a chalcopyrite specimen were measured after the chalcopyrite was anodically polarized at 706 mV vs SHE , which corresponds to the mixed potential of chalcopyrite in 0.2 mol dm^{-3} HCl- 0.5 mol dm^{-3}

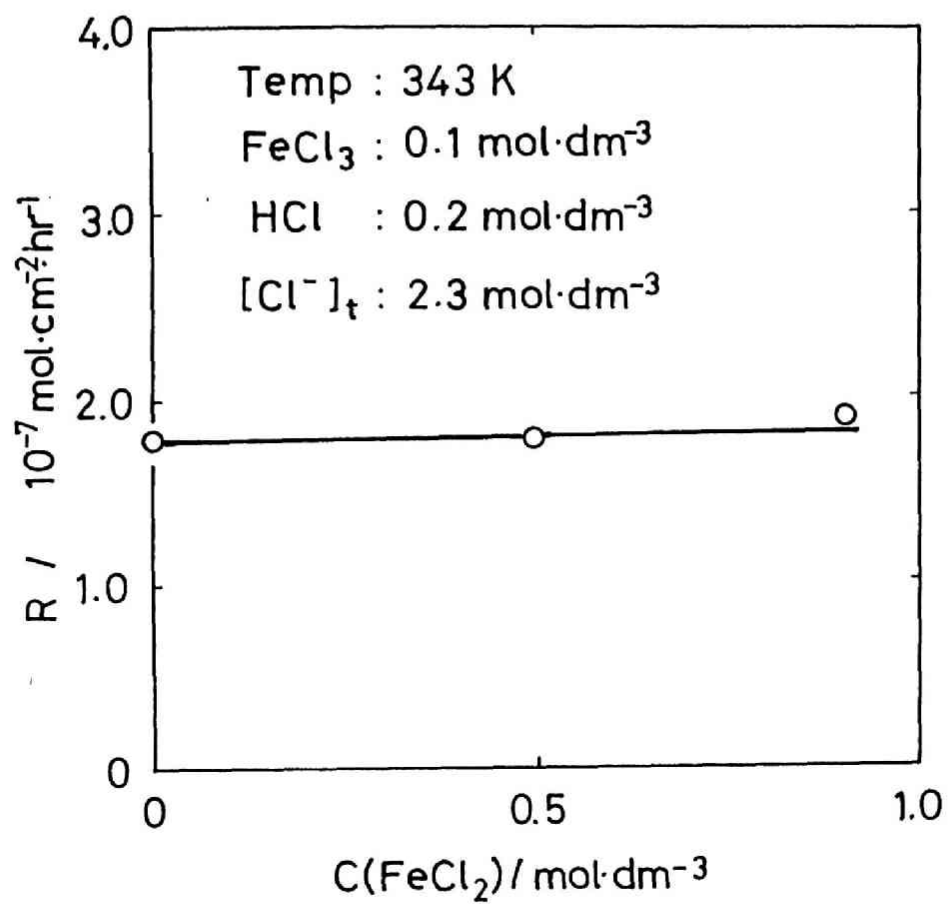


Fig. 2-10 Effect of ferrous chloride concentration on the leaching rate of chalcopyrite.

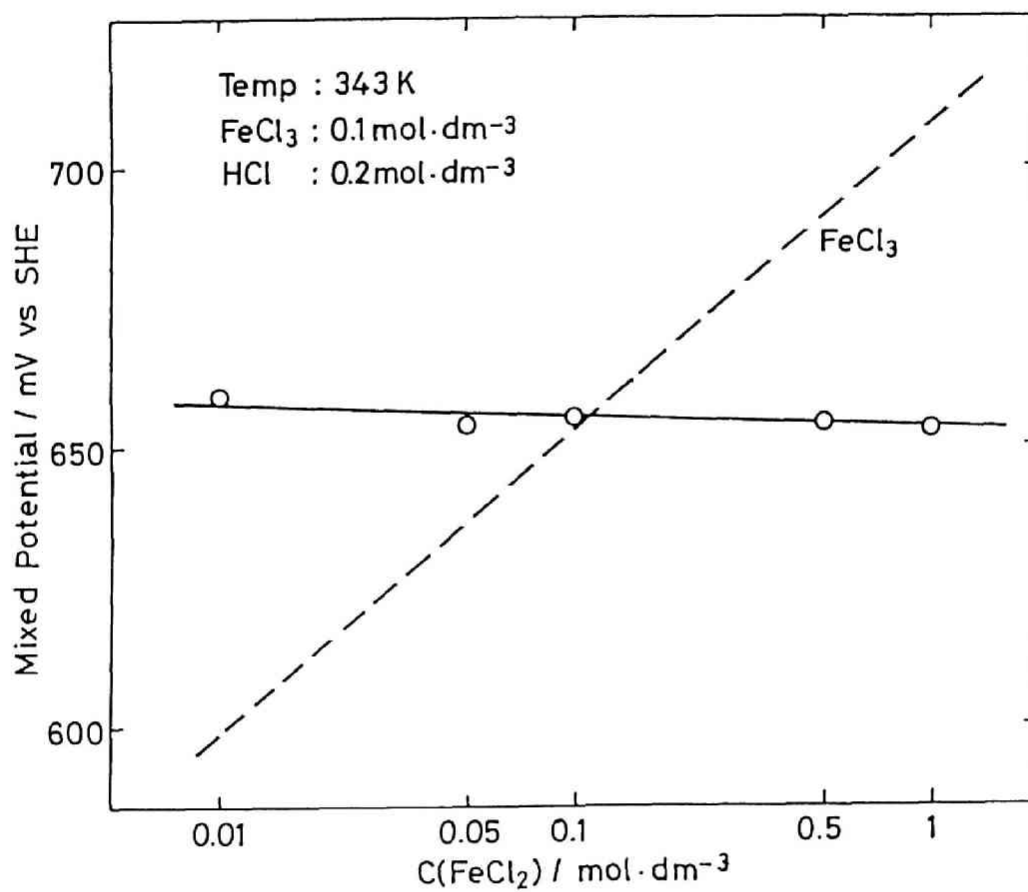


Fig. 2-11 Effect of ferrous chloride concentration on the mixed potential of chalcopyrite. (Dotted line shows the effect of ferric chloride concentration.)

FeCl_3 , in 0.2 mol dm^{-3} HCl containing various amounts of ferrous chloride. The results obtained are depicted in Fig. 2-12. Two series of measurements were made by using the same chalcopyrite specimen without re-polishing. In the performance of the experiment, a cell containing test solution of a given composition was replaced before the subsequent measurement without a further polishing of the specimen. No significant variation in the current density was observed by the change in ferrous chloride concentration. However, the anodic polarization is interrupted after each measurement when using this method. The scatter of the values of the determined current density shown in Fig. 2-12 may be caused by the interruption of the anodic polarization.

A similar measurement was made without any interruption of anodic polarization. In order to determine the effect of ferrous chloride addition on the stable current density, an anodic polarization experiment at 706 mV vs SHE was made in 0.2 mol dm^{-3} HCl solution whose total chloride concentration was adjusted with sodium chloride to a constant value of 2.2 mol dm^{-3} . Prior to the polarization experiment, the solution was purged with nitrogen gas. After the stable current density was achieved, ferrous chloride was added to be 0.1 mol dm^{-3} , without the interruption of anodic polarization, to continue the polarization. The experimental result is depicted in Fig. 2-13. Immediately after the polarization of chalcopyrite, the current density decreased sharply and then gradually increased to reach a constant level of $18.5 \mu\text{A cm}^{-2}$. By adding ferrous chloride, the

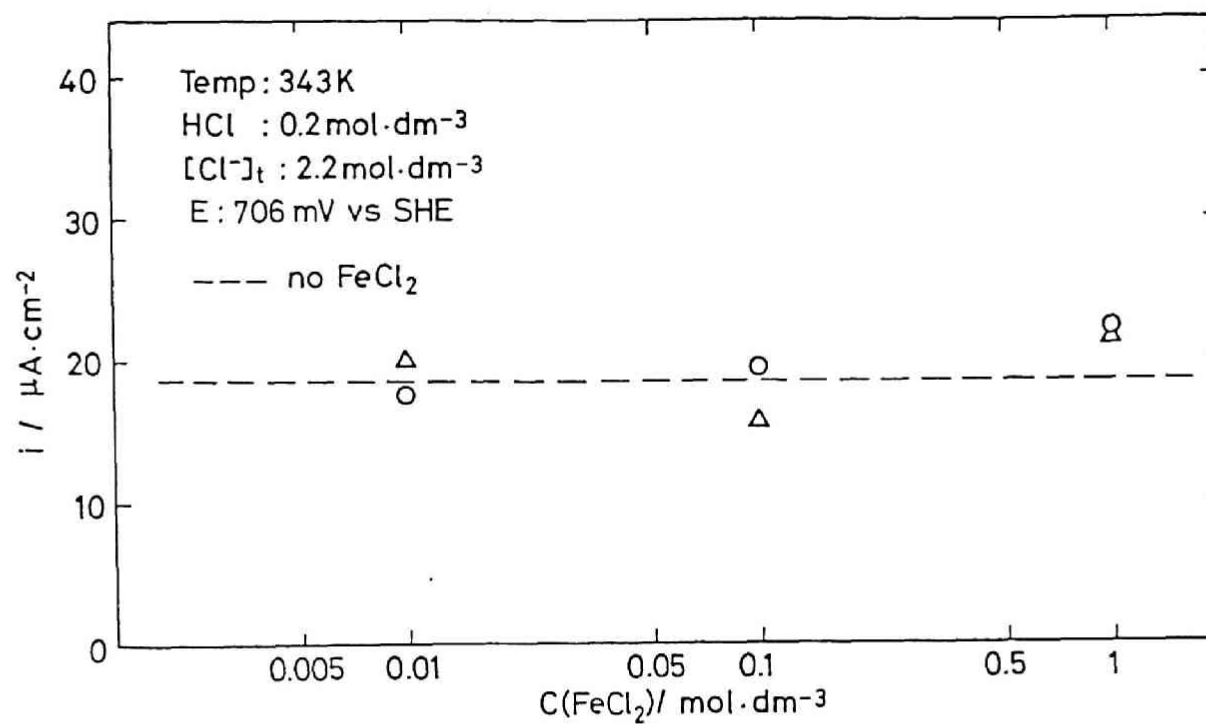


Fig. 2-12 Effect of ferrous chloride concentration on the stable current density of the anodic polarization of chalcopyrite specimen at 706 mV vs SHE.

(○:first series and Δ:second series)

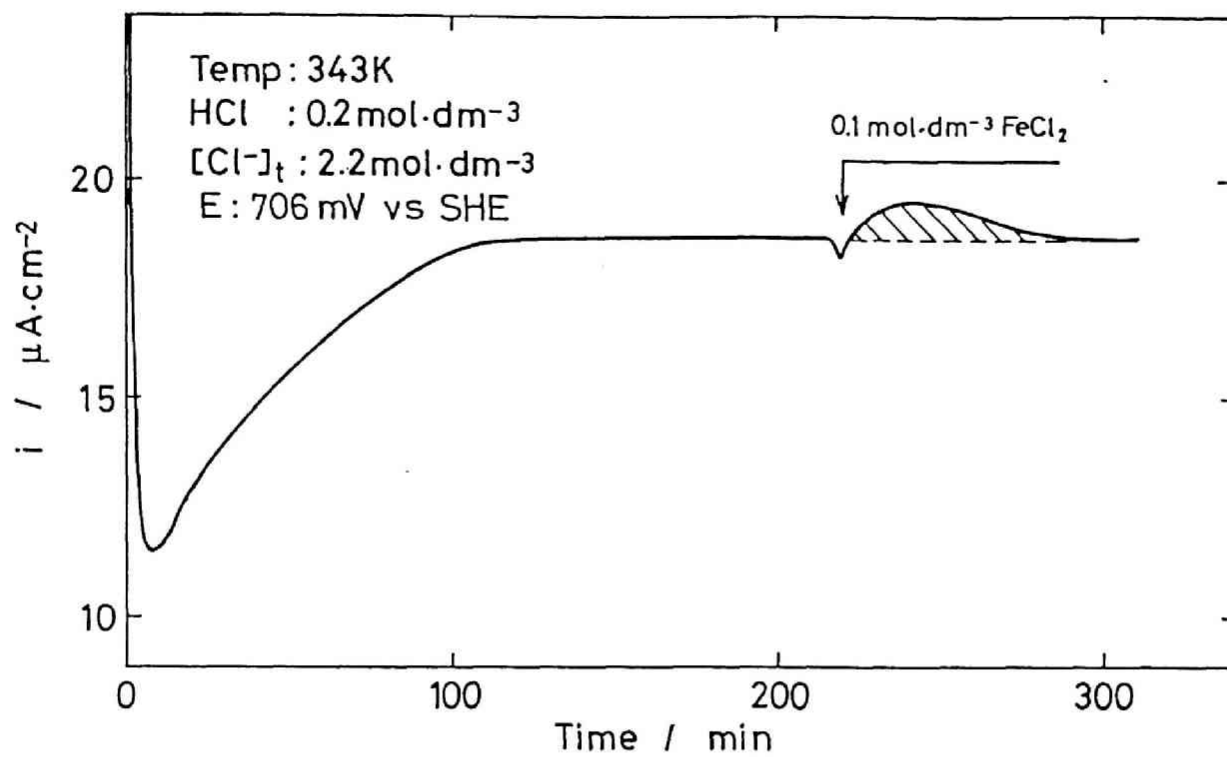


Fig. 2-13 Effect of the addition of ferrous chloride on the stable current density of anodic polarization of chalcopyrite.

current density slightly decreased and then showed a small peak in the current density curve. After one hour the current density again returned to the same constant value of $18.5 \mu\text{A cm}^{-2}$. Judging from the area shaded on the current density curve, the amount of oxidized product was estimated to be 1.3×10^{-8} moles, showing a great difference from that of the ferrous chloride added (2×10^{-2} moles). The results obtained in these experiments indicate that ferrous ions have no significant influence on the electrochemical leaching of chalcopyrite. In another words, it is supposed that the oxidation reaction of ferrous ions on a chalcopyrite electrode is extremely slow.

2.3.6 Effect of the Concentration of Cupric Chloride on the Mixed Potential

In the leaching of chalcopyrite with ferric chloride, cupric and ferrous ions are the products of dissolution. The reduction of ferric ions yields ferrous ions. Cupric chloride is also known as an effective leachant of chalcopyrite, and cupric chloride itself is reduced to the cuprous state. Although the oxidation reaction of ferrous chloride is accelerated by the presence of a Cu(II) catalyzer, it is still controlled by a chemical reaction step²⁸⁻³⁰. Also as mentioned before, the electrochemical oxidation of Fe(II) on chalcopyrite was very slow in 0.2 mol dm^{-3} HCl solutions. By contrast, the homogeneous oxidation of Cu(I) with dissolved molecular oxygen is very fast in chloride media³¹. The absorption rate of oxygen gas into the aqueous phase control the oxidation rate of Cu(I)³¹. Therefore,

ferric chloride is certainly the oxidant for chalcopyrite during the initial stage of leaching but the accumulated cupric ions may take the place of the ferric leachant during the later stage of leaching. In order to examine such a possibility, the effect of the addition of cupric chloride on the mixed potential of chalcopyrite in acidic ferric chloride solution was studied. The mixed potential of a chalcopyrite specimen in 0.2 mol dm^{-3} HCl- 0.1 mol dm^{-3} FeCl_3 is controlled by cupric chloride at the concentration range above 0.01 mol dm^{-3} . It shows the slope of $44 \text{ mV decade}^{-1}$ as can be seen in Fig. 2-14. A similar result was reported by Jones and Peters⁹. Judging from the fact a concentration of cupric chloride an order of magnitude lower than that of ferric chloride is enough to control the mixed potential, it may be concluded that cupric chloride is a more reactive reagent than ferric chloride.

2.3.7 Effect of Temperature

Temperature is an important parameter of the rate determining step. Temperature dependence of chalcopyrite leaching in 0.1 mol dm^{-3} ferric chloride is shown in Fig. 2-15. It can be seen that the leaching rate increases with an increase in temperature. The data is summarized on the Arrhenius plot in Fig. 2-16. The results obtained in two series of leaching experiments using two different specimens are plotted. The apparent activation energy for both specimens was found to be 69.0 kJ mol^{-1} , thus showing a good correlation. Table 2-1 shows the activation energies for the dissolution of relatively pure chalcopyrite reported by

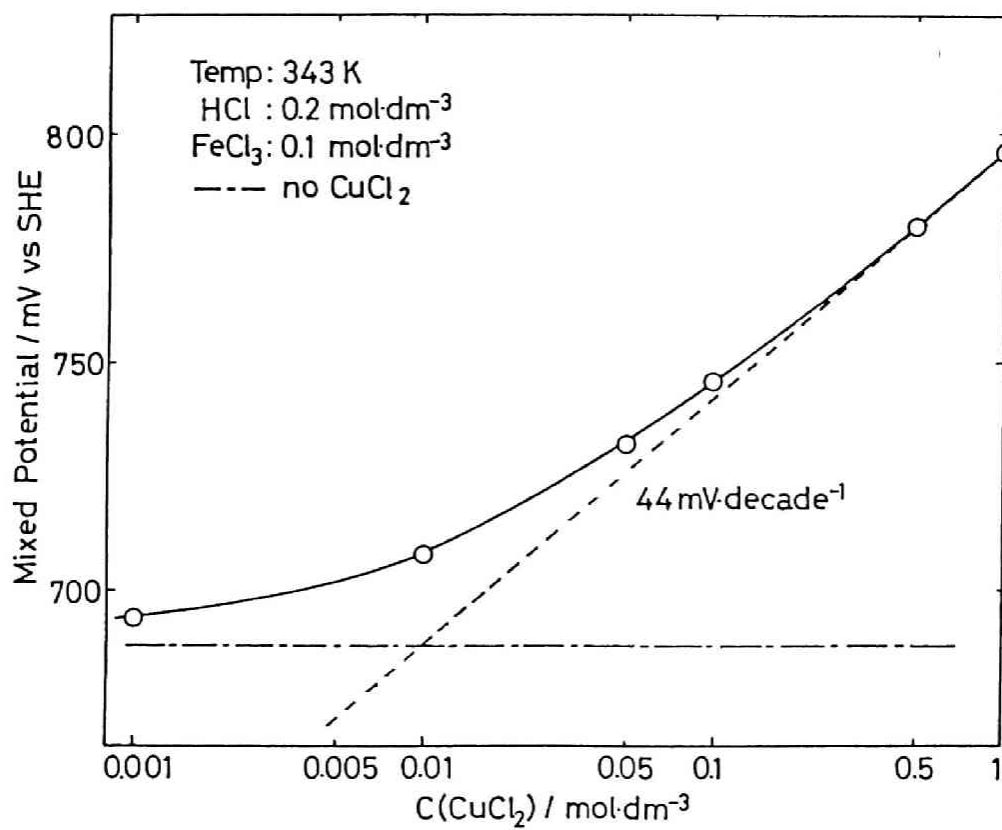


Fig. 2-14 Effect of the addition of cupric chloride on the mixed potential of chalcopyrite in acidic ferric chloride solution.

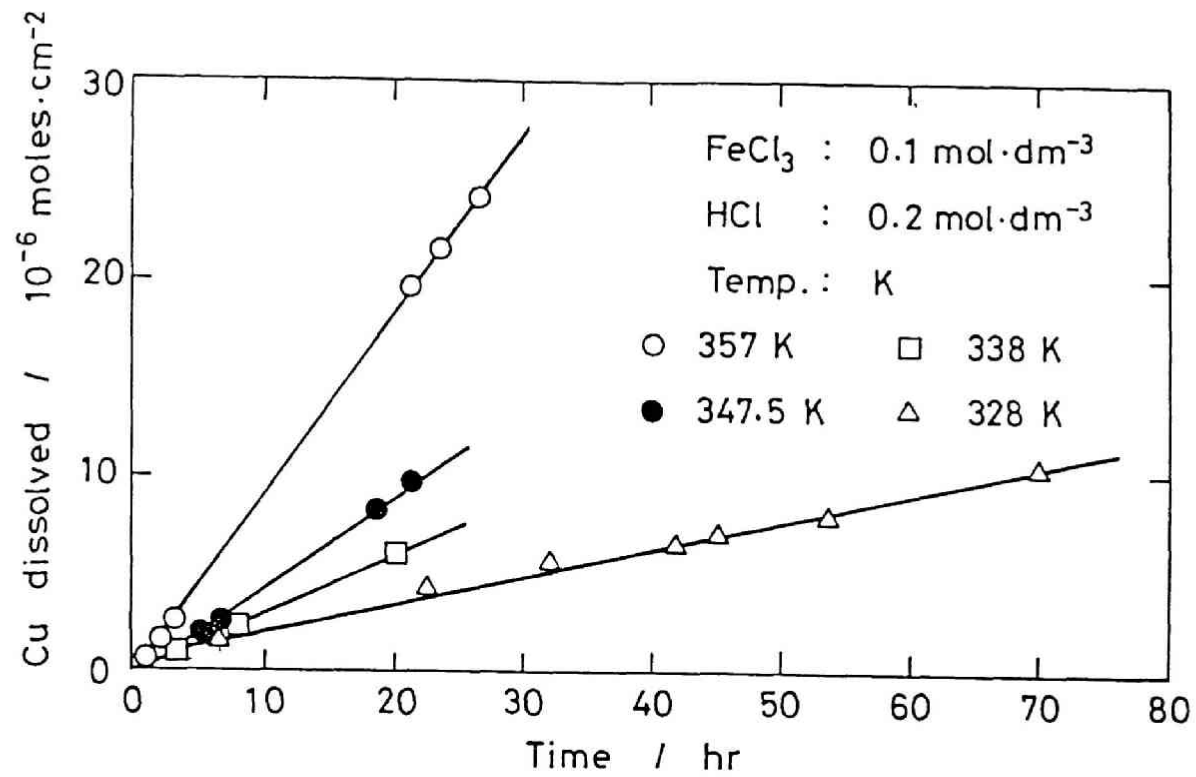


Fig. 2-15 Effect of temperature on the leaching of chalcopyrite with ferric chloride.

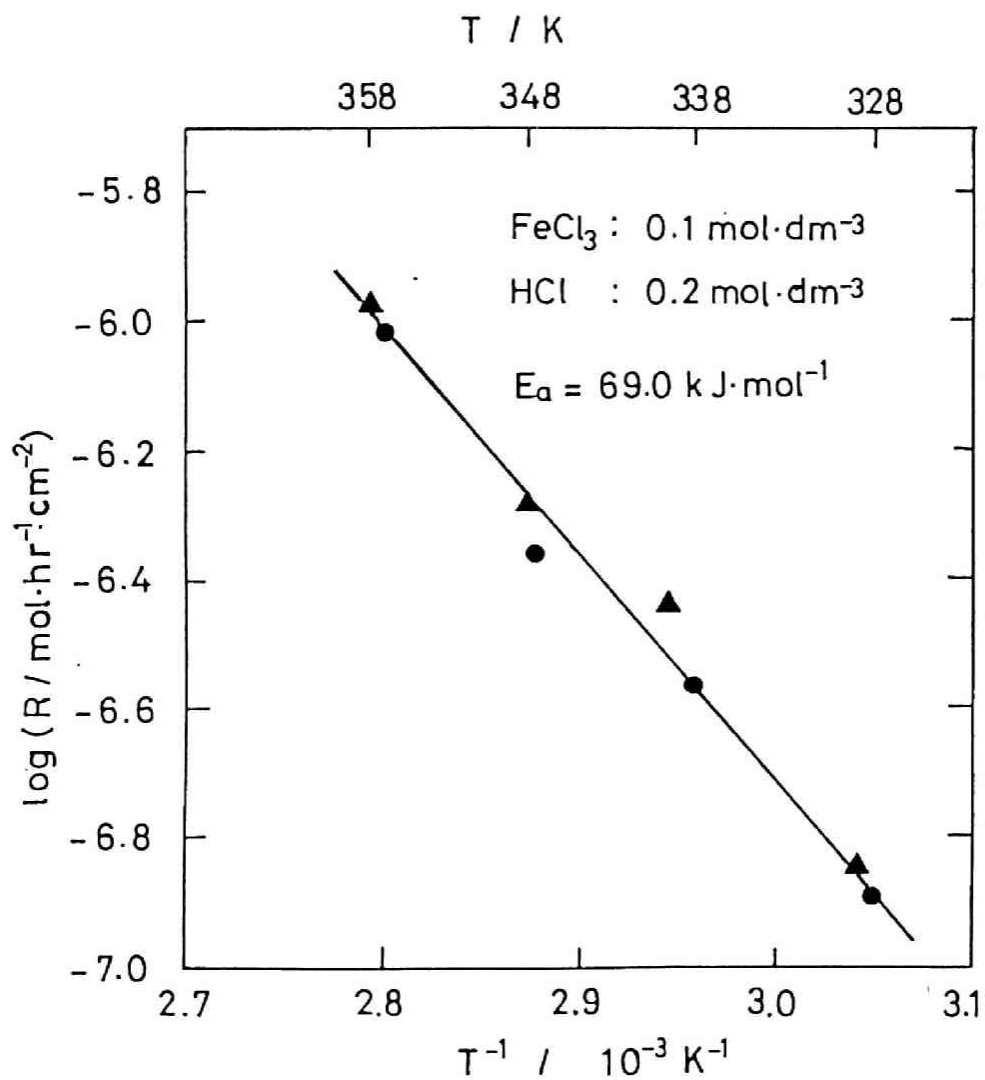


Fig. 2-16 Arrhenius plots for the leaching of chalcopyrite with ferric chloride. (Two different specimens were used.)

Table 2-1 Reported activation energies for the leaching of chalcopyrite in ferric chloride media.

Mineral	Temperature range / K	Activation Energy / kJ mol ⁻¹	Reference
Natural chalcopyrite	333-379	50	Ermilof et al. (26)
Synthetic chalcopyrite	298-348	38 ±4	Ammou-Chokroum et al. (27)
Synthetic chalcopyrite	323-373	46 ±4	Dutrizac (10)
Natural chalcopyrite	303-373	42 ±4	Dutrizac (10)
Natural chalcopyrite	313-373	63 ±8	Dutrizac (12)
Natural chalcopyrite	348-369	62	Palmer et al. (13)
Natural chalcopyrite	333-368	70	Dutrizac (14)
Natural chalcopyrite	328-358	69	Present study

various workers (part of the data shown in this table were also reported by Dutrizac¹²). It can be seen that these activation energies are highly variable. The value for leaching of chalcopyrite in ferric chloride solutions ranged from 38.0 to 62.0 kJ mol⁻¹. The activation energy of 69.0 kJ mol⁻¹ which was found in this study on a chalcopyrite crystal of museum grade, is thus compatible with the upper value of the reported range. Palmer et al.¹³ also reported an activation energy of 62.0 kJ mol⁻¹ for monosized chalcopyrite particles obtained from the Temagami mine, Ontario, Canada.

The anodic dissolution of chalcopyrite was studied potentiostatically at 706 mV vs SHE in a solution containing 0.2 mol dm⁻³ HCl and 0.3 mol dm⁻³ NaCl. Temperature dependence of the stable current density of the anodic polarization of chalcopyrite is shown in Fig. 2-17. It can be seen that the stable current density increases with an increase in temperature. The data is summarized on the Arrhenius plot in Fig. 2-18. The apparent activation energy of 59.5 kJ mol⁻¹ was obtained. These findings suggest the possibility of an electrochemical mechanism in the leaching of chalcopyrite with ferric chloride.

2.3.8 Effect of the Addition of Sodium Chloride

The effect of sodium chloride on the leaching rate was investigated by leaching a chalcopyrite specimen in 0.1 mol dm⁻³ FeCl₃ with or without the addition of sodium chloride. As shown in Fig. 2-19, the leaching rate of chalcopyrite increases with

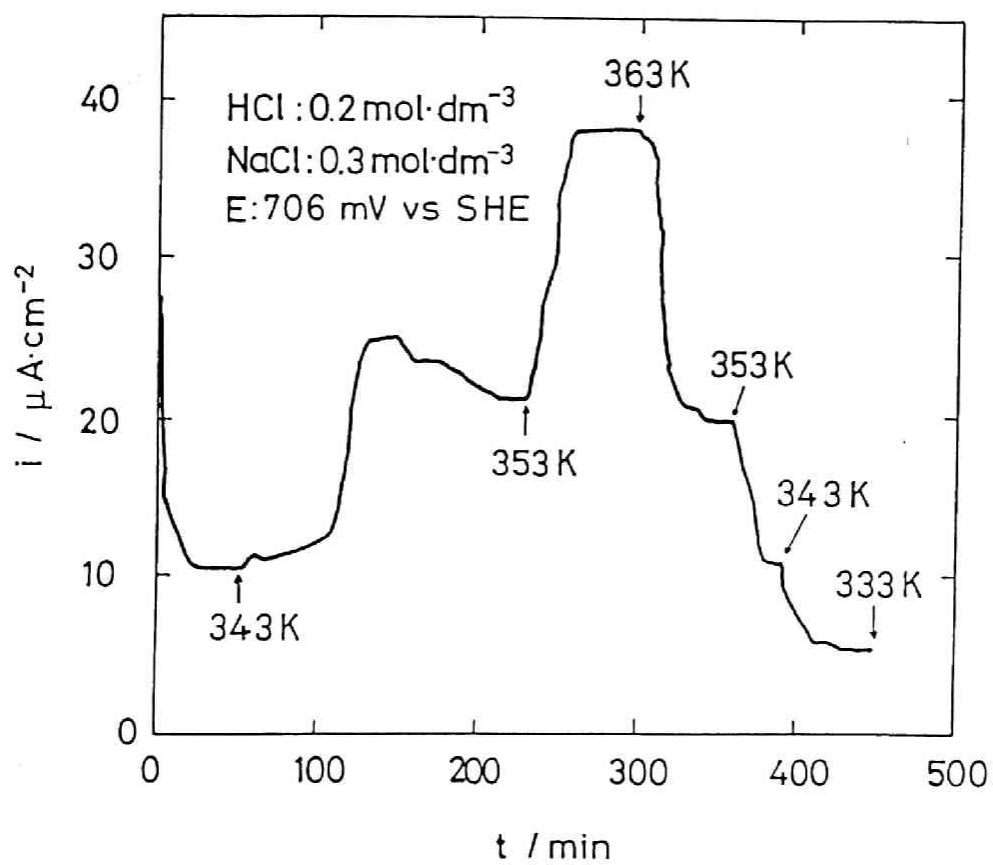


Fig. 2-17 Effect of temperature on the stable current density of the anodic polarization of chalcopyrite.

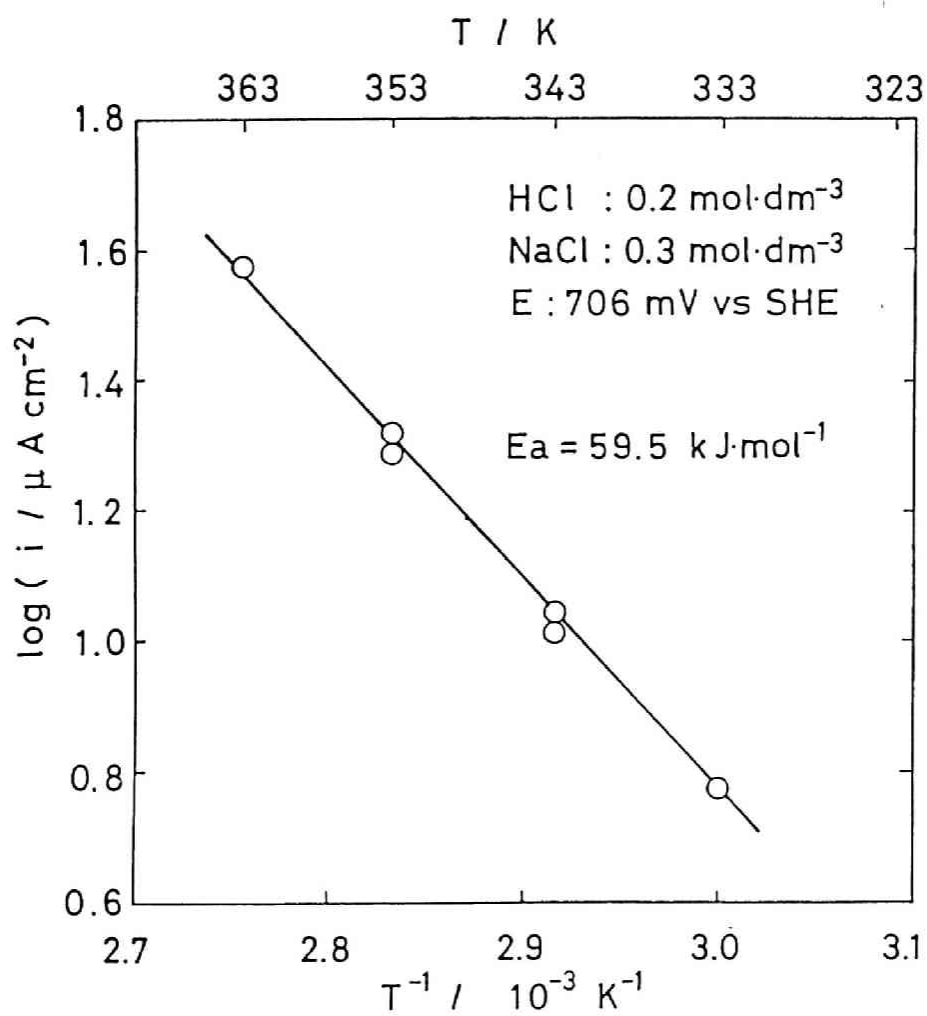


Fig. 2-18 Arrhenius plots for the stable current density of the anodic polarization of chalcopyrite.

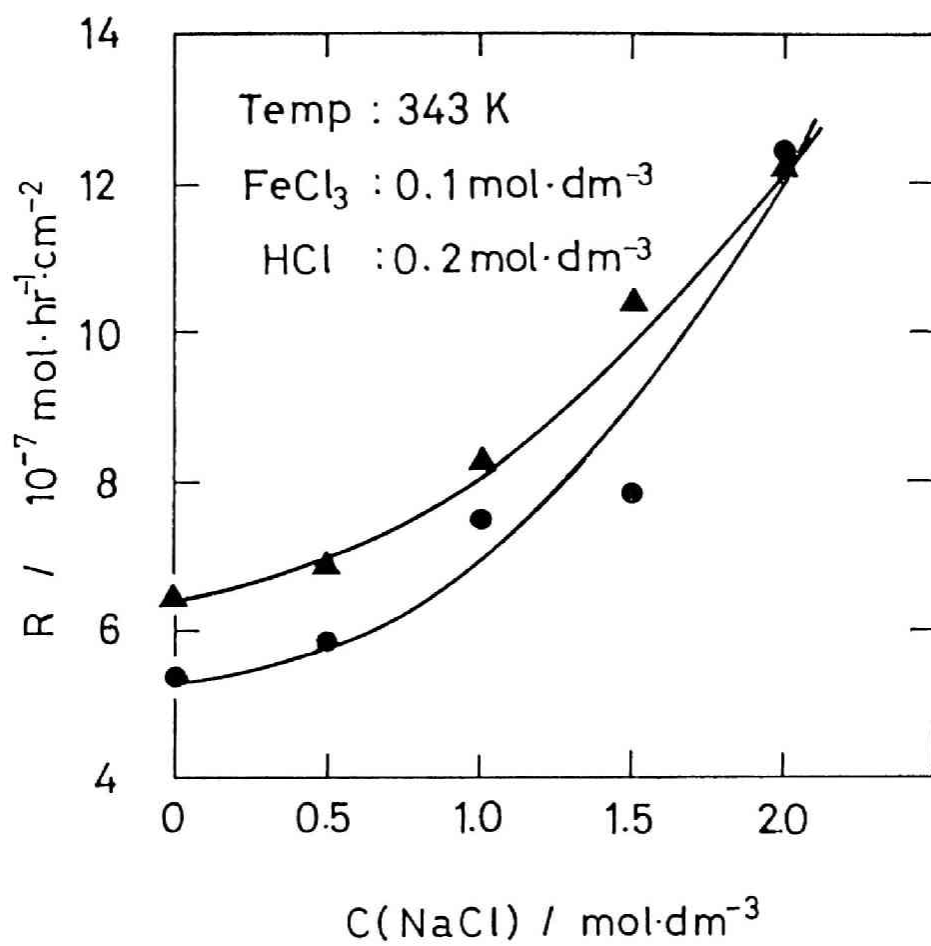


Fig. 2-19 Effect of sodium chloride concentration on the leaching rate of chalcopyrite.

an increase in the concentration of sodium chloride. When the leaching rate of chalcopyrite at 2 mol dm^{-3} NaCl was compared to that without sodium chloride, it was found that the leaching rate doubled in the presence of sodium chloride.

Meanwhile, the increase in the mixed potential of chalcopyrite due to the addition of sodium chloride to 2 mol dm^{-3} was only several millivolts as shown in Fig. 2-20, and such a potential change is insufficient to attribute to the increase in the leaching rate. This means that the role of sodium chloride in the oxidative leaching of chalcopyrite in acidic ferric chloride can not be explained by an electrochemical mechanism, leaving the possibility of other chemical mechanisms.

Dutrizac¹⁰ and Palmer et al.¹³ showed that the leaching rate of chalcopyrite increased with an increase in chloride concentration at its lower level, and that the increase in rate tended to taper off with further increases in total chloride concentration. On the other hand, Ammou-Chokroum et al.¹⁶ reported that the anodic dissolution of chalcopyrite in HCl was independent of the total chloride concentration. The results obtained in this study are very different from those reported by these researchers, suggesting a necessity for further investigation.

2.3.9 Correlation of the Leaching Rates of Chalcopyrite

Chemically Leached and Those Electrochemically Leached

Leaching rates of chalcopyrite with ferric chloride depicted in Fig. 2-8 were converted to electric current densities by

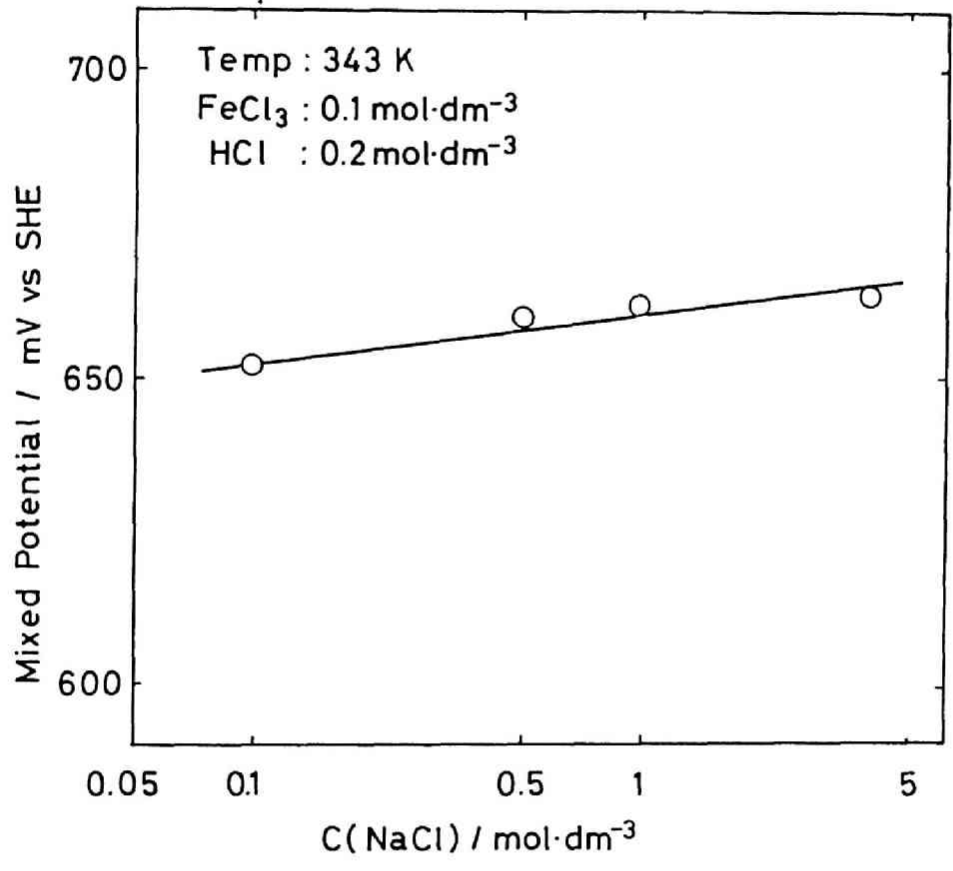
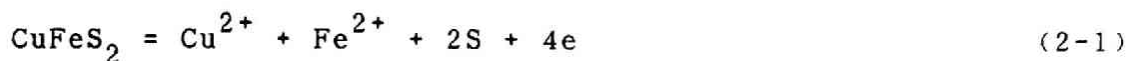


Fig. 2-20 Effect of sodium chloride concentration on the mixed potential of chalcopyrite.

assuming the following reaction:



At the same time, the mixed potentials of chalcopyrite were measured during its leaching with ferric chloride.

By plotting the mixed potential, E_M , thus determined against the logarithm of current density, straight lines as shown in Fig. 2-21 were obtained. The slopes of these straight lines were both found to be $140 \text{ mV decade}^{-1}$.

For comparison purposes, the logarithms of the anodic current density of chalcopyrite leached electrochemically are plotted against excitation voltage. The results obtained are shown comparatively in Fig. 2-21.

Apparently, a Tafel relationship does not hold in electrochemical leaching in this current-potential region. A suppressing tendency of current density at higher potential regions is shown in this figure. Also it is clearly recognized that the rate obtained in chemical leaching is always larger than that of electrochemical leaching at an identical potential.

Although the chalcopyrite specimens used in these experiments were all different, it is impossible to attribute such a large difference in the Tafel plots to the difference in specimens.

The morphological observation of the surface of chemically and electrochemically leached chalcopyrite is vital to provide a basis for understanding the differences in their leaching behaviors.

The morphology of the surface of chalcopyrite anodized in $0.2 \text{ mol dm}^{-3} \text{ HCl}$ at a constant potential of 706 mV vs SHE at 363 K

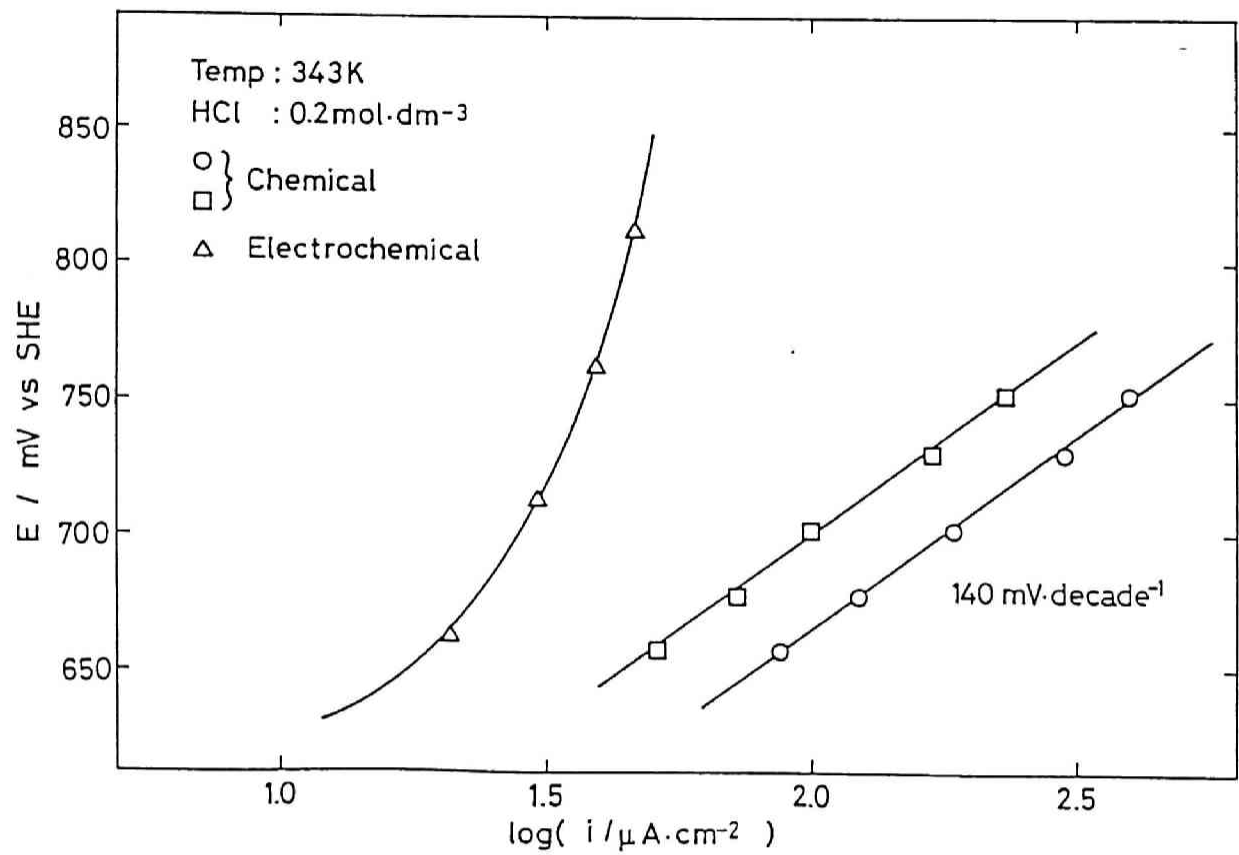


Fig. 2-21 A comparison of leaching rates of chalcopyrite with ferric chloride and those of electrochemical leaching.

for 24 hr was examined by means of SEM. The results of observation are shown in Plate 2-6. The formation of a porous layer, which was identified as elemental sulfur by X-ray analysis using an EPMA, is observable on the anodized chalcopyrite surface. Mushroom cap-like elemental sulfur having several or more pores can be detected from this photo.

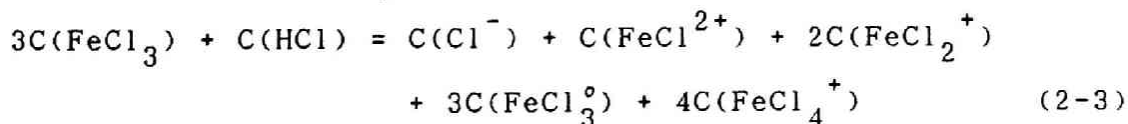
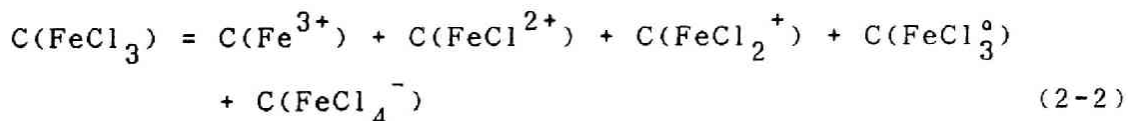
Judging from the current passed during the anodization, the conditions of Plate 2-6 should be close to those of Plate 2-2(a), the morphological appearance of these surfaces are, however, quite different.

2.4 Discussion

2.4.1 Complex Formation

Prior to discussing the experimental results obtained in this study, the formation reactions of chloro complexes of Fe(III) were examined. The formation constants of Fe(III)-chloro complexes are reported in Table 2-2³².

The mass balances on Fe(III) and chloride are



These relations are sufficient to provide a unique solution for the 6 unknowns.

By using the formation constants at 343 K determined by an interpolation method, the concentrations of complexes in 0.2 mol dm⁻³ HCl were calculated as a function of the ferric chloride



Plate 2-6 Morphology of the surface of chalcopyrite anodized in
0.2 mol dm⁻³ HCl at 706 mV SHE at 363 K for 24 hr.

Table 2-2 Formation reactions of Fe(III)-chloro complexes and their complex formation constants.³²

Reaction	Equilibrium relationship	Log of equilibrium constant		
		(323 K)	(373 K)	(423 K)
$\text{Fe}^{3+} + \text{Cl}^{-} = \text{FeCl}^{2+}$	$C(\text{FeCl}^{2+}) = k_1 C(\text{Fe}^{3+}) C(\text{Cl}^{-})$	1.96	2.94	3.98
$\text{Fe}^{3+} + 2\text{Cl}^{-} = \text{FeCl}_2^{+}$	$C(\text{FeCl}_2^{+}) = \beta_2 C(\text{Fe}^{3+}) C(\text{Cl}^{-})^2$	2.62	3.63	4.72
$\text{Fe}^{3+} + 3\text{Cl}^{-} = \text{FeCl}_3^{\circ}$	$C(\text{FeCl}_3^{\circ}) = \beta_3 C(\text{Fe}^{3+}) C(\text{Cl}^{-})^3$	1.76	3.00	4.30
$\text{Fe}^{3+} + 4\text{Cl}^{-} = \text{FeCl}_4^{-}$	$C(\text{FeCl}_4^{-}) = \beta_4 C(\text{Fe}^{3+}) C(\text{Cl}^{-})^4$	0.05	1.63	3.23

concentration. The results obtained are illustrated in Fig. 2-22. The principal chemical species in the concentration range studied in this work is FeCl_2^+ , exhibiting an approximate proportionality to the concentration of ferric chloride.

By contrast, in an aqueous solution containing excess chloride ions, it is reported that the predominant species of Fe(II) is FeCl_2 ^{33.34}.

From these findings, the main cathode reaction of Fe(III) was assumed to be



The subsequent discussion is based on this assumption.

2.4.2 Leaching Mechanism of Chalcopyrite in Ferric Chloride Solutions

As shown in Figs. 2-8 and 2-10, the leaching rate of chalcopyrite is a function of ferric chloride concentration, whereas it is independent of ferrous chloride concentration. The dependency of the leaching rate upon ferric chloride concentration appeared to be half order. In regard to this, the mixed potential of chalcopyrite exhibits 72 mV decade⁻¹ dependency upon ferric chloride concentration as shown in Fig. 2-9, while no influence on the mixed potential was observed by the addition of ferrous chloride (Fig. 2-11). Similar dependencies of the mixed potential upon the concentrations of ferric chloride and ferrous chloride were reported by Jones and Peters⁹.

Based on these observations, the following half cell reactions can be written by assuming the electrochemical mechanism of

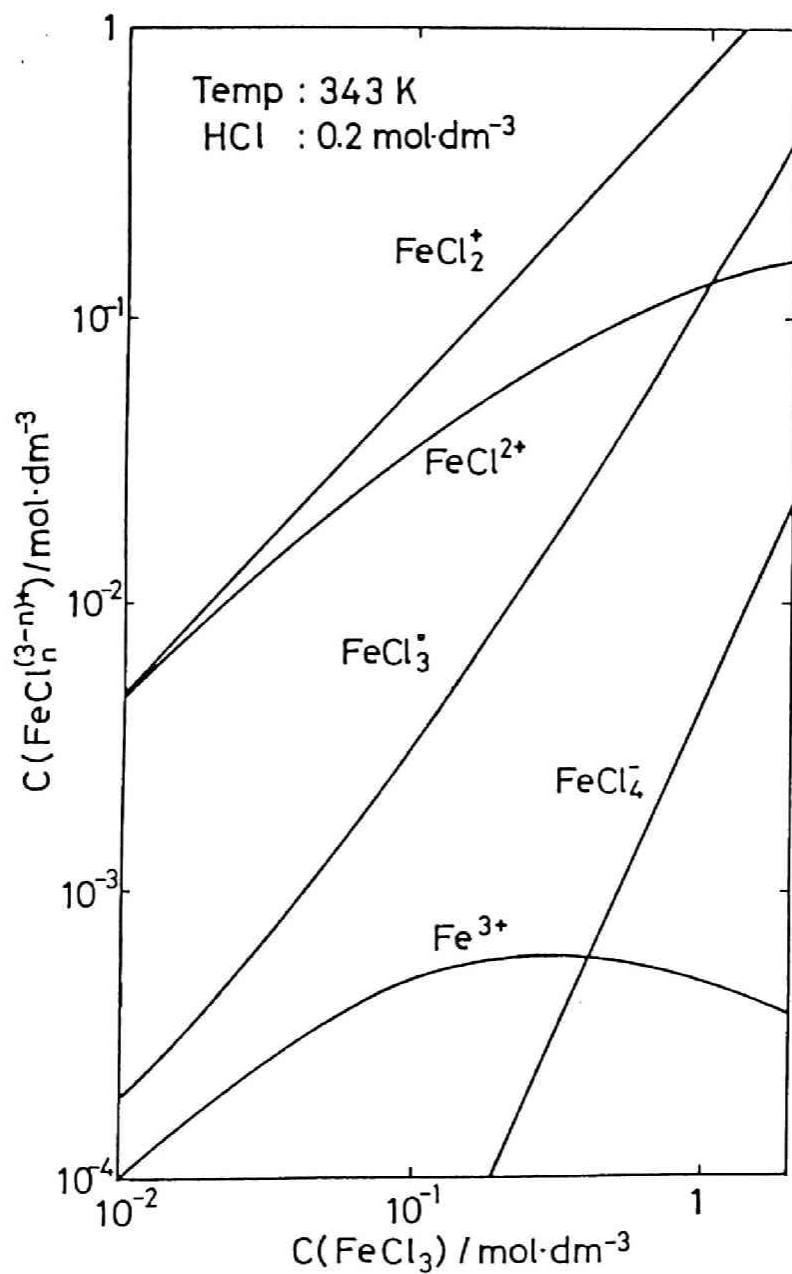
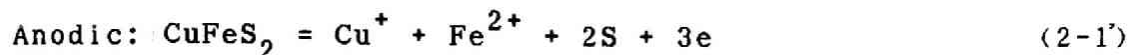


Fig. 2-22 Concentrations of Fe(III)-chloro complexes in 0.2 mol dm⁻³ HCl solutions at different ferric chloride concentrations.

chalcopyrite leaching in ferric chloride solution schematically shown in Fig. 2-23:



Although a similar combination of anodic and cathodic reactions expressed by equations (2-1') and (2-4) was proposed by Palmer et al.¹³, they assumed that the cathodic reaction of the uncomplexed, hydrated ferric ion, the first, second, and third chloro complexes of Fe(III) occur in parallel. It is more realistic to assume that the easy-to-reduce species is preferentially reduced among all species, instead of taking parallel paths. The reduced species is supplied by achieving the equilibrium conditions. For this reason, the cathodic reduction of FeCl_2^+ , which is the most predominant species, is considered. This assumption can also satisfy the requirement of the proportionality between the concentration of FeCl_2^+ and ferric chloride. By contrast, Jones and Peters⁹ assumed that the reversible reaction of the $\text{Fe}^{3+}/\text{Fe}^{2+}$ redox controls the mixed potential. However, the oxidation reaction of ferrous chloride on a chalcopyrite anode was so slow that it is difficult to consider the $\text{Fe}^{3+}/\text{Fe}^{2+}$ redox reaction for the 72 mV decade⁻¹ dependency.

Applying a Butler-Volmer equation to reactions (2-1') and (2-4), the rate equations of electrode reactions are given by equations (2-5) and (2-6).

$$i_a = 3Fk_a \exp\left(\frac{\alpha_a zF}{RT} E_a\right) \quad (2-5)$$

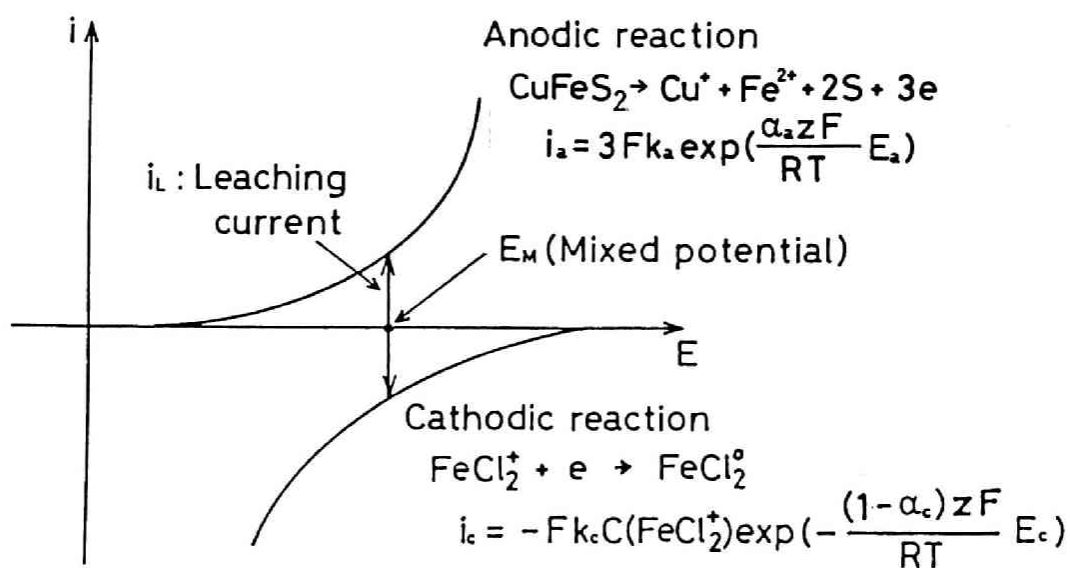


Fig. 2-23 Schematic illustration of the leaching of chalcopyrite in ferric chloride solution.

$$i_c = -Fk_c C(\text{FeCl}_2^+) \exp\left[-\frac{(1-\alpha_c)zF}{RT} E_c\right] \quad (2-6)$$

where i is current density, k is rate constant, E is potential, F is Faraday constant, α is the transfer coefficient, and z is the number of electrons transferred in the rate controlling step. Also the suffixes a and c denotes anodic and cathodic reactions, respectively.

If the overall reaction is controlled by an electrochemical step, then a one electron transfer mechanism can be considered. Thus, z is assumed to be unity. On the other hand Despic' and Bockris have demonstrated that the value of each transfer coefficient should fall in the range of 0.4 to 0.6³⁵. By taking the average of these values, the transfer coefficient was assumed to be $\alpha_a = \alpha_b = 0.5$.

The rate expression for the leaching of chalcopyrite is obtained from the electron conservation equation which necessitates that

$$i_a A_a = -i_c A_c \quad (2-7)$$

where A_a and A_c are areas of anodic site and cathodic site respectively. Additionally, since chalcopyrite is a relatively good electrical conductor, the potentials of the anodic and cathodic sites will be equal to the mixed potential, E_M .

By substituting Eqs. (2-5) and (2-6) into Eq. (2-7) Eq. (2-8) is obtained.

$$3FA_a k_a \exp\left(\frac{F}{2RT} E_M\right) = FA_c k_c C(\text{FeCl}_2^+) \exp\left(-\frac{F}{2RT} E_M\right) \quad (2-8)$$

Re-arrangement of Eq. (2-8) yields Eq. (2-9).

$$E_M = \frac{2.3RT}{F} \log C(\text{FeCl}_2^+) + \log \frac{A_c k_c}{3A_a k_a} \quad (2-9)$$

At 343 K, the following equation is obtained.

$$E_M = 0.068 \log C(\text{FeCl}_2^+) + \text{const} \quad (2-10)$$

Although the reduction of FeCl_2^+ is considered as the cathodic reaction, the concentration of FeCl_2^+ is approximately proportional to that of ferric chloride as depicted in Fig. 2-22. Therefore the concentration of ferric chloride can be replaced by that of FeCl_2^+ . Then Eq. (2-10) is rewritten as

$$E_M = 0.068 \log C(\text{FeCl}_3) + \text{const.} \quad (2-11)$$

This means that the $C(\text{FeCl}_3)$ dependency upon the mixed potential of chalcopyrite should be 68 mV decade⁻¹ as far as one electron transfer reaction is assumed. The experimental value obtained in this work was 72 mV decade⁻¹, and this value coincides well to that theoretically calculated.

The Butler-Volmer equation applied to chalcopyrite anodically dissolved at the mixed potential, E_M , is expressed as

$$i_L = 3Fk_a \exp\left(\frac{F}{2RT} E_M\right) \quad (2-12)$$

Rearranging Eq. (2-12) and inserting the numerical values for 343 K, Eq. (2-13) is obtained:

$$E_M = 0.136 \log i_L + \text{const} \quad (2-13)$$

The slope, 140 mV decade⁻¹, of the Tafel plot for the leaching of chalcopyrite in ferric chloride solution agrees well with that of the theoretically obtained, 136 mV decade⁻¹.

Jones¹⁵ obtained 130 mV decade⁻¹ by measuring the current densities of chalcopyrite anodized in 4 mol dm⁻³ KCl solution at

363 K. However, their result has no direct relation to the current results which results were deduced from the chemical leaching rate of chalcopyrite in ferric chloride solutions.

On the other hand, the substitution of Eq. (2-13) into Eq. (2-11) yields

$$0.068 \log C(\text{FeCl}_3) = 0.136 \log i_L + \text{const.} \quad (2-14)$$

Thus Eq. (2-15) is obtained:

$$\log i_L = 1/2 \log C(\text{FeCl}_3) + \text{const.} \quad (2-15)$$

This finding supports the one half order dependency of the leaching rate with ferric chloride as shown in Fig. 2-8. A similar treatment was also proposed by Palmer et al.¹³.

As depicted in Fig. 2-21, the Tafel relationship for the leaching of chalcopyrite with ferric chloride does not coincide to that of electrochemical leaching. In order to elucidate this discrepancy, some additional experiments were made. As mentioned above, the determination of the absolute leaching rate of chalcopyrite in ferric chloride solution is almost impossible as long as polished chalcopyrite specimens are used, due to the specimens' different leaching response. Therefore, the chalcopyrite leached in ferric chloride solutions containing $0.2 \text{ mol dm}^{-3} \text{ HCl}$ was subjected to electrochemical leaching in $0.2 \text{ mol dm}^{-3} \text{ HCl}$ solution without further polishing of the specimen.

The mixed potentials, E_M , and the leaching rates were determined for the chemical leaching of chalcopyrite at 343 K with ferric chloride. Then the value of i was calculated from the leaching rates. By plotting E_M against $\log i$, Fig. 2-24 was obtained. As can be seen in this figure, a linear relationship

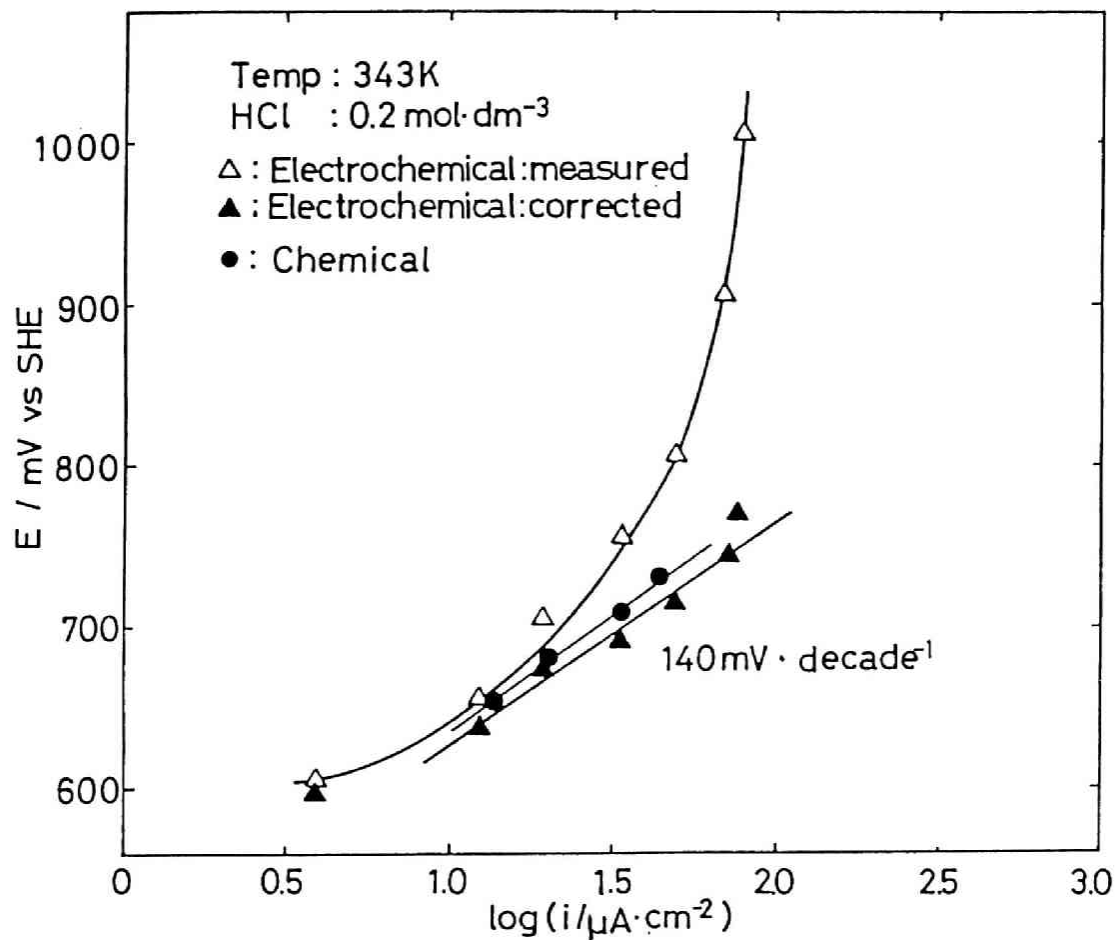


Fig. 2-24 Correlation of E-log i relationship for chemical leaching of chalcopyrite with ferric chloride and that of electrochemical leaching.

whose slope was $140 \text{ mV decade}^{-1}$ was obtained.

By contrast, the E-log i plot obtained through the anodic polarization at constant potential using the same specimen appears to be quite different from that for chemical leaching. Apparently a Tafel relationship does not hold in electrochemical leaching. A suppressing tendency of electric current was distinct in the a higher potential region. Also, it is clearly recognized that the rate obtained in chemical leaching is always larger than that of electrochemical leaching. Such a discrepancy of leaching rates may be caused either by the semiconductive property of chalcopyrite itself, intermediate semiconductive products or the insulating materials formed on the chalcopyrite surface. If a smaller voltage (due to the electric resistance of these materials) than the excitation voltage (set by a potentiostat) is actually applied on the chalcopyrite electrode, then the resultant current must be smaller than expected.

It is difficult to consider the electron or hole transfer mechanism in semiconductive materials, however, because a large current can flow when cuprous chloride is electrochemically oxidized on the chalcopyrite surface. Also, it is observed that a large current can flow during the anodization of chalcopyrite at higher potentials.

By considering these facts, the following equation may be obtained.

$$E_X - IR = a + b \log i \quad (2-16)$$

where E_X is the excitation voltage and R is the electric

resistance. In order to determine the value of R , a method similar to the current interrupter method was used.

Chalcopyrite was anodized at a constant potential until a stable current was obtained. Then the excitation voltage was cut off to measure the electrode potential afterwards. By so doing, a potential-time curve as schematically shown in Fig. 2-25 was obtained.

A linearly sharp decrease in potential at the instance of cut off of excitation voltage was observed, followed by a gradual decrease in mixed potential.

Assuming such a sharp drop of potential, ΔE , is caused by the electric resistance of the products on the chalcopyrite surface, the electric resistance, determined from the values of ΔE and stable currents, was found to be $2.1 \text{ k} \Omega \text{ cm}^2$.

The values of $(E_X - \Delta E)$ were plotted against $\log i$, and the results are depicted in Fig. 2-24. As shown in this figure, a straight line whose slope is $140 \text{ mV decade}^{-1}$ was obtained. This slope agreed well with that of chemical leaching. Not only the slopes, but also the positions of these straight lines coincide well with each other.

Compared to such a large resistance of the oxidation products on the chalcopyrite surface, that of the test solution was determined to be about $10 \Omega \text{ cm}$, and those of the chalcopyrite specimens used in the present study were always less than 100Ω .

It should be noted that a stable current is obtainable by an anodization of chalcopyrite, suggesting that a surface product was formed on the chalcopyrite by prolonged anodization but its

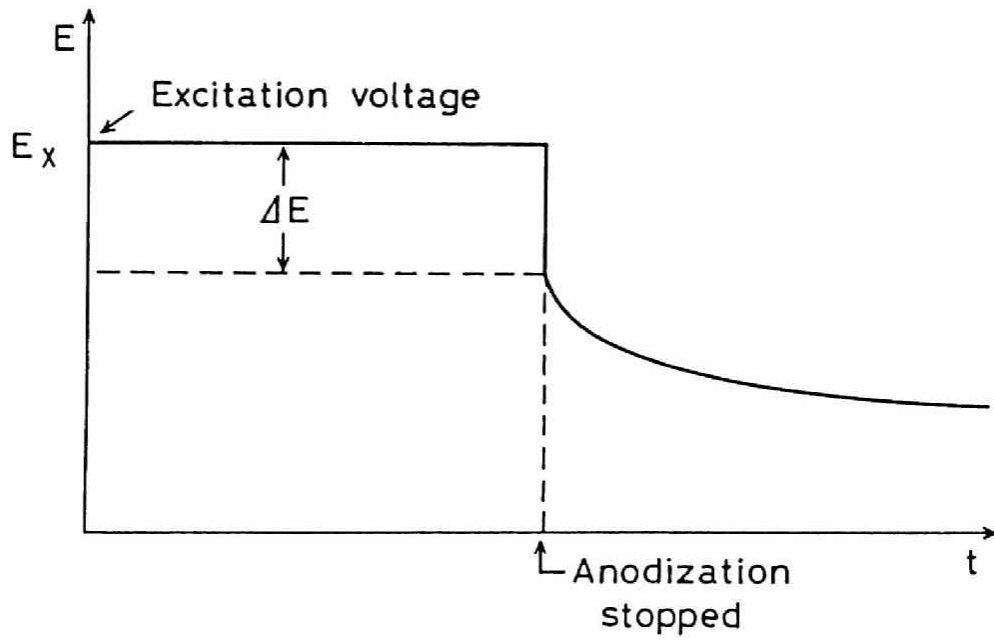


Fig. 2-25 Schematic illustration of current interrupter experiment of chalcopyrite.

amount was almost constant. The resistance of the surface product showed a decay tendency at the cut off of the excitation voltage. Furthermore, the recovery of resistivity was found to be very fast by the re-excitation of the voltage.

It is difficult to conclude at this stage what kind of products on the surface of chalcopyrite play this role, although the distinct difference can be observed between the morphology of the surfaces leached chemically and electrochemically as seen in Plate 2-5.

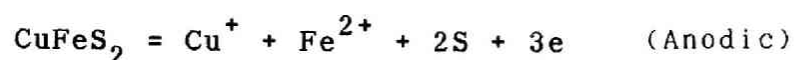
From these findings it is concluded that the leaching of chalcopyrite in ferric chloride solution is controlled by an electrochemical mechanism, showing satisfactory agreement between chemical and electrochemical leaching behavior.

2.5 Conclusions

The leaching of natural chalcopyrite crystal with ferric chloride or ferric sulfate was studied kinetically. The morphology of the leached chalcopyrite was also investigated. A comparative study of electrochemical leaching and chemical leaching of chalcopyrite was done to elucidate the leaching mechanism of chalcopyrite in ferric chloride media. The principal conclusions obtained are as follows:

1. The elemental sulfur layer formed on the chalcopyrite surface after leaching in a ferric chloride solution is porous and not a barrier to further leaching.
2. Ferric chloride is a more reactive leachant than ferric sulfate for chalcopyrite.

3. The leaching rate of several chalcopyrite specimens varied significantly, even though the chalcopyrite crystals originated from the same deposit of the same mine. The leaching rate cannot be reproduced if repeat leaching tests utilize the same specimen which is polished by Emery paper prior to each experiment. A new method has been developed to obtain reliable kinetic data.
4. The leaching rate of chalcopyrite was of a half order with respect to ferric chloride concentration.
5. The effect of ferrous chloride on the leaching of chalcopyrite in a ferric chloride solution was found to be almost insignificant.
6. The leaching rate of chalcopyrite increases with an increase in sodium chloride concentration.
7. The apparent activation energies for the ferric chloride leaching of chalcopyrite and for the electrochemical leaching were found to be 69.0 kJ mol^{-1} and 59.5 kJ mol^{-1} , respectively. This similarity of the values of activation energy suggests that the leaching of chalcopyrite in a ferric chloride solution should be chemically controlled.
8. The mixed potential of chalcopyrite in ferric chloride solution is determined by a combination of the following anodic and cathodic reactions:



The dependency of the mixed potential upon ferric chloride concentration was found to be $72 \text{ mV decade}^{-1}$ at 343 K, showing a

satisfactory agreement with the theoretical value.

9. By displaying the leaching rates of chalcopyrite in ferric chloride on a Tafel plot, a straight line, whose slope was $140 \text{ mV decade}^{-1}$ was obtained. This finding suggests that the leaching kinetics are controlled by a one electron transfer mechanism.

10. The dependency of E upon $\log i$ for chemical leaching of chalcopyrite in ferric chloride well agrees with that for electrochemical leaching. This finding strongly supports the electrochemical mechanism of ferric chloride leaching of chalcopyrite.

11. Cupric chloride, the resultant product of leaching, may play an important role in the later stages of leaching as an oxidizing agent, since cupric chloride is thought to be a more reactive reagent than ferric chloride.

References

1. H. Majima, Y. Awakura, T. Hirato and T. Tanaka: *Can. Metall. Quart.*, 1985, vol. 24, p. 283.
2. T. Hirato, M. Kinoshita, Y. Awakura, and H. Majima: *Metall. Trans. B*, 1986, vol. 17B, p. 19.
3. M. Ichikuni: *Bull Chem. Soc. Japan*, 1960, vol.33, p.1052; 1962, vol. 35, p. 1765.
4. S.S. Kim, and J.I. Kim: *J. Korean Inst. Met.*, 1973, vol. 11, p. 324.
5. D.R. Nagaraj and K.I. Vasu, *Electrochem. Soc. India*, 1973, vol. 22, p. 217.
6. G. Basu, P.K. Sinha, S.C. Aush, N. Dhananjayan, and V.A. Altekar: *NML J. Tech*, 1975, vol. 18, p. 29.
7. D.R. Nagaraj, S. Illangovan, T.G. Prakash, and K.I. Vasu: *J. Electrochem. Soc. India*, 1978, vol. 27, p. 11.
8. F.P. Haver and M.M. Wong: *J. Metals*, 1971, vol. 23(2), p. 25.
9. D.L. Jones and E. Peters: "Extractive Metallurgy of Copper", J.C. Yannopoulos and J.D. Agarwal, eds., AIME, New York, NY, 1976, vol. 2, p. 633.
10. J.E. Dutrizac: *Metall. Trans. B*, 1978, vol. 9B, p. 431.
11. E. Peters, C.M. Swinkels and A. Vizsolyi: *Process and Fundamental Considerations of Selected Hydrometallurgical System*. M.C. Kuhn eds AIME, New York, NY, 1981, p. 71.
12. J.E. Dutrizac: *Metall. Trans. B.*, 1981, vol. 12B, p. 371.
13. B.R. Palmer, C.O. Nebo, M.F. Rau and M.C. Fuerstenau: *Metall. Trans. B*, 1981, vol. 12B, p. 595.

14. J.E. Dutrizac: *Metall. Trans. B*, 1982, vol. 13B, p. 5.
15. M. Ammou-Chokroum, P.K. Sen, and F. Fouques: *Mem. Sci. Revue Metallurgie*, 1979, vol. 76, p. 333.
16. M. Ammou-Chokroum, P.K. Sen, and F. Fouques: *Proc. XIII Intern. Mineral Proc. Cong., Warsaw, Poland, 1979*, vol. 1, p. 527.
17. D.L. Jones: *Ph.D. Thesis, Univ. British Columbia, Vancouver, B.C., 1974*.
18. A.J. Parker, R.L. Paul, and G.P. Power: *Aust. J. Chem.*, 1981, vol. 34, p. 13.
19. Idem. *J. Electroanal. Chem.*, 1981, vol. 118, p. 305.
20. R.S. McMillan, D.J. MacKinnon, and J.E. Dutrizac: *J. Applied Electrochem.*, 1982, vol. 12, p. 743.
21. T. Biegler and M.D. Horne: *Proc. Electrochem. Soc. No.84-10. Cincinnati, 1984*, p. 321.
22. G.W. Warren: *Ph.D. Thesis, Univ. Utah, Salt Lake City, UT, 1978*.
23. G.W. Warren, M.E. Wadsworth, and S.M. El-Raghy: *Metall. Trans.B*, 1982, vol. 13B, p. 571.
24. G.W. Warren and M.E. Wadsworth: *Metall. Trans. B*, 1984, vol. 15B, p. 289.
25. M.E. Wadsworth: *Proceedings of Copper '84, Quebec, CIM, 1984*.
26. V.V. Ermilov, O.B. Tkachenko and A.L. Tseft: *Inst. Met., Obogashch, Alma Acta, 1969*, vol. 30, p. 3.
27. M. Ammou-Chokroum, M. Cambozoglou and D. Steinmetz, *Bull. Soc. Mineral. Cristallogr.*, 1977, vol. 100, p. 149.
28. M. Iwai, H. Majima and Izaki: *Denki Kagaku*, 1979, vol. 47, p. 409.

29. M.Iwai and H.Majima: *Denki Kagaku*, 1979, vol. 47, p.717.
30. H.Majima, M.Iwai, and Y.Awakura: paper presented to Zenkoku Chikashigen Kankeigakukai Shunki Taikai, Section M Autoxidation, Kyoto, 1979.
31. Y. Awakura, M. Iwai, K. Nabeoka, and H. Majima: *Denki Kagaku*, 1980, vol. 48, p. 104.
32. "Stability Constants of Metal-Ion Complexes, Part A - Inorganic Ligands", p. 209, IUPAC Chemical Data Series No. 21, Pergamon Press, New York, 1982.
33. J.P. Wilson and W.W. Fisher: *J. Metals*, 1981, vol. 33(2), p. 52.
34. R.T. Kimura, P.A. Haunschild, and K.C. Liddell: *Metall. Trans. B*, 1984, Vol. 15B, P. 213.
35. A.R. Despic' and J.O'M. Bockris: *J. Chem. Phys.*, 1960, vol. 32, p. 389.

Chapter 3

The Leaching of Chalcopyrite with Cupric Chloride¹

3.1 Introduction

Cupric chloride is used as a leachant of chalcopyrite in the CLEAR process². As reported by Jones and Peters³, cupric chloride is a more reactive oxidant than ferric chloride for chalcopyrite leaching. Also, it was pointed out in Chapter 2 that the cupric chloride accumulated during the leaching of chalcopyrite concentrate with ferric chloride may play an important role in the later stage of leaching.

Many researchers have studied the leaching of chalcopyrite in acidic cupric chloride solutions. Some of them postulated that the leaching occurs electrochemically. Papers reported by Bonan et al.⁴ and Wilson and Fisher⁵ are typical examples, although no direct experimental support has been provided for an electrochemical mechanism of chalcopyrite leaching in the acidic cupric chloride solution. Also only a limited amount of knowledge about the morphological aspect of chalcopyrite leaching is available.

To obtain a fuller understanding of the mechanism of chalcopyrite leaching, chalcopyrite leaching was examined chemically, electrochemically and morphologically. The correlation between the chemical leaching of chalcopyrite in acidic cupric chloride solutions and the electrochemical leaching of chalcopyrite in acidic chloride media was examined to test the appropriateness of the electrochemical mechanism proposed by previous researchers.

3.2 Experimental Procedures

3.2.1 Sample and Chemicals

Chalcopyrite crystals of museum grade supplied from Shakanai Mine, Akita prefecture, Japan, were used in leaching experiments in this work. Their copper, iron, and sulfur contents were 34.8 %, 30.4 %, and 34.8 %, respectively. The mineral crystals were not associated with any gangue minerals and the purity of the specimens appeared to be good. Disk specimen was prepared by cementing a chalcopyrite crystal in an epoxy resin such that one surface ($0.3-0.5 \text{ cm}^2$) was exposed to the leaching solution. Moreover, electrical contact was made by soldering copper wire with silver paste on the rear face of each specimen for electrochemical measurements. After fine wet grinding with Emery paper, the specimen was subjected to experiments. The exposed surface area was measured prior to each experiment by using a planimeter on an enlarged photograph.

Deionized water whose specific resistivity was $5 \times 10^6 \Omega \text{ cm}$ and reagent grade chemicals were used to prepare all electrolyte solutions.

3.2.2 Leaching Experiments

A 0.5 dm^3 glass separable flask with a fitted lid having five necks was used as a reaction vessel for all leaching experiments. The centre hole of the lid was used for the accommodation of a rod holding a disk specimen of chalcopyrite. The other four necks were used for the introduction and discharge of nitrogen gas, the accommodation of a thermometer, and the accommodation of a sampling tube, respectively. Also, a condenser was placed at

the outlet of nitrogen gas of the reaction vessel to avoid the vaporization of water from the leaching solution during the experiment. A water bath provided with a temperature controller was used as a thermostat (± 0.5 K).

A disk specimen was placed facing sideways in a leaching solution. The leaching solution was agitated by a magnetic stirrer at a constant speed of 300 r min^{-1} , and nitrogen gas was bubbled into the leaching solution throughout each experiment. Temperature of the solution ranged from 333 to 363 K and cupric chloride concentrations ranged from 0.01 to 1 mol dm^{-3} . The pH of the solution was adjusted to less than 1 by using hydrochloric acid. Aliquots of 10 cm^3 each were withdrawn from the solution at an appropriate time interval and were subjected to quantitative analysis for dissolved iron by using an atomic absorption spectrophotometer (Jarell-Ash, Type AA-1).

As mentioned in Chapter 2, the leaching rate of chalcopyrite specimen were significantly different even though the chalcopyrite crystal originated from the same deposit of the same mine. It was also observed that the same leaching rate cannot be obtained even if repeated leaching tests utilize the same specimen which is polished by automatic precise grinding wheel prior to each experiment. Therefore, a leaching technique similar to that used in Chapter 2, was employed in this study to obtain reliable kinetic data. The specimen was subjected to wet polishing with Emery paper before only first leaching and the same specimen without further polishing was used in successive leaching experiments. On the other hand, preliminary experiments showed that the dissolution of chalcopyrite with

cupric chloride proceeded at a constant rate unless the total dissolved iron from chalcopyrite was less than 1×10^{-4} moles cm^{-2} . Thus, the leaching experiments were all designed to keep the total dissolved iron to less than 1×10^{-4} moles cm^{-2} .

3.2.3 Electrochemical Measurements

To determine the mechanism of chalcopyrite leaching, three types of electrochemical experiments were performed; measurement of the mixed potential of chalcopyrite in aqueous hydrochloric acid solutions containing cupric chloride or cuprous chloride, measurement of the electrochemical dissolution rate of chalcopyrite at constant potential in acidic chloride solutions without any oxidants, and measurement of the electrochemical oxidation or reduction rate of Cu(I) or C(II) on the surface of chalcopyrite.

These electrochemical measurements were made using a typical three electrode system, consisting of the chalcopyrite working electrode, platinum counter electrode and 3.3 mol dm^{-3} KCl AgCl-Ag reference electrode, with a potentiostat (Nikko Keisoku Model DPGS-10). All potentials measured are presented with respect to the standard hydrogen electrode (SHE) instead of the 3.3 mol dm^{-3} KCl AgCl-Ag electrode.

The volume of solution used in the electrochemical measurements was 0.2 dm^3 and the cell was maintained in a thermostatted water bath to keep a constant temperature at 343 K unless otherwise stated. Agitation of solution was accomplished with a magnetic stirrer at a speed of 300 r min^{-1} , keeping the working electrode stationary. Nitrogen gas was also bubbled into the

solution during the experiment.

3.2.4 Morphological Observation

Observation of surface of chalcopyrite leached chemically was done for (1) a grain-sized crystal of chalcopyrite leached without wet fine grinding and (2) a cross-section of the chalcopyrite prepared by breaking it into two with a knife edge. In both cases, the product of the leaching reaction was observed by using a scanning electron microscope (SEM) and analysed by an electron probe micro analyser (EPMA).

3.3 Experimental Results

3.3.1 Leaching Rate Curve

Figure 3-1 illustrates the typical extent of the leaching curve of chalcopyrite with cupric chloride. The leaching curve is linear for approximately 200 hr until the amount of the dissolved iron is approximately 1×10^{-4} moles cm^{-2} , as in the case of leaching of chalcopyrite with ferric chlororide. Thereafter the leaching rate is gradually enhanced with leaching time.

3.3.2 Morphology

Plate 3-1 shows the surface and cross section of chalcopyrite specimens after 100 hr and 480 hr leaching with $1 \text{ mol dm}^{-3} \text{ CuCl}_2 - 0.2 \text{ mol dm}^{-3} \text{ HCl}$ solution at 363 K. The product formed on the surface of chalcopyrite after 480 hr leaching was identified as elemental sulfur by X-ray analysis. These micrographs clearly show that the sulfur layer is porous.

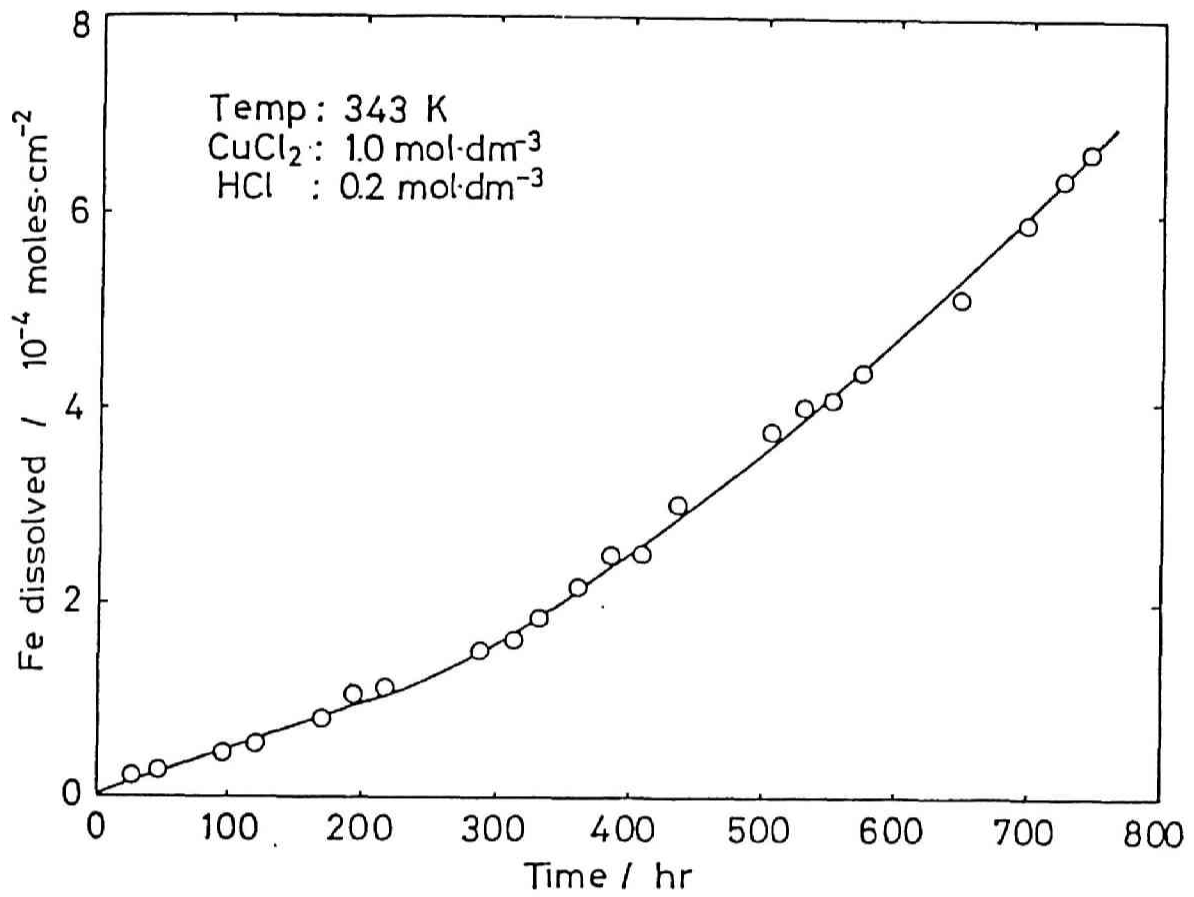


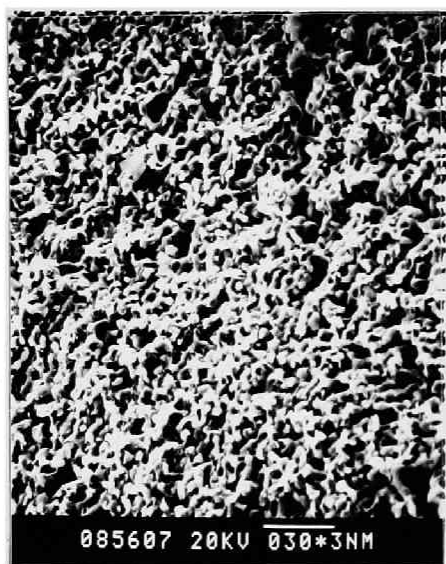
Fig. 3-1 A typical leaching curve of chalcopyrite with cupric chloride.



(100 hr)



(100 hr)



(480 hr)



(480 hr)

(a) Surface

(b) Cross Section

Plate 3-1 Surface and cross section of chalcopyrite leached with cupric chloride.

(after leaching for 100 hr and 480 hr in 1.0 mol dm^{-3} CuCl_2 - 0.2 mol dm^{-3} HCl at 363 K)

As is clear in Plate 3-1, the interface between the unreacted chalcopryrite and elemental sulfur was roughened by prolonged leaching and this finding indicates an increase in the effective reaction surface area. On the other hand, the leaching rate of chalcopryrite was accelerated by prolonged leaching, as shown in Fig. 3-1. During the leaching, only small amounts of iron and copper dissolved, so that the increased leaching rate does not reflect an autocatalytic effect. The leaching was also carried out under the condition of nitrogen gas atmosphere. Therefore, the acceleration of chalcopryrite leaching is attributable to the increase in the effective reaction surface area of chalcopryrite.

A leaching experiment was done to examine the effect of surface roughness on the leaching rate. After the leaching rate reached the final linear stage, leaching was repeated using a fresh, re-prepared leaching solution. The observed leaching rate was much greater than that in the initial linear stage, showing almost the same rate as the final stage.

3.3.3 Effect of the Concentrations of Cupric Chloride and Cuprous Chloride

(a) Leaching Rate

To examine the effect of cupric chloride concentration on chalcopryrite leaching, the successive leaching experiments were carried out at 343 K in acidic cupric chloride solutions whose concentrations were 0.1, 1.0, 0.01, 0.5, 0.2, and 0.03 mol dm⁻³, respectively. The sequence of the concentrations described above indicates the order of the leaching experiments.

Figure 3-2 illustrates the leaching curves obtained at 343 K. All the leaching curves are essentially linear and the leaching rate, R , increases with the cupric chloride concentration.

Figure 3-3 shows the relationship between $\log R$ and $\log C(\text{CuCl}_2)$. Despite the random sequence of the leaching experiment, the leaching rates lie on the same straight line. A good linear relationship was obtained over the concentration range from 0.01 to 1 mol dm⁻³, the slope of the graph being 0.54. This indicates that the leaching rate of chalcopyrite is of a half order with respect to cupric chloride concentration.

To examine the effect of the cuprous chloride concentration on the leaching rate, a series of experiments was done at 343 K in aqueous cuprous chloride solutions containing 0.1 mol dm⁻³ CuCl₂ - 0.2 mol dm⁻³ HCl - 3 mol dm⁻³ NaCl, in which the cuprous chloride concentration was changed from 0.005 to 0.1 mol dm⁻³. Since the leaching rate was found to be fairly sensitive to the chloride concentration, an excess amount of sodium chloride, 3 mol dm⁻³ NaCl was added to the leaching solutions to avoid the change of the total chloride concentration due to the addition of cuprous chloride.

Figure 3-4 shows the relationship between $\log R$ and $\log C(\text{CuCl})$. A good linear relationship was obtained over the whole concentration range studied, the slope of the graph being -0.5. This indicates that the leaching rate of chalcopyrite is inversely proportional to $C(\text{CuCl})^{0.5}$.

(b) Mixed Potential

The effect of cupric chloride concentration on the mixed

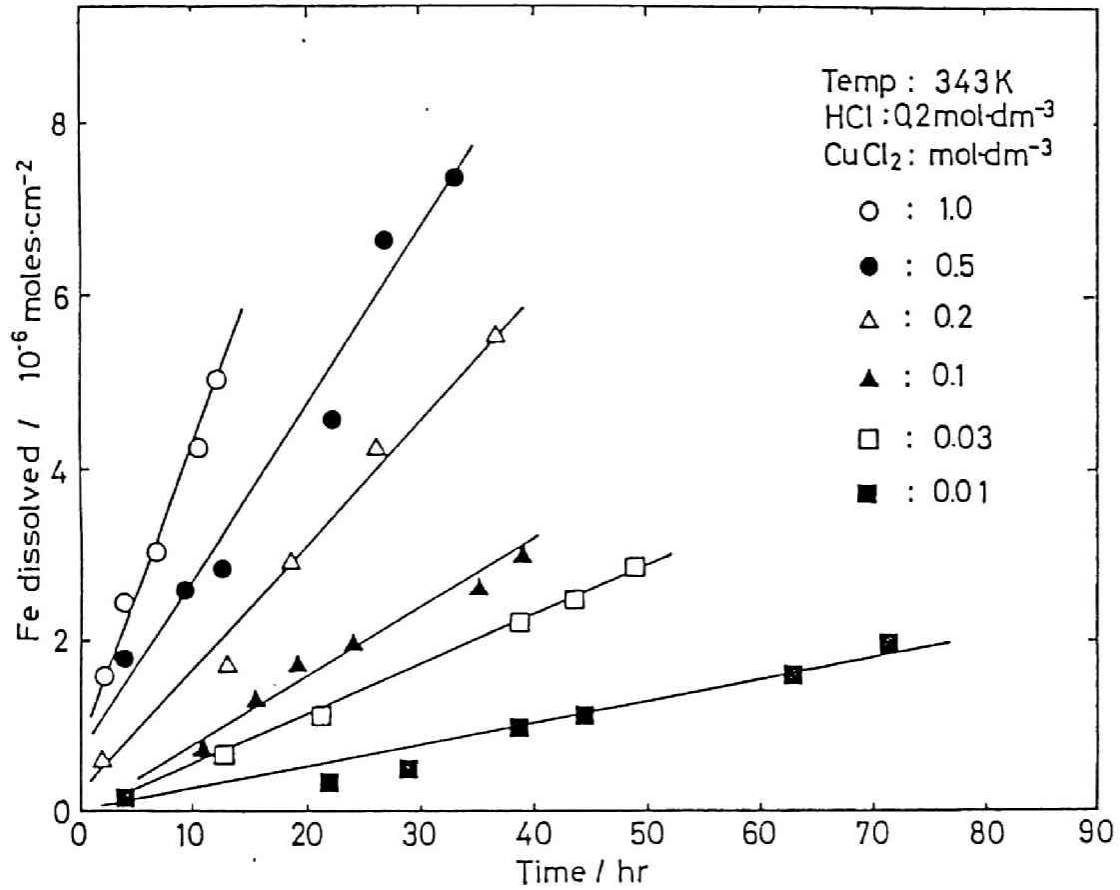


Fig. 3-2 Leaching curves of chalcopyrite with cupric chloride.

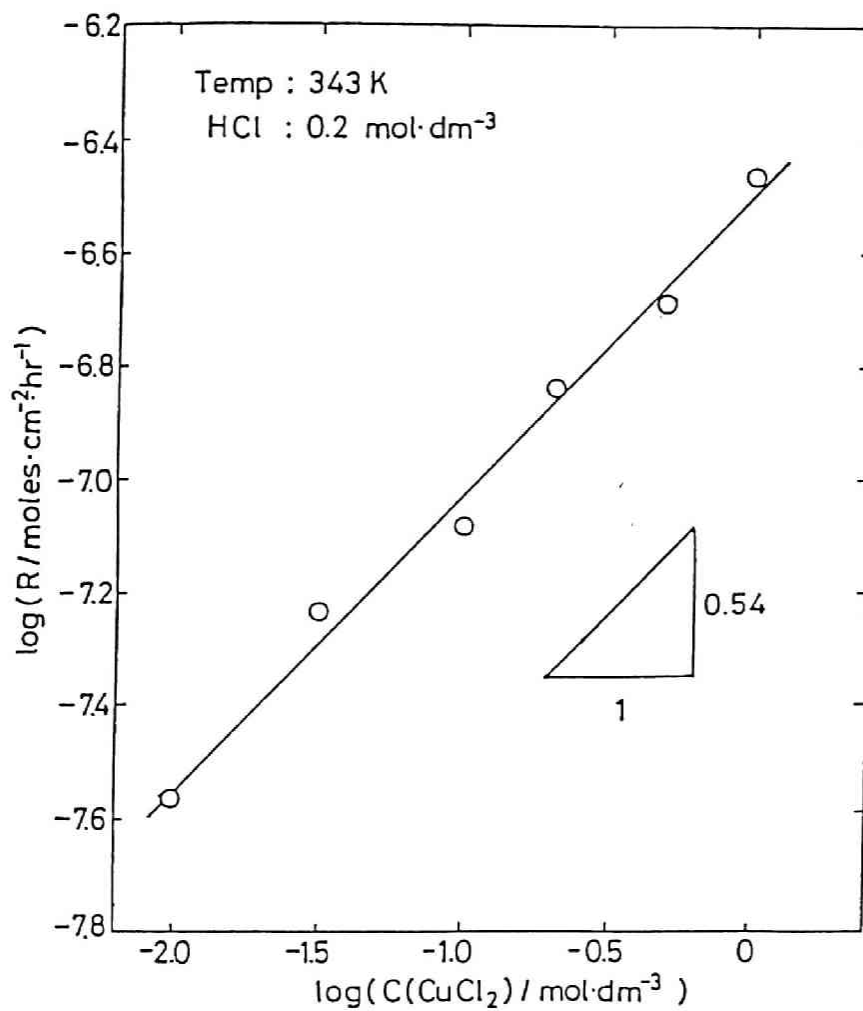


Fig. 3-3 Effect of cupric chloride concentration on the leaching rate of chalcopyrite.

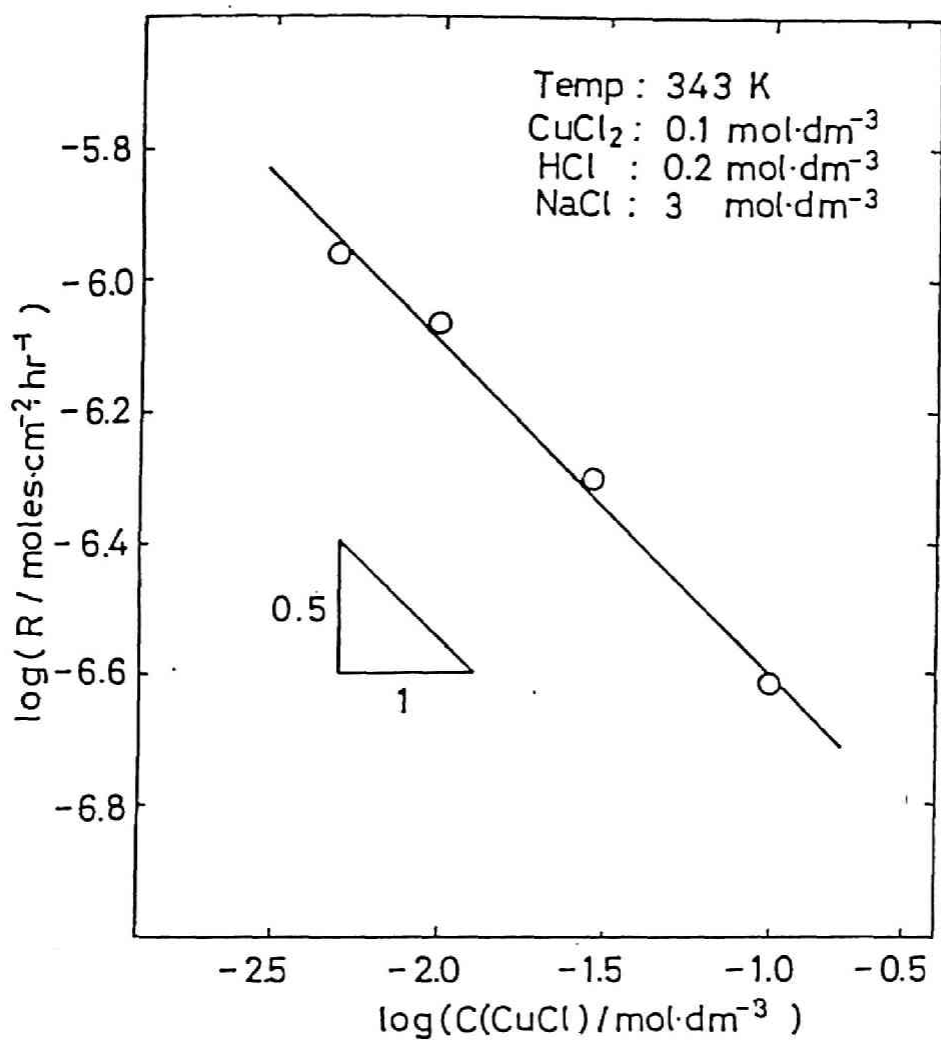


Fig. 3-4 Effect of cuprous chloride concentration on the leaching rate of chalcopyrite.

potential of chalcopyrite was examined at 343 K in 0.2 mol dm^{-3} HCl solutions containing cupric chloride whose concentrations ranged from 0.01 to 1 mol dm^{-3} . A linear relationship was obtained between the mixed potential and the concentration of cupric chloride, with a slope of $66 \text{ mV decade}^{-1}$ (Fig. 3-5).

Also the effect of cuprous chloride concentration on the mixed potential of chalcopyrite was investigated at 343 K in $0.1 \text{ mol dm}^{-3} \text{ CuCl}_2$ - $0.2 \text{ mol dm}^{-3} \text{ HCl}$ - $3 \text{ mol dm}^{-3} \text{ NaCl}$ solutions containing cuprous chloride. As is shown in Fig. 3-6, the dependency of mixed potential upon the cuprous chloride concentration was $-69 \text{ mV decade}^{-1}$. Jones and Peters³ reported similar findings. Note that cuprous chloride affects the mixed potential of chalcopyrite, while ferrous chloride had no effect on the mixed potential in acidic FeCl_3 - FeCl_2 solutions.

(c) Oxidation of Cuprous Chloride on the Surface of
Chalcopyrite Electrode

Judging from the results shown in Fig. 3-6, the oxidation of cuprous chloride may proceed rapidly on the surface of chalcopyrite. To verify such a speculation, the electrochemical oxidation of cuprous chloride on the surface of chalcopyrite electrode was studied. Figure 3-7 depicts the electric current densities measured at 343 K at the constant electrode potential of 706 mV vs SHE in $0.2 \text{ mol dm}^{-3} \text{ HCl}$ - $2 \text{ mol dm}^{-3} \text{ NaCl}$ containing cuprous chloride whose concentration was between 0 and 0.01 mol dm^{-3} . As can be seen in this figure, the current densities increased immediately after each addition of cuprous chloride to the solution, followed by almost a steady state.

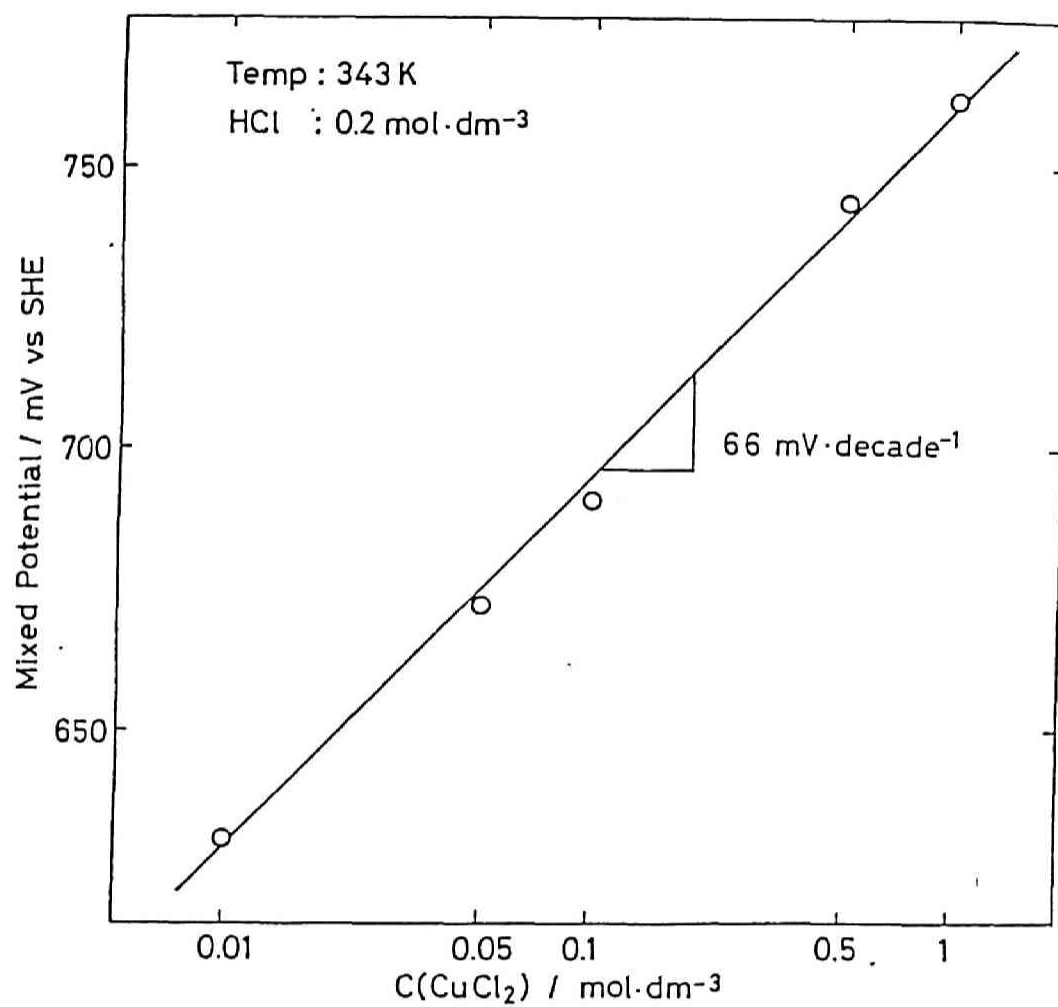


Fig. 3-5 Effect of cupric chloride concentration on the mixed potential of chalcopyrite.

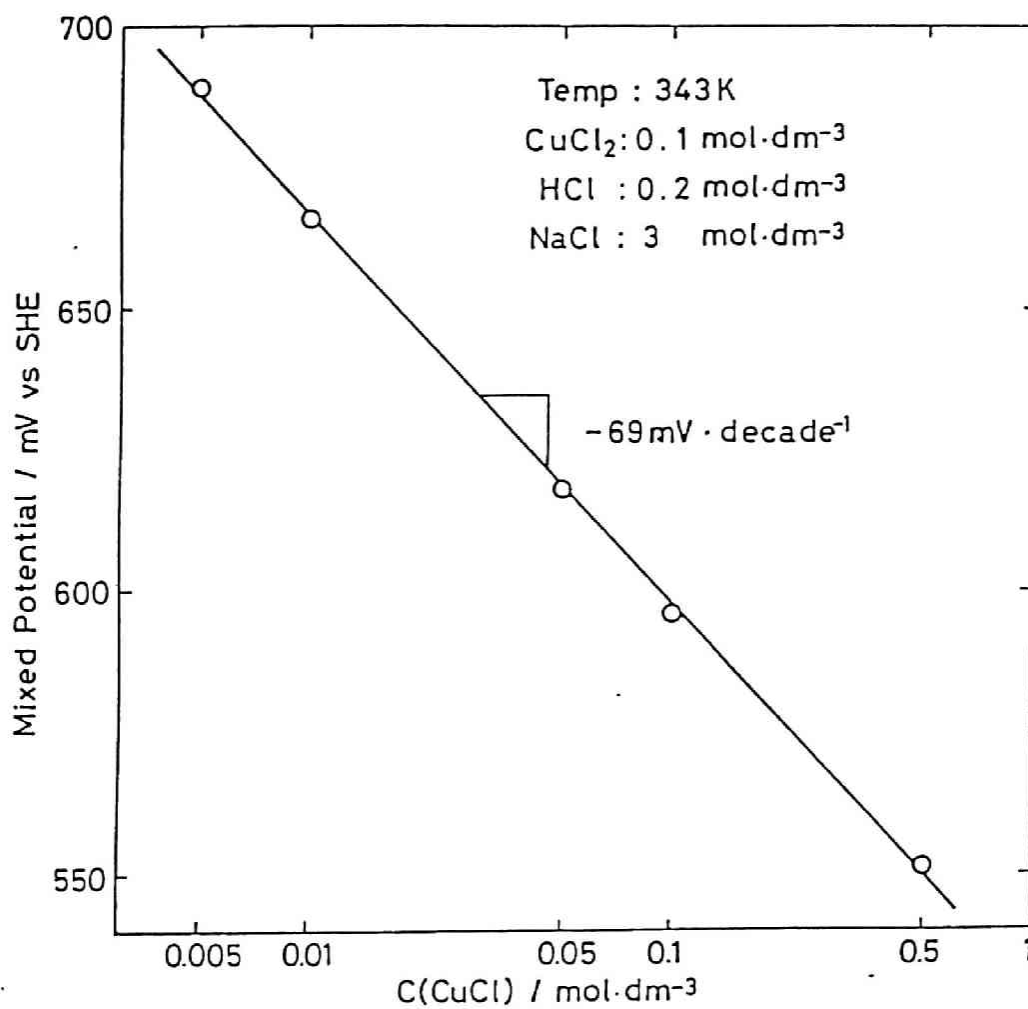


Fig. 3-6 Effect of cuprous chloride concentration on the mixed potential of chalcopyrite.

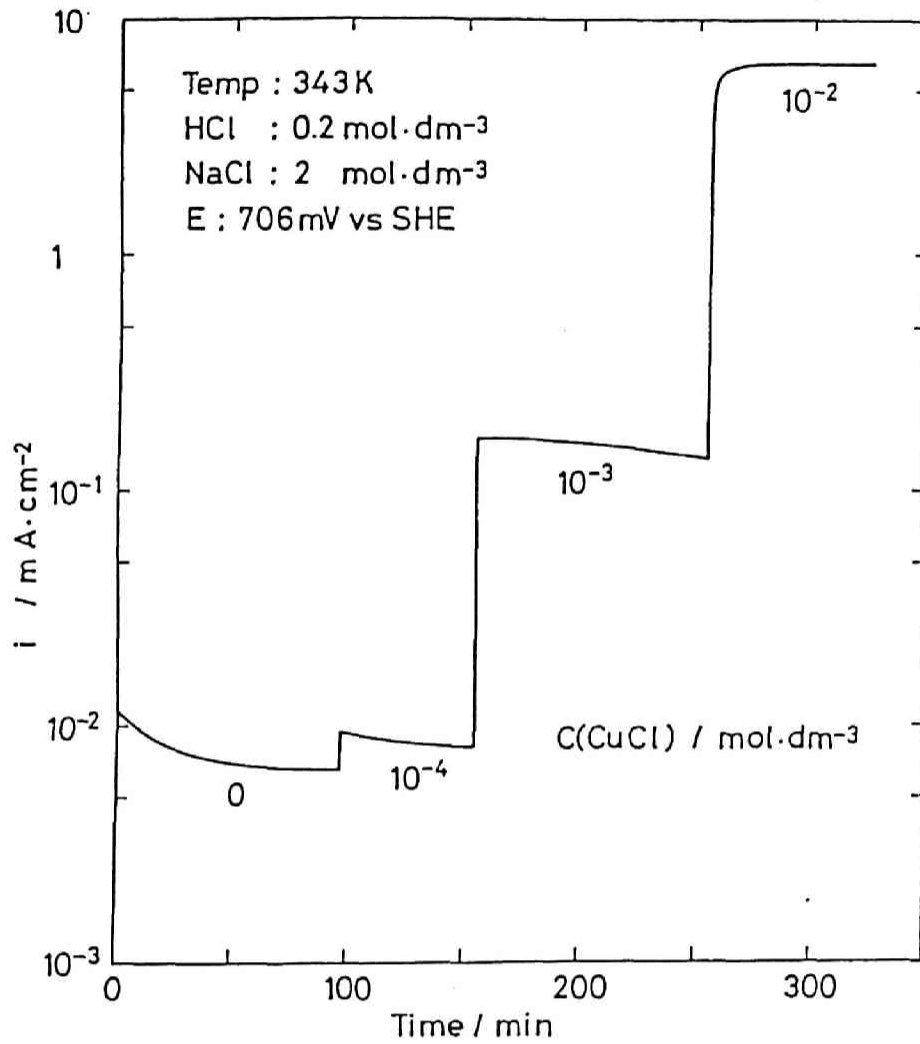


Fig. 3-7 Effect of cuprous chloride concentration on the stable current density of the anodic polarization of chalcopyrite specimen at 706 mV vs SHE.

The results shown in Fig. 3-7 tell us that a considerably large discharge can occur on the surface of chalcopyrite, and at the same time, that cuprous chloride is readily oxidized. This is very different from the oxidation behavior of Fe(II) on the surface of chalcopyrite electrode, which was mentioned in Chapter 2. A rapid oxidation of Cu(I) on the surface of chalcopyrite would cause the effect of cuprous chloride concentration on the leaching rate and the mixed potential of chalcopyrite.

3.3.4 Effect of the Concentration of Sodium Chloride

Figure 3-8 shows the effect of sodium chloride concentration on the leaching rate of chalcopyrite, when leaching experiments were made at 343 K in $0.1 \text{ mol dm}^{-3} \text{ CuCl}_2$ - $0.2 \text{ mol dm}^{-3} \text{ HCl}$ containing different amounts of sodium chloride. The leaching rate increases with an increase in the sodium chloride concentration up to 2 mol dm^{-3} , showing a declining tendency above that.

Figure 3-9 shows the effect of sodium chloride concentration on the mixed potential of chalcopyrite at 343 K. The mixed potential increases with the concentration of sodium chloride, which may be one of the reasons for the increase in leaching rates with the addition of sodium chloride. However, no quantitative correspondence can be detected between the leaching rate and mixed potential. For example, the leaching rate increased by around 4 times with the addition of $1 \text{ mol dm}^{-3} \text{ NaCl}$, while the mixed potential was increased only by 21 mV.

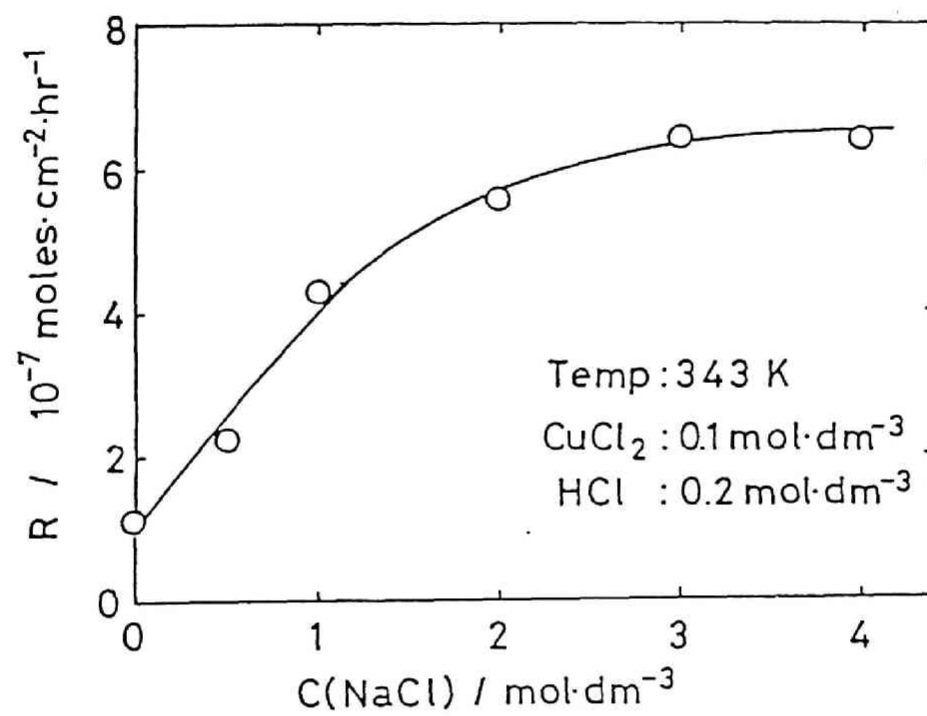


Fig. 3-8 Effect of sodium chloride concentration on the leaching rate of chalcopyrite.

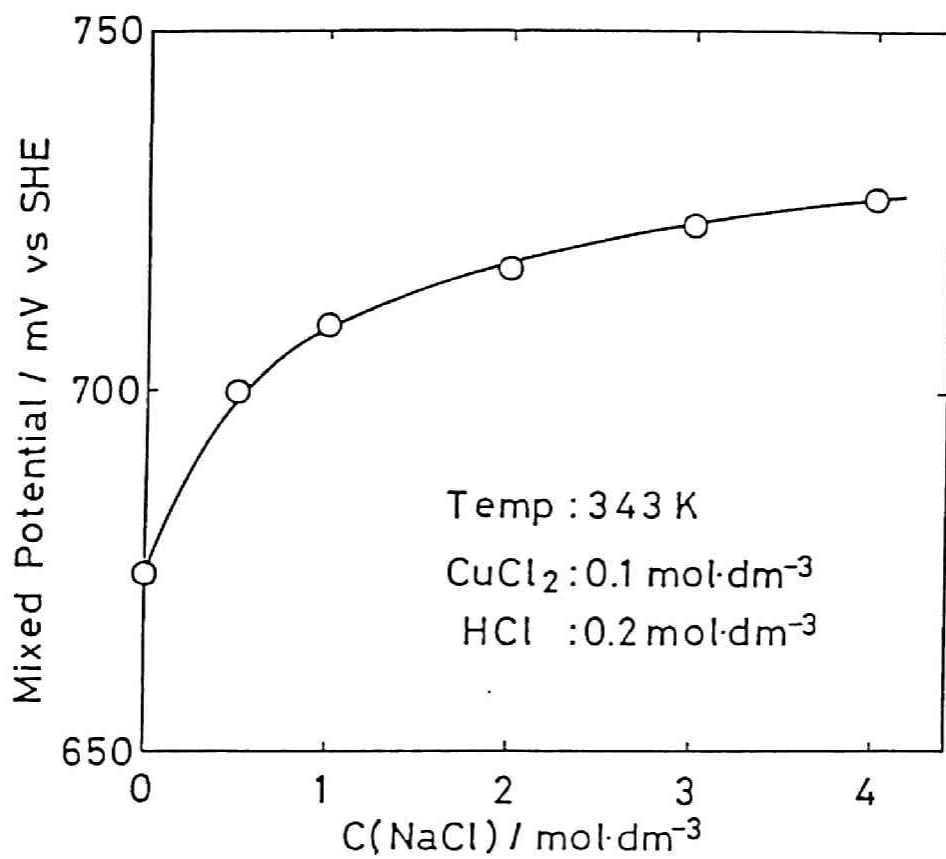


Fig. 3-9 Effect of sodium chloride concentration on the mixed potential of chalcopyrite.

3.3.5 Effect of Temperature

The leaching rates of chalcopyrite were studied in $0.1 \text{ mol dm}^{-3} \text{ CuCl}_2$ - $0.2 \text{ mol dm}^{-3} \text{ HCl}$ at different temperatures ranging from 333 to 358 K. The apparent activation energy for the chemical leaching of chalcopyrite was found to be 81.5 kJ mol^{-1} , as shown in Fig. 3-10.

Bonan et al.⁴ studied the temperature dependence of the leaching rate of chalcopyrite in $4 \text{ mol dm}^{-3} \text{ NaCl}$ solutions containing cupric chloride and cuprous chloride at a $C(\text{Cu(II)})/C(\text{Cu(I)})$ ratio of unity between 348 and 377 K and reported on activation energy of 71 kJ mol^{-1} above 358 K and 336 kJ mol^{-1} below 358 K. However, the drastic change in the activation energy within such a narrow temperature region seems rather unrealistic. On the other hand, Wilson and Fisher⁵ found that the apparent activation energy was $134.7 \text{ kJ mol}^{-1}$ above 353 K.

In this respect, the effect of temperature on the steady rate of electrochemical dissolution of chalcopyrite was studied between 333 and 363 K at a constant potential of 706 mV vs SHE in $0.2 \text{ mol dm}^{-3} \text{ HCl}$ - $0.3 \text{ mol dm}^{-3} \text{ NaCl}$ solution. The apparent activation energy was 59.5 kJ mol^{-1} .

3.4 Discussion

3.4.1 Speciation of Aqueous Solution System of $\text{HCl-CuCl}_2\text{-CuCl-NaCl}$.

Before discussing the reaction mechanism of chalcopyrite leaching based upon the experimental results obtained in this

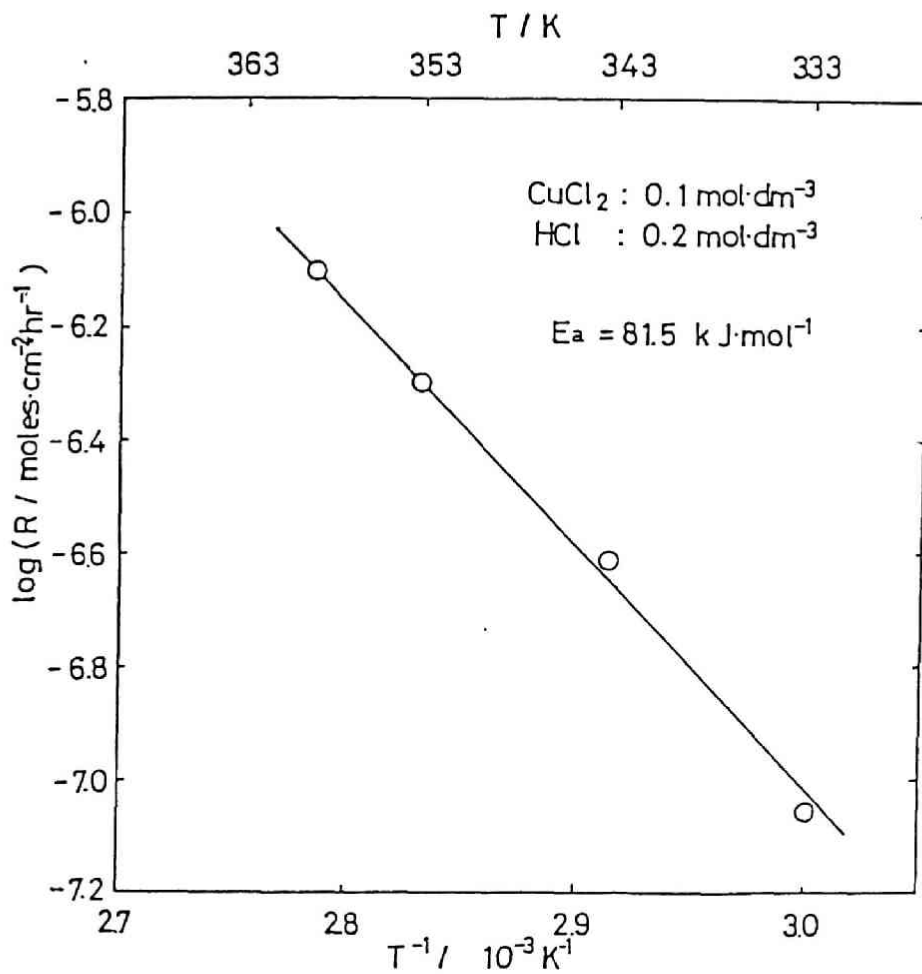


Fig. 3-10 Arrhenius plots for the leaching of chalcopyrite with cupric chloride.

work, the speciation for the aqueous solution system of HCl-CuCl₂-CuCl-NaCl was examined at 343 K. Since the amounts of Fe and Cu dissolved from chalcopyrite under the experimental conditions employed in this study were less than 1.3×10^{-2} % of the amount of cupric chloride originally present in leaching solutions, the effect of Fe and Cu dissolved were neglected in the speciation calculation.

Table 3-1 shows the equilibrium relations of Cu(II)- and Cu(I)-chloro complex formation reaction concerned with this solution system and their equilibrium constants⁶. Moreover, the mass balance equations on Cu(II), Cu(I) and chlorine are as follows:

$$C(\text{Cu(II)}) = C(\text{Cu}^{2+}) + C(\text{CuCl}^+) + C(\text{CuCl}_2^0) + C(\text{CuCl}_3^-) + C(\text{CuCl}_4^{2-}) \quad (3-1)$$

$$C(\text{Cu(I)}) = C(\text{Cu}^+) + C(\text{CuCl}_2^-) + C(\text{CuCl}_3^{2-}) \quad (3-2)$$

$$C_T(\text{Cl}) = C(\text{Cl}^-) + C(\text{CuCl}^+) + 2C(\text{CuCl}_2^0) + 3C(\text{CuCl}_3^-) + 4C(\text{CuCl}_4^{2-}) + 2C(\text{CuCl}_2^-) + 3C(\text{CuCl}_3^{2-}) \quad (3-3)$$

where $C(\text{Cu(II)})$ and $C(\text{Cu(I)})$ and $C_T(\text{Cl})$ are the total concentrations of cupric, cuprous and Cl^- in the solution, respectively.

By using these relations as well as the equilibrium relations, the concentrations of Cu(II) species in 0.2 mol dm^{-3} HCl solutions containing various amounts of cupric chloride were calculated at 343 K (Fig. 3-11). The principal chemical species in the concentration range of cupric chloride studied is CuCl^+ , whose concentration is approximately proportional to the analytical concentration of cupric chloride. Thus CuCl^+ is thought to be a reaction species in the chalcopyrite leaching.

Table 3-1 Formation reactions of Cu(II)-, Cu(I)-chloro complexes and their complex formation constants.⁶

Reaction	Equilibrium relationship	Log of equilibrium constant		
		(323 K)	(373 K)	(423 K)
$\text{Cu}^{2+} + \text{Cl}^{-} = \text{CuCl}^{+}$	$c(\text{CuCl}^{+}) = k_1 c(\text{Cu}^{2+}) c(\text{Cl}^{-})$	0.53	1.54	2.57
$\text{Cu}^{2+} + 2\text{Cl}^{-} = \text{CuCl}_2^{\circ}$	$c(\text{CuCl}_2^{\circ}) = \beta_2^{\text{II}} c(\text{Cu}^{2+}) c(\text{Cl}^{-})^2$	-0.06	1.15	2.36
$\text{Cu}^{2+} + 3\text{Cl}^{-} = \text{CuCl}_3^{-}$	$c(\text{CuCl}_3^{-}) = \beta_3^{\text{II}} c(\text{Cu}^{2+}) c(\text{Cl}^{-})^3$	-1.48	0.04	1.52
$\text{Cu}^{2+} + 4\text{Cl}^{-} = \text{CuCl}_4^{2-}$	$c(\text{CuCl}_4^{2-}) = \beta_4^{\text{II}} c(\text{Cu}^{2+}) c(\text{Cl}^{-})^4$	-3.54	-1.63	0.18
$\text{Cu}^{+} + 2\text{Cl}^{-} = \text{CuCl}_2^{-}$	$c(\text{CuCl}_2^{-}) = \beta_2^{\text{I}} c(\text{Cu}^{+}) c(\text{Cl}^{-})^2$	4.94	5.06	5.35
$\text{Cu}^{+} + 3\text{Cl}^{-} = \text{CuCl}_3^{2-}$	$c(\text{CuCl}_3^{2-}) = \beta_3^{\text{I}} c(\text{Cu}^{+}) c(\text{Cl}^{-})^3$	5.18	5.39	5.77

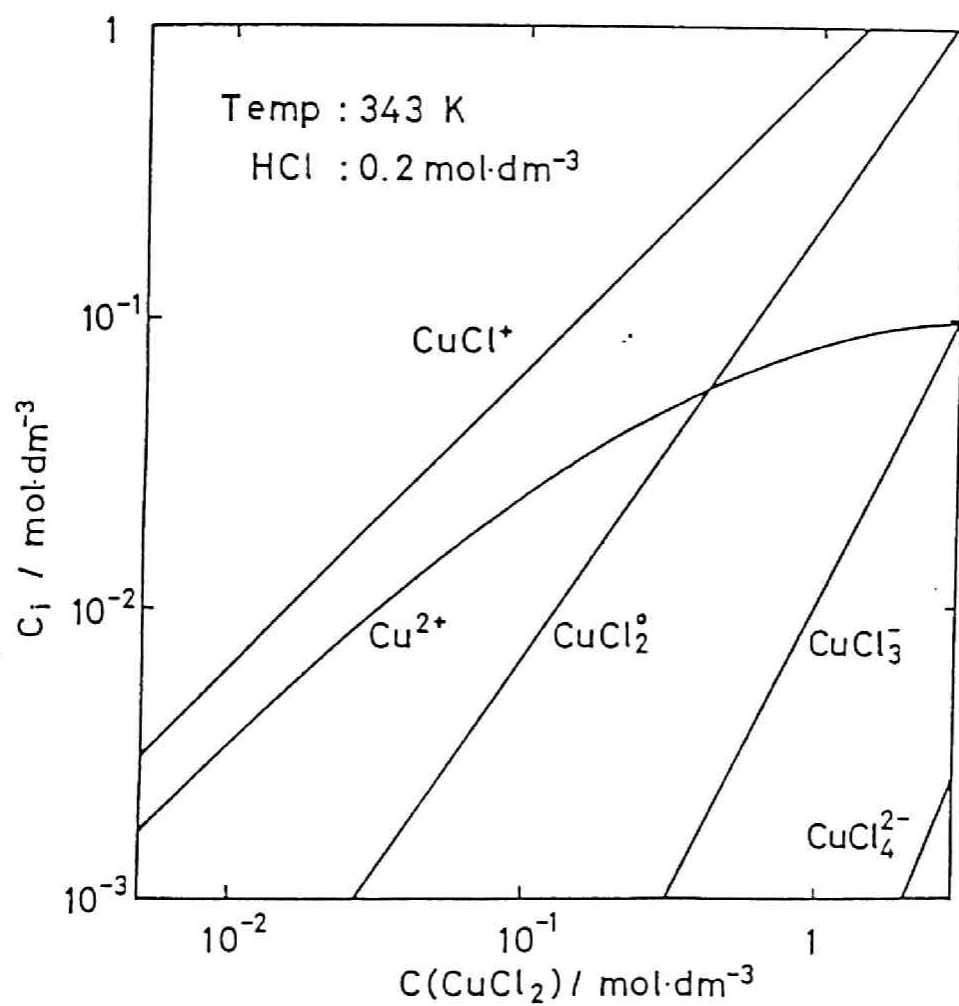


Fig. 3-11 Concentrations of Cu(II)-chloro complexes in 0.2 mol dm⁻³ HCl solutions at different cupric chloride concentrations.

The concentrations of Cu(I) and Cu(II) species in 0.1 mol dm^{-3} CuCl_2 - 0.2 mol dm^{-3} HCl - 3 mol dm^{-3} NaCl solutions containing various amounts of cuprous chloride were also calculated (Fig. 3-12). The principal chemical species of Cu(I) are CuCl_2^- and CuCl_3^{2-} , the concentrations of each being approximately proportional to the analytical concentration of cuprous chloride. A similar calculation with different concentrations of sodium chloride and a constant concentration of cuprous chloride showed that with the increase in the sodium chloride concentration, the concentration of CuCl_3^{2-} increases but the concentration of CuCl_2^- decreases.

Bonan et al.⁴ assumed that the reaction species of Cu(I) would be CuCl_3^{2-} which is the predominant cuprous species, according to Vasilev and Kunin's data⁷ for an ionic strength of 5. The author examined the effect of sodium chloride concentration on the electrochemical oxidation rate of Cu(I) on chalcopyrite and found that the oxidation rate of Cu(I) decreases with the increase in the concentration of sodium chloride. This suggests that it is more realistic to consider CuCl_2^- as a principal reaction species of Cu(I), since the speciation mentioned above shows a decrease in the concentration of CuCl_3^{2-} with an increase in sodium chloride concentration.

Thus, the main redox reaction on the chalcopyrite surface in the Cu(II)/Cu(I) system was assumed to be:



followed by the reaction (3-5)



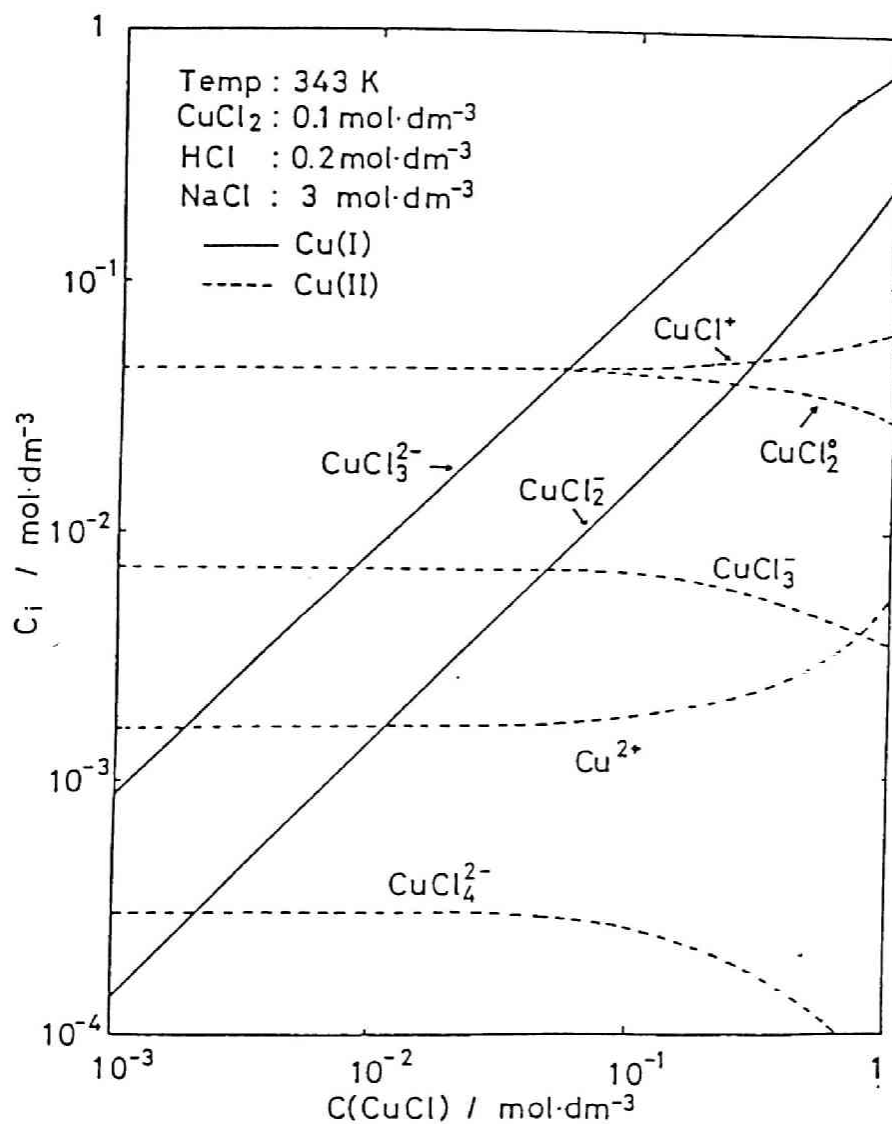
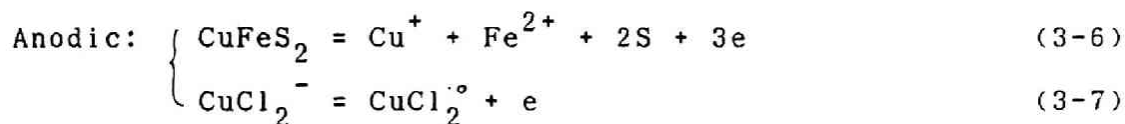


Fig. 3-12 Concentrations of Cu(I)-chloro complexes in 0.1 mol dm⁻³ CuCl₂-0.2 mol dm⁻³ HCl-3 mol dm⁻³ NaCl solutions at different cuprous chloride concentrations.

The following discussion is based on this assumption.

3.4.2 Leaching Mechanism of Chalcopyrite in Cupric Chloride Solutions

To explain the experimental results obtained in this work, the following half cell reaction on the chalcopyrite surface can be proposed by assuming the electrochemical mechanism of chalcopyrite leaching in the cupric chloride solution as schematically shown in Fig. 3-13.



The reactions (3-7) and (3-8) are followed by quick reactions of CuCl^+ and CuCl_2^- formation by releasing and capturing a Cl^- ion, respectively, because the CuCl^+ and CuCl_2^- are stable species of Cu(II) and Cu(I), respectively, in the solution.

By applying a Butler-Volmer equation to each current density for these anodic and cathodic reactions, the single electron transfer process is assumed as a rate controlling step because this process is more favorable energetically than simultaneous multi electron transfer. The anodic and cathodic partial current densities on the chalcopyrite surface are given as follows:

$$i_a = 3Fk_1 \exp\left(\frac{\alpha_1 F}{RT} E\right) + Fk_2 C(\text{CuCl}_2^-) \exp\left(\frac{\alpha_2 F}{RT} E\right) \quad (3-9)$$

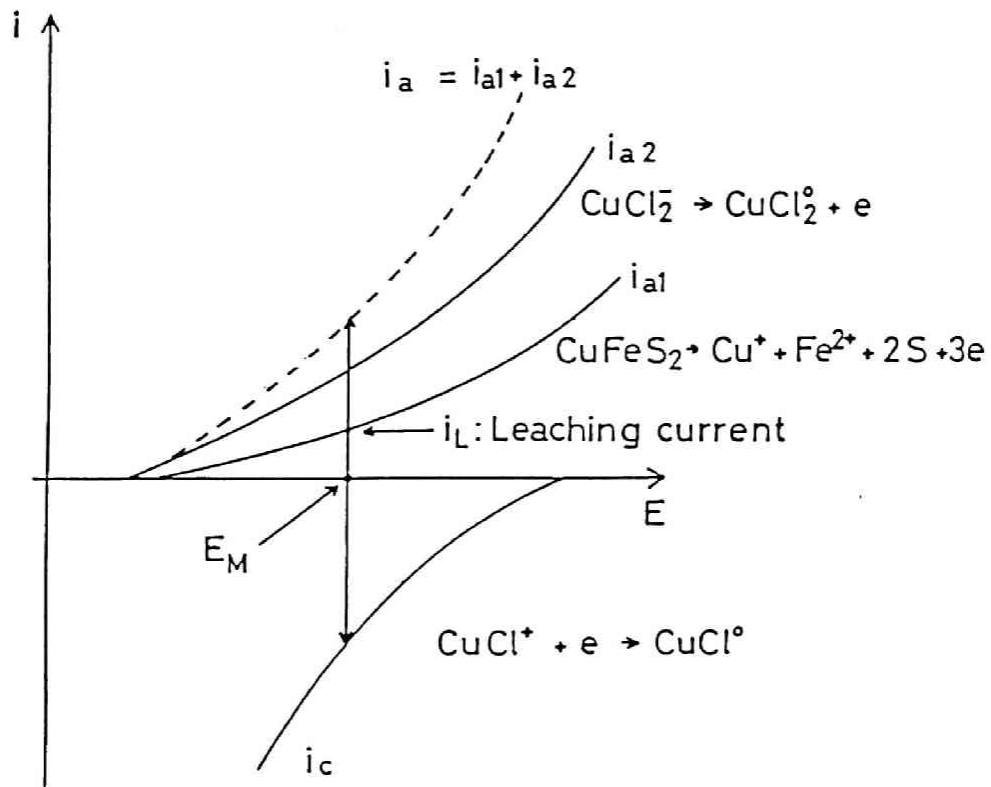


Fig. 3-13 Schematical illustration of the leaching of chalcopyrite in a cupric chloride solution.

$$i_c = - Fk_3 C(\text{CuCl}^+) \exp\left(-\frac{(1-\alpha_2)F}{RT} E\right) \quad (3-10)$$

where the symbols of i , k , E , F , and α are current density, rate constant, potential, Faraday constant, and transfer coefficient, respectively.

In the chalcopyrite leaching under the steady-state condition, the net current density, i , corresponding to $i_a + i_c$, should be zero, and thus the following equation of the mixed potential, E_M , of chalcopyrite can be obtained.

$$\begin{aligned} 3Fk_1 \exp\left(\frac{\alpha_1 F}{RT} E_M\right) + Fk_2 C(\text{CuCl}_2^-) \exp\left(\frac{\alpha_2 F}{RT} E_M\right) \\ = Fk_3 C(\text{CuCl}^+) \exp\left(-\frac{(1-\alpha_2)F}{RT} E_M\right) \end{aligned} \quad (3-11)$$

In general, the transfer coefficient, α , involved in the above equation can be determined experimentally from the Tafel slope of each electrode reaction concerned. Figure 3-14 shows the polarization curves for the oxidation of Cu(I) and the reduction of Cu(II) on the surface of chalcopyrite, which was measured at 343 K. No distinct linear portion, which corresponds to a Tafel region, was obtained on these plots, and this may be because the exchange current density for this redox reaction even on the chalcopyrite surface is extremely large and thus the effect of concentration polarization becomes significant soon after the situation comes into the Tafel region. However, judging from the satisfactorily symmetrical shape of anodic and cathodic polarization curves, it would be reasonable to assume that $\alpha_2 = 0.5$. On the other hand, as mentioned in Chapter 2, a

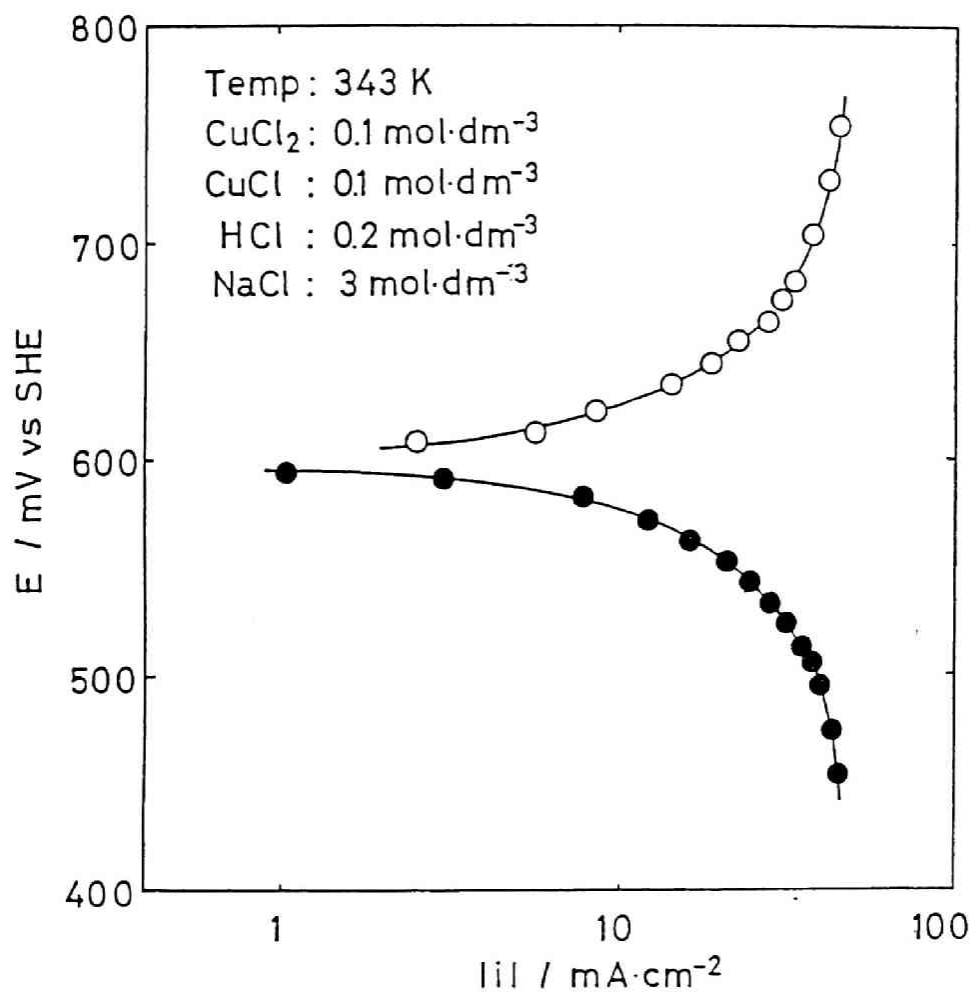


Fig. 3-14 Tafel plots of the oxidation current of Cu(I) (\circ) and the reduction current of Cu(II) (\bullet).

Tafel slope of chalcopyrite oxidation was $140 \text{ mV decade}^{-1}$ at 343 K. The transfer coefficient calculated from this value is 0.44, supporting the appropriateness of the assumption of $\alpha_1 = 0.5$.

Assuming that α_1 and α_2 are both equal to 0.5, Eq. (3-9) yields an expression of mixed potential, E_M :

$$E_M = \frac{2.3RT}{F} \log \left(\frac{k_3 C(\text{CuCl}^+)}{3k_1 + k_2 C(\text{CuCl}_2^-)} \right) \quad (3-12)$$

Furthermore, substitution of Eq. (3-12) into the first term in the right hand side of Eq. (3-9) gives the current density, i_L , corresponding to the leaching rate of chalcopyrite:

$$i_L = 3Fk_1 \left(\frac{k_3 C(\text{CuCl}^+)}{3k_1 + k_2 C(\text{CuCl}_2^-)} \right)^{0.5} \quad (3-13)$$

These equations are discussed below for the leaching conditions employed in this work.

(a) Effect of Cupric Chloride Concentration

When the analytical concentration of cupric chloride is varied in acidic cupric chloride solutions, the concentration of CuCl^+ , one of the predominant species, is approximately proportional to that of cupric chloride as depicted in Fig. 3-11. Therefore, by replacing a term of $C(\text{CuCl}^+)$ in Eqs. (3-12) and (3-13) by $C(\text{CuCl}_2)$, and neglecting the $C(\text{CuCl}_2^-)$

in these equations, the following equations are given at 343 K:

$$E_M = 0.068 \log C(\text{CuCl}_2) + \text{const.} \quad (3-14)$$

$$i_L = 3Fk_1 k_3^{0.5} C(\text{CuCl}_2)^{0.5} \quad (3-15)$$

these equations mean that the mixed potential of chalcopyrite

depends on the $\log C(\text{CuCl}_2^-)$ theoretically with $68 \text{ mV decade}^{-1}$ and the current density due to the leaching rate is proportional to $C(\text{CuCl}_2^-)^{0.5}$. These experimentally determined values are $66 \text{ mV decade}^{-1}$ and 0.54 , respectively; they are in good agreement with the theoretical values.

(b) Effect of Cuprous Chloride Concentration

When the analytical concentration of cuprous chloride is varied in acidic cuprous chloride solutions containing cupric chloride and sodium chloride, where the concentrations of cupric chloride and sodium chloride are kept constant, $C(\text{CuCl}_2^-)$ is approximately proportional to $C(\text{CuCl})$ as depicted in Fig. 3-12. Furthermore, $k_1 \ll k_2 C(\text{CuCl}_2^-)$ is assumed in Eq. (3-12) and (3-13) since the oxidation rate of CuCl_2^- is so fast. Then Eqs. (3-12) and (3-13) can be rewritten at 343 K as

$$E_M = -0.068 \log C(\text{CuCl}) + \text{const.} \quad (3-16)$$

$$i_L = 3Fk_1k_2^{-0.5} C(\text{CuCl})^{-0.5} \quad (3-17)$$

These equations signify that cuprous chloride concentration dependency of the mixed potential is theoretically $-68 \text{ mV decade}^{-1}$ and the dependency of the leaching rate upon cuprous chloride concentration is inversely a half order. These values also coincide well with those obtained experimentally.

(c) Effect of Sodium Chloride Concentration

As shown in Fig. 3-8, the mixed potential of chalcopyrite in acidic cupric chloride solutions increased with the increase in the sodium chloride concentration. In these experiments, the concentration of cuprous chloride is negligible and thus the Eq. (3-11) can be rewritten as

$$E_M = 0.068 \log C(\text{CuCl}^+) + \text{const.} \quad (3-18)$$

On the other hand, the speciation for acidic cupric chloride solution containing sodium chloride shows that the concentration of CuCl^+ slightly decreases with the increase in the concentration of sodium chloride. Therefore, Eq. (3-18) could not explain the effect of sodium chloride concentration on the mixed potential of chalcopyrite in these solutions. In the electrochemical mechanism of chalcopyrite leaching proposed here, the addition of sodium chloride in the solution and thus the increase in the concentration of Cl^- ions was taken into consideration only as a controlling factor for determining the concentration of CuCl^+ in the solution. The discrepancy between the experimental and the theoretical values suggests the necessity for considering some physico-chemical action of Cl^- ions such as the adsorption of Cl^- ions on the chalcopyrite surface, which may favor chalcopyrite dissolution as an anodic reaction or reduction of CuCl^+ as a cathodic reaction. However, this point requires further research.

3.4.3 Correlation of the Leaching Rate and Electrochemical Dissolution Rate of Chalcopyrite

By eliminating the concentration terms from Eqs. (3-12) and (3-13), the following equation can be obtained at 343 K:

$$E_M = 0.136 \log i_L + \text{const.} \quad (3-19)$$

The leaching rates of chalcopyrite determined in two types of solutions in this work, e.g. in acidic cupric chloride solutions and acidic cuprous chloride solutions containing 0.1 mol dm^{-3}

CuCl_2 and 3 mol dm^{-3} NaCl , were converted into corresponding current densities, i_L . According to Eq.(3-19), the mixed potential of chalcopyrite in these solutions was plotted against the logarithm of the current density as shown in Fig. 3-15. Linear relationships were obtained for both solution systems, their slopes being 121 and 135 mV decade^{-1} , respectively. These values of the slope are in good agreement with the theoretical value of 136 mV decade^{-1} shown by Eq.(3-19).

On the other hand, the E vs. $\log i$ plot obtained through the anodic polarization measurement at 343 K in 0.1 mol dm^{-3} HCl solution using the same chalcopyrite specimen as in the chemical leaching was also depicted in Fig. 3-15. This plot, however, is not linear and is quite different from the plots obtained for chemical leaching. As mentioned in Chapter 2, on the chalcopyrite leaching with ferric chloride such a discrepancy is considered to be caused by an effect of the resistance layer in the chalcopyrite surface, and so its resistivity was measured by a current interrupter method. The potential, E , of chalcopyrite in the anodic polarization was corrected by the ohmic potential drop through the resistance layer. The corrected E vs. $\log i$ plot in Fig. 3-15 shows a straight line with its slope of 130 mV decade^{-1} , which agrees well with those of chemical leaching. Furthermore, the position of the straight line for the anodic polarization is close to that of the chemical leaching in an acidic cupric chloride solution.

It is concluded that the leaching of chalcopyrite in the cupric chloride solution is controlled by an electrochemical

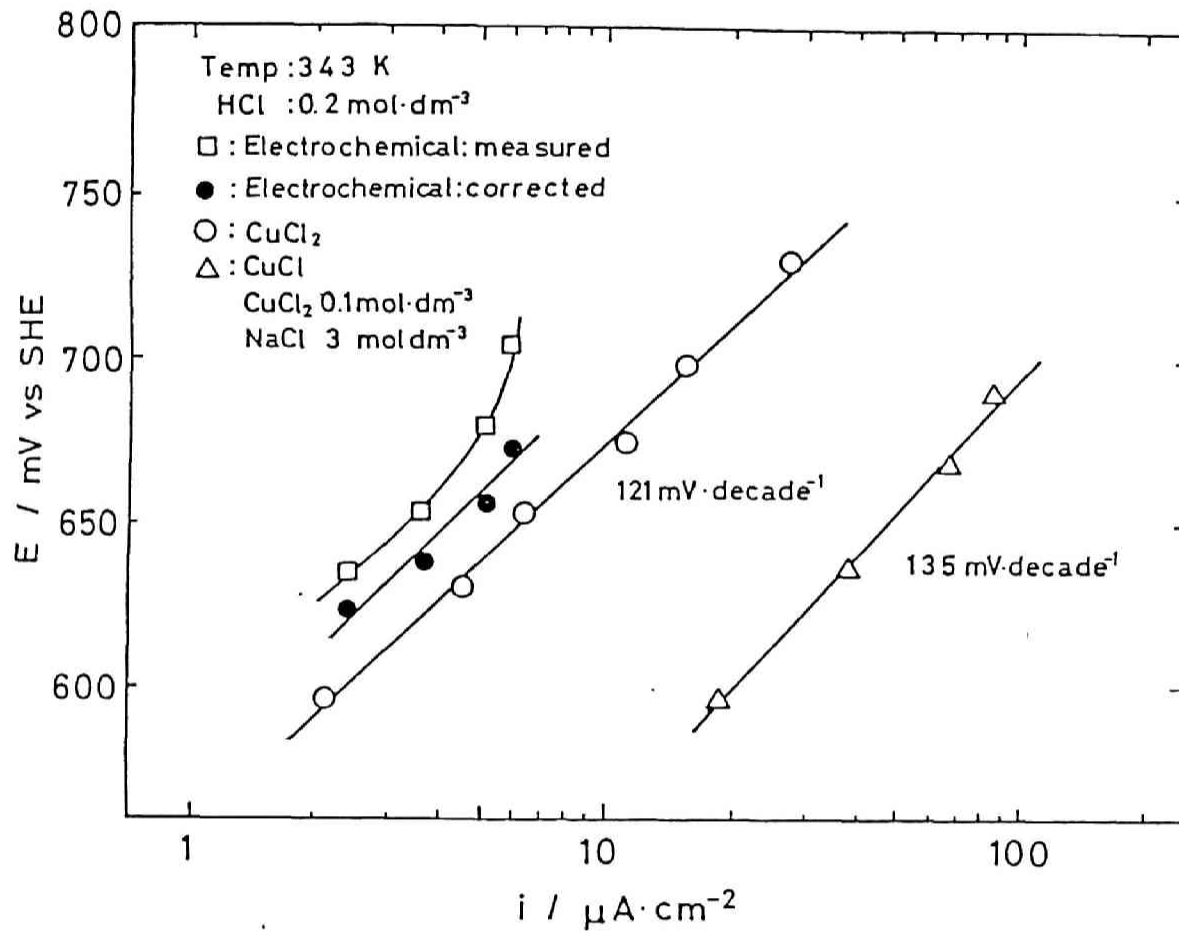


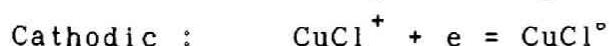
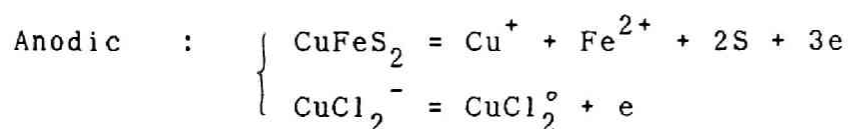
Fig. 3-15 Correlation of E-log i relationship for chemical leaching of chalcopyrite with cupric chloride and that of electrochemical leaching.

mechanism, and that the chemical and electrochemical leaching behavior are in good agreement.

3.5 Conclusions

The electrochemical leaching and chemical leaching of chalcopyrite were compared to elucidate the leaching mechanism of chalcopyrite with cupric chloride. Also the morphology of the surface of leached chalcopyrite was studied using a single chalcopyrite crystal. The principal results are as follow:

1. The elemental sulfur layer formed on the chalcopyrite surface during the leaching in acidic cupric chloride solutions is porous and not a barrier to further leaching.
2. The leaching of chalcopyrite with cupric chloride shows linear kinetics and its leaching rate is proportional to $C(\text{CuCl}_2)^{0.5}$, whereas it is inversely proportional to $C(\text{CuCl})^{0.5}$.
3. The mixed potential of chalcopyrite exhibits a 66 mV decade⁻¹ dependency upon cupric chloride concentration and -69 mV decade⁻¹ upon cuprous chloride concentration. These dependencies are in good agreement with the theoretical values expected from the mixed potential determined by a combination of the following anodic and cathodic reactions on the chalcopyrite surface:



Furthermore, the dependencies of leaching rate upon the concentrations of cupric chloride and cuprous chloride were explained by the application of a Butler-Volmer equation to each anodic or

cathodic reaction.

4. The plots of mixed potential against the logarithm of the current density calculated from the leaching rate of chalcopyrite in acidic cupric chloride solutions and in acidic cuprous chloride solutions containing $0.1 \text{ mol dm}^{-3} \text{ CuCl}_2$ and $3 \text{ mol dm}^{-3} \text{ NaCl}$ both gave straight lines, whose slopes were $121 \text{ mV decade}^{-1}$ and $135 \text{ mV decade}^{-1}$, respectively. These findings suggest the validity of the leaching kinetics controlled by a one electron transfer mechanism.

5. The dependency of $121 \text{ mV decade}^{-1}$ and $135 \text{ mV decade}^{-1}$ mentioned above for the chemical leaching of chalcopyrite both agree fairly well with the dependency of $130 \text{ mV decade}^{-1}$ for the electrochemical leaching. This strongly supports the electrochemical mechanism of chalcopyrite leaching with Cupric chloride.

6. The activation energy obtained for the chemical leaching was fairly close to that obtained for electrochemical leaching, this again supports an electrochemical mechanism.

References

1. T. Hirato, H. Majima, and Y. Awakura: Metall. Trans. B, in press.
2. G.E. Atwood and C.H. Curtis: U.S. Patent 3879272, April 22, 1975.
3. D.J. Jones and E. Peters: "Extractive Metallurgy of Copper", J.C. Yannopoulos and J.D. Agarwal, eds., AIME, New York, NY, 1976, pp. 633-653.
4. M. Bonan, J.M. Demarthe, H. Renon and F. Baratin: Metall. Trans. B, 1981, vol. 12B, pp. 269-274.
5. J.P. Wilson and W.W. Fisher: J. Metals, 1981, vol. 33(2), pp. 52-57.
6. "Stability Constants of Metal-Ion Complexes, Part A - Inorganic Ligands", IUPAC Chemical Data Series No. 21, Pergamon Press, New York, NY, 1982, pp. 216-217.
7. V.P. Vasilev and B.T. Kunin: Zh. Neorg. Khim., 1975, vol.20, pp. 1881-1886.

Chapter 4

The Leaching of Chalcopyrite with Ferric Sulfate¹

4.1 Introduction

The kinetics of the leaching of chalcopyrite with ferric chloride and cupric chloride have been studied in Chapters 2 and 3. A similar investigation has been extended to the leaching of chalcopyrite with ferric sulfate.

Ferric sulfate is one of the most important oxidative leaching reagents for sulfides. A number of investigations have been conducted to elucidate the reaction kinetics and to delineate the important leaching variables with chalcopyrite by Dutrizac et al.²⁻⁵, Wadsworth and his co-workers^{6,7}, Jones and Peters⁸, and other investigators⁹⁻¹¹, but some problems still remain to be solved. Most of these researchers concluded that the leaching of chalcopyrite with ferric sulfate follows a parabolic rate law^{2,6,7}. In contrast, Jones and Peters⁸ found that the leaching curve is linear over an extended leaching period. This is an example of the ambivalent results which require further investigation.

As mentioned in Chapter 2, that the observations of the leached surface provide useful information on the leaching mechanism. This study was conducted to obtain a fundamental understanding of the reaction kinetics of chalcopyrite leaching with ferric sulfate. For this purpose, the kinetics of the chemical and electrochemical leaching of chalcopyrite crystals of museum grade was investigated.

4.2 Experimental Procedures

4.2.1 Sample and Chemicals

Chalcopyrite crystals of museum grade supplied from Shakanai Mine, Akita prefecture, Japan, were used in the leaching experiments. Their copper, iron, and sulfur contents were 34.8 %, 30.4 %, and 34.8 %, respectively. The mineral crystals were not associated with any gangue minerals and the purity of the specimens appeared to be good. The disk specimen was prepared by cementing a chalcopyrite crystal in an epoxy resin such that one surface ($0.3\text{-}0.5\text{ cm}^2$) was exposed to the leaching solution. Moreover, electrical contact was made by soldering copper wire with silver paste on the rear face of each specimen for electrochemical measurements. After fine wet grinding with Emery paper, the specimen was subjected to the experiment. The exposed surface area was measured prior to each experiment by using a planimeter on an enlarged photograph.

Deionized water whose specific resistivity was $5 \times 10^6 \Omega\text{ cm}$ and reagent grade chemicals were used to prepare all electrolyte solutions.

4.2.2 Leaching Experiments

A 0.25 dm^3 glass vessel with a silicon rubber plug having three holes was used as a leaching reactor. The center hole of the plug was used for accommodation of the rod holding a disk specimen of chalcopyrite. The other two holes were used for accommodation of a thermometer for temperature control and a sampling tube, respectively. Also this reaction vessel had a

Nichrome heater on its outer wall, and the temperature of the leaching solutions was kept constant during the experiment. The leaching solution was agitated at constant speed of 300 r min^{-1} with a magnetic stirrer. Temperature of the solution ranged from 323 to 363 K and ferric sulfate concentrations ranged from 0.001 to 1 mol dm^{-3} . The pH of the solution was adjusted to less than 1 by using sulfuric acid. The rate curve was determined by analyzing the total copper content in the aliquots which were periodically withdrawn from the leaching solution with an atomic absorption spectrophotometer (Jarell-Ash, Type AA-1).

4.2.3 Electrochemical Measurements

Two types of electrochemical experiments were performed; measurement of the mixed potential of chalcopyrite in aqueous sulfuric acid solutions containing ferric sulfate or ferrous sulfate, and measurement of the electrochemical oxidation or reduction rate of Fe(II) or Fe(III) on the surface of chalcopyrite.

These electrochemical measurements were made using a typical three electrode system, consisting of the chalcopyrite working electrode, platinum counter electrode and 3.3 mol dm^{-3} KCl AgCl-Ag reference electrode, with a potentiostat (Nikko Keisoku Model DPGS-10). Agitation of solution was accomplished with a magnetic stirrer at a speed of 300 r min^{-1} keeping the working electrode stationary. All potentials measured are presented with respect to the standard hydrogen electrode (SHE) instead of the 3.3 mol dm^{-3} KCl AgCl-Ag electrode.

4.2.4 Morphology

The surface of chalcopyrite leached chemically was observed for (1) a grain-sized crystal of chalcopyrite leached without wet fine grinding and (2) a cross-section of the chalcopyrite prepared by breaking it into two with a knife edge. In both cases, the product of the leaching reaction was observed by using a SEM and analysed by an EPMA.

4.3 Results and Discussion

4.3.1 Leaching Rate Curve

Figure 4-1 illustrates a typical leaching rate curve of chalcopyrite in acidic ferric sulfate solutions. The leaching curve is parabolic for approximately 100 hr, thereafter the leaching rate is gradually enhanced with leaching time, showing a linear kinetics.

Jones and Peters⁸ studied the leaching of chalcopyrite in acidic ferric sulfate solutions with a massive chalcopyrite specimen and found that the kinetics were linear over an extended period. On the other hand, Dutrizac et al.² and Munoz et al.⁷ reported that the kinetics of the particulate chalcopyrite sample was parabolic. The leaching experiments done by Dutrizac et al.² or Munoz et al.⁷ were completed within about 100 hr. By contrast, Jones and Peters⁸ who used a leaching time of over 55 days, found a linear kinetics. They also reported the existence of an induction period. However, a parabolic kinetics for the initial stage of the leaching was observed to be followed by a linear stage over an extended leaching period, in this work.

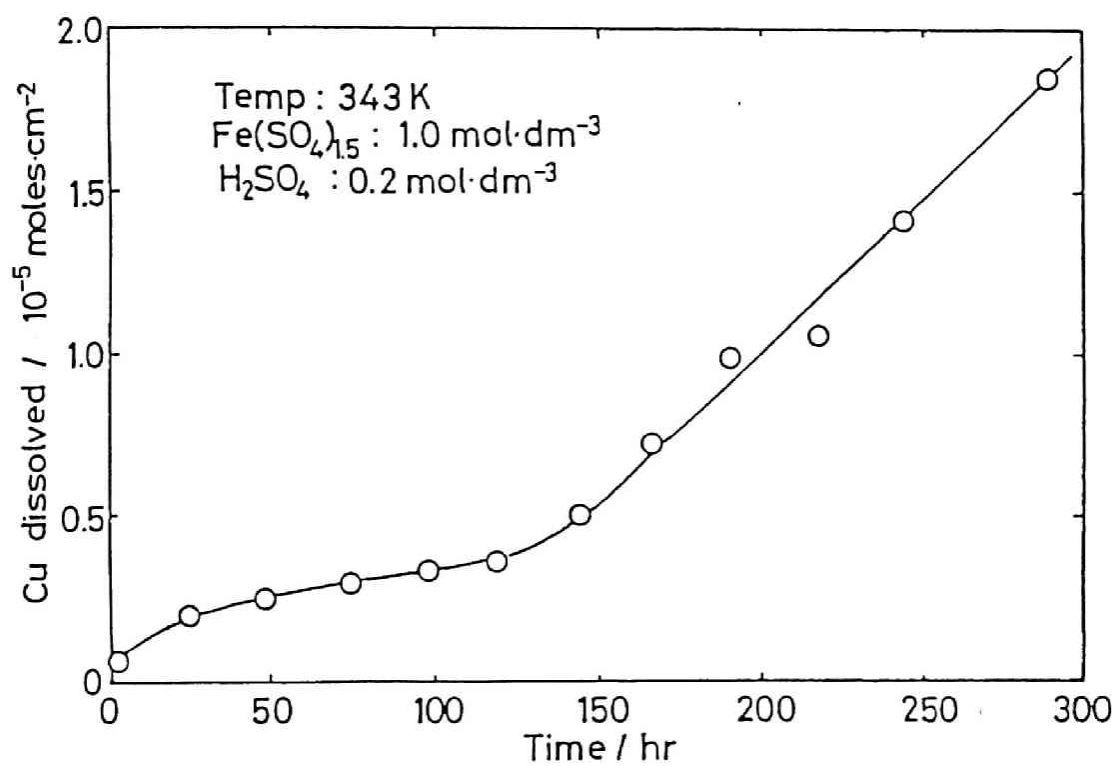


Fig. 4-1 Leaching rate curve of chalcopyrite with ferric sulfate.

4.3.2 Morphology

This change of the leaching kinetics from parabolic to linear may be attributed to the difference in the morphology of the leached surface of chalcopyrite. In this respect, Munoz et al.⁷ and Beckstead et al.⁶ reported the formation of a dense, tenacious sulfur layer on the leached chalcopyrite surface. On the other hand, Jones and Peters⁸ reported the formation of sulfur only in certain fissures or grain boundaries.

Plate 4-1 shows the morphology of the chalcopyrite surface leached with ferric sulfate at 363 K. Plate 4-1(a) shows the edge of the broken specimen after leaching. The upper part of this picture shows the unleached surface and the lower part the leached surface. Plate 4-1(b) shows a magnified picture of the leached surface. It is obvious in this picture that the elemental sulfur layer formed by ferric sulfate is considerably denser. This is a big difference from the layer of elemental sulfur on chalcopyrite surface leached with ferric chloride. The elemental sulfur layer formed by an aggregate of two-dimensional flakes was partly peeled-off from the chalcopyrite surface during leaching. The formation of flaky floats were observed at the solution-gas interface during the leaching with ferric sulfate. Plate 4-2(a) shows one of these flakes and Plate 4-2(b) shows its X-ray analysis. After 738 hr of leaching a conchoidally roughened surface was formed as shown in Plate 4-1(c).

From these observations, the formation of the dense sulfur layer was thought to have slowed the leaching rate. Once the

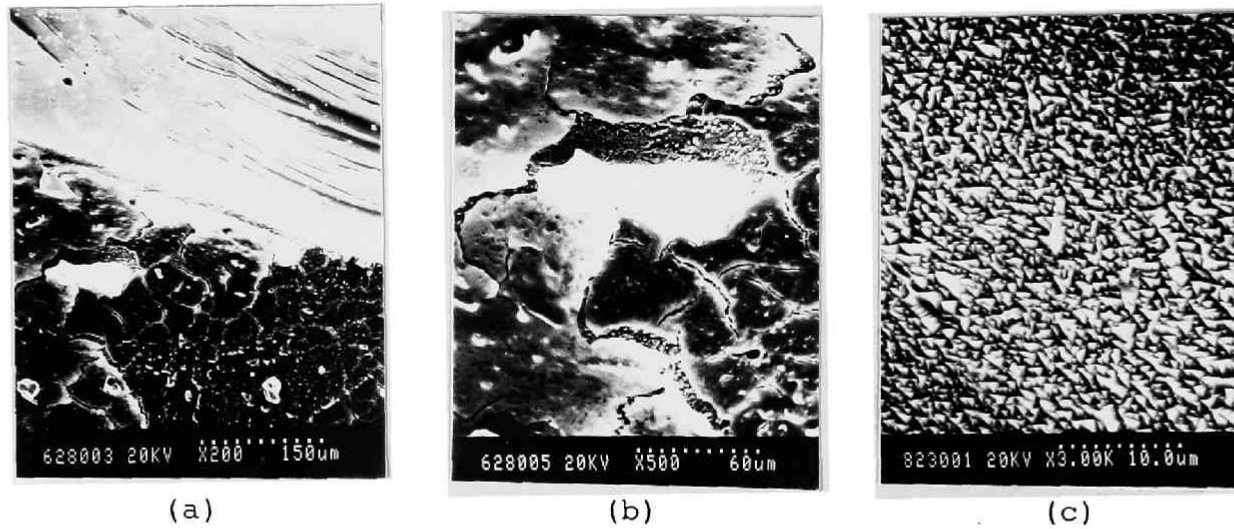


Plate 4-1 Morphology of chalcopyrite surface leached with ferric sulfate. ($1.0 \text{ mol dm}^{-3} \text{ Fe}(\text{SO}_4)_{1.5} - 0.2 \text{ mol dm}^{-3} \text{ H}_2\text{SO}_4$ at 363 K)

(a) Cross section of chalcopyrite leached for 432 hr.

(b) Magnified picture of Plate 4-1(a).

(c) Chalcopyrite surface leached for 738 hr.

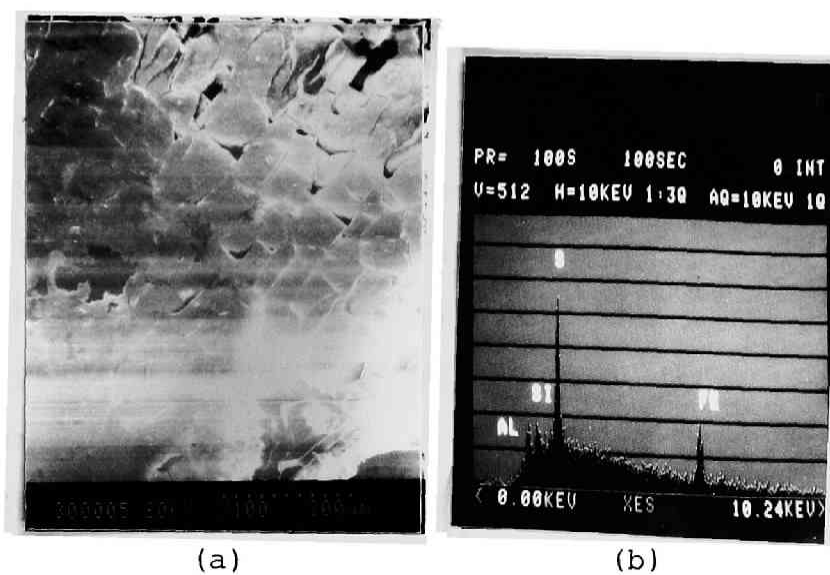
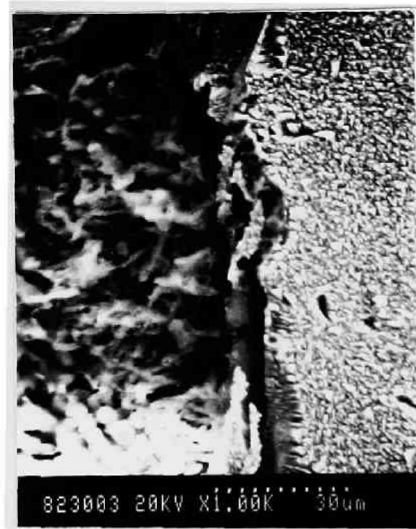


Plate 4-2 Flaky float formed during the leaching of chalcopyrite (a) and its X-ray analysis (b).

elemental sulfur layer was peeled off, a roughened surface remained. On the roughened surface, the whole surface could not be covered with a dense elemental sulfur layer, and under these circumstances, the leaching kinetics come to be linear.

Plate 4-3(a) shows a picture of a fissure in the same specimen shown in Plate 4-1(c), and Plates 4-3(b) and (c) show the results of its X-ray analyses. As is clear in these pictures, elemental sulfur exists in the fissure. The deposit of elemental sulfur formed in the fissure remains after the dense layer of elemental sulfur was peeled off from the surface of chalcopyrite. In this respect, Jones and Peters⁸ report was only on the formation of sulfur in certain fissures or grain boundaries. The possibility remains that the sulfur remaining was observed after the surface sulfur had been peeled off.

As mentioned above, the leaching of chalcopyrite with ferric sulfate shows a two stage kinetics. The first stage which obeys the parabolic rate law has been studied by a number of investigators. For this stage, the activation energies for the chalcopyrite leaching ranged from 38 to 83 kJ mol⁻¹ 2,3,5,7,10,11 It was also reported^{3,4,6,7,9-11} that the leaching rate increased with an increase in the concentration of ferric sulfate in dilute solutions, but it was almost independent of the concentration of ferric sulfate in the concentrated solution. On the other hand, no studies have been reported on the second stage of chalcopyrite leaching with ferric sulfate, which follows a linear kinetics. Therefore, the second stage was mainly studied here.



(a)



(b)



(c)

Plate 4-3 Picture of a fissure remaining in the same sample shown in Plate 1(c) and the X-ray analyses of the fissure (b) and the leached surface (c).

4.3.3 Effect of Temperature

The chalcopyrite specimen was leached in a $1 \text{ mol dm}^{-3} \text{ Fe}(\text{SO}_4)_{1.5}$ - $0.2 \text{ mol dm}^{-3} \text{ H}_2\text{SO}_4$ solution until the leaching kinetics was recognized to be linear. Then the successive leaching experiments were made under different conditions by using the same specimen without further polishing.

The leaching rate determined at the last experiment of successive leaching which was made under the same conditions as the first leaching experiment, coincided well with that of the first one. Therefore the change of surface morphology does not affect significantly the leaching rate of chalcopyrite throughout a series of leaching experiments.

Figure 4-2 shows the leaching curves in $0.1 \text{ mol dm}^{-3} \text{ Fe}(\text{SO}_4)_{1.5}$ - $0.2 \text{ mol dm}^{-3} \text{ H}_2\text{SO}_4$ solution at different temperatures. All the leaching curves are essentially linear and the leaching rate increases with the rise in temperature. Similar results were obtained at three different ferric sulfate concentrations and the data are summarized on the Arrhenius plots in Fig. 4-3. The apparent activation energies ranged from 76.8 to 87.7 kJ mol^{-1} .

The activation energies reported for the leaching of relatively pure chalcopyrite in acidic ferric sulfate solutions all correspond to the one for the first stage which follows a parabolic kinetics, and no data is available for the second stage which follows a linear kinetics. However, the amounts of activation energies obtained in this work suggest that the leaching of chalcopyrite in the second stage is chemically controlled.

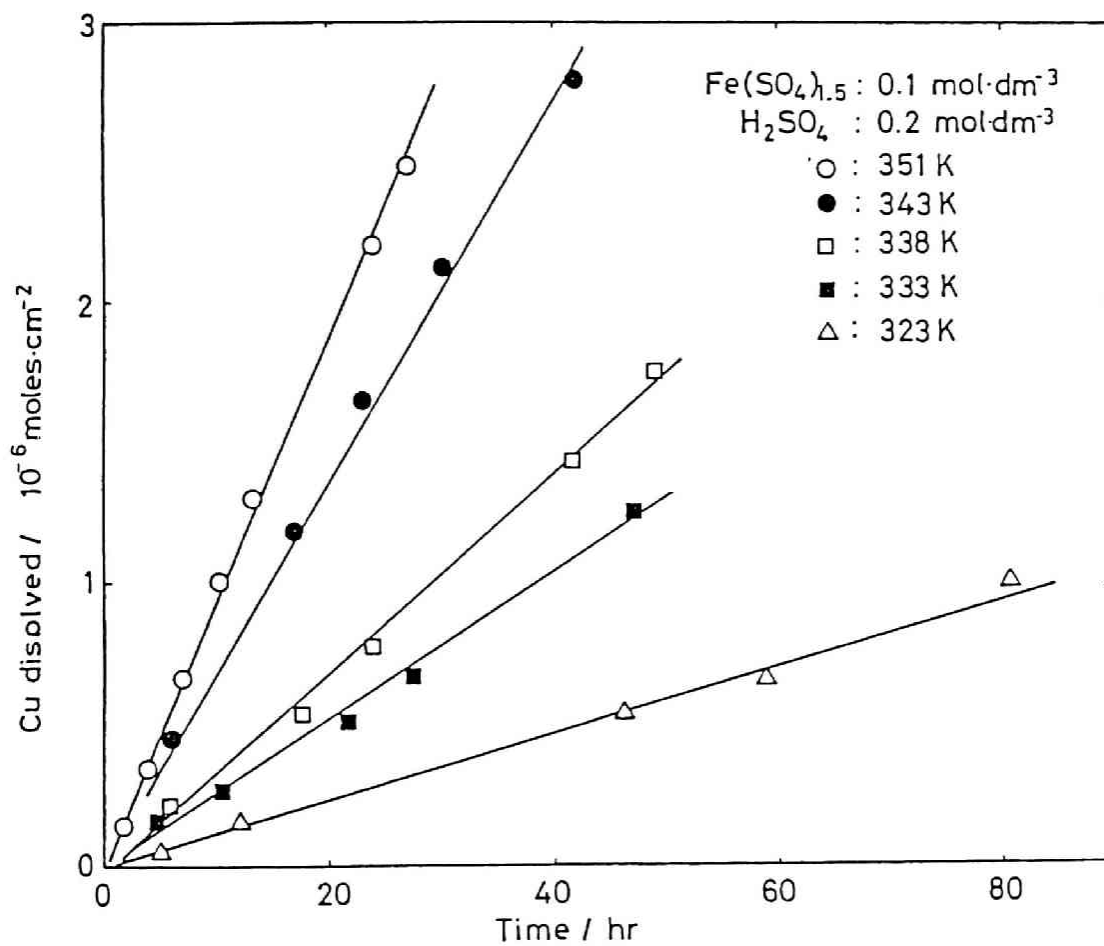


Fig. 4-2 Effect of temperature on the leaching of chalcopyrite with ferric sulfate.

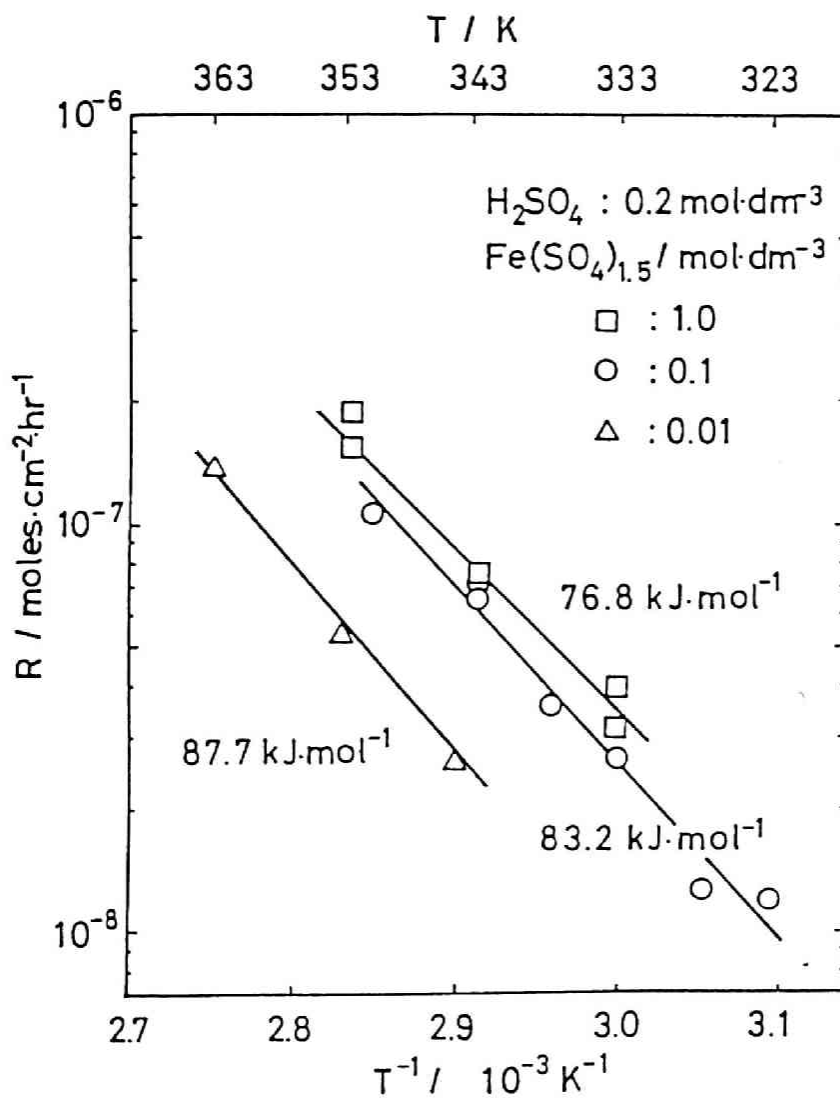


Fig. 4-3 Arrhenius plots of the leaching rate of chalcopyrite in acidic ferric sulfate solutions.

4.3.4 Effect of the Concentrations of Ferric Sulfate

(a) Leaching Rate

Figure 4-4 shows the effect of ferric sulfate concentration on the leaching rate of chalcopyrite at 343 K. The three curves shown in this figure were obtained by using three different specimens. Although the magnitude of the leaching rate differed distinctly with the three different specimens in the solution of the same ferric sulfate concentration, the dependency of the leaching rate upon the ferric sulfate concentration was similar. The leaching rate increased with the increase in the ferric sulfate concentration up to $0.1 \text{ mol dm}^{-3} \text{ Fe}(\text{SO}_4)_{1.5}$, showing a first order dependency, but tended to decline at a higher concentration. The declining tendency of the effect of ferric sulfate concentration on the leaching rate at a high ferric sulfate concentration may be attributed to the effect of the distribution of the species in the solution. The speciation for the aqueous solution system of $\text{H}_2\text{SO}_4\text{-Fe}(\text{SO}_4)_{1.5}$ was next examined. According to the data of Sapeieszko et al.¹², the principal Fe(III) species in this solution system are Fe^{3+} , FeSO_4^+ and FeHSO_4^{2+} . The reactions of the Fe(III)-sulfato and -bisulfato complex formation and their equilibrium constants are

$$\text{Fe}^{3+} + \text{SO}_4^{2-} = \text{FeSO}_4^+ \quad K(\text{FeSO}_4) = 1020 \quad (4-1)$$

$$\text{Fe}^{3+} + \text{HSO}_4^- = \text{FeHSO}_4^{2+} \quad K(\text{FeHSO}_4) = 4 \quad (4-2)$$

These equilibrium constants are quoted from the data of Speieszko et al.¹² for an ionic strength of 2.67 at 353 K. The dissociation constant of HSO_4^+ , K_a , was estimated as a function

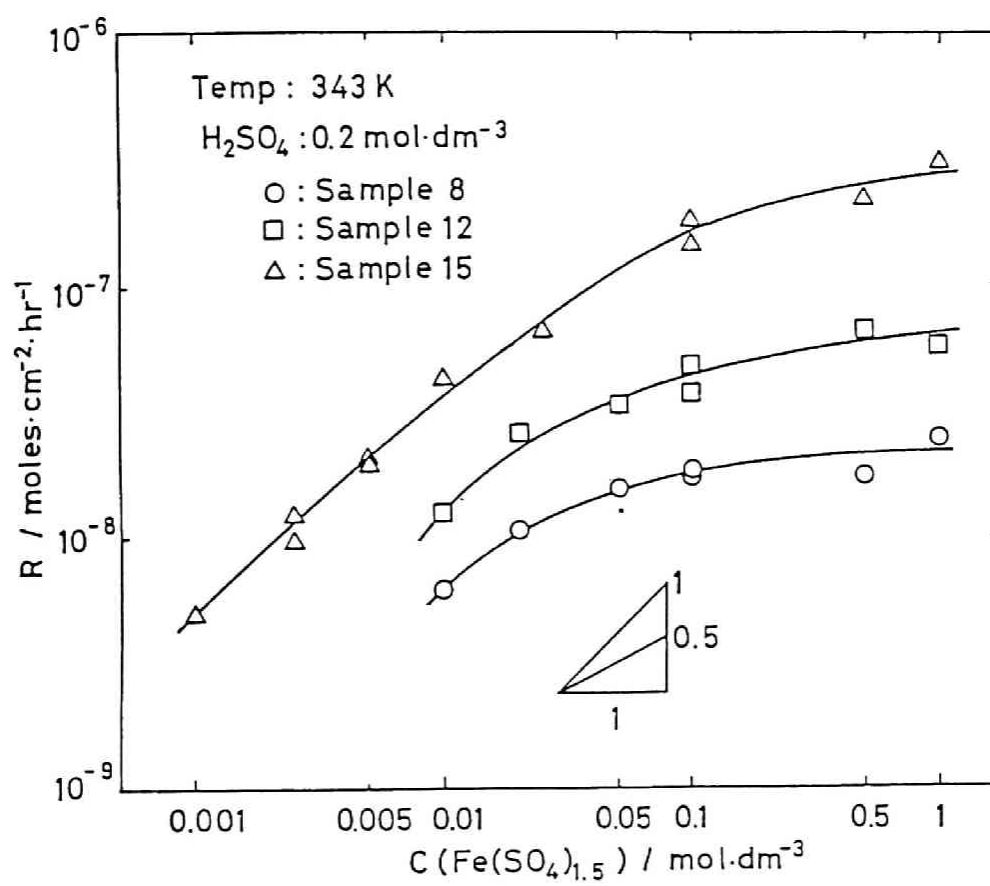


Fig. 4-4 Effect of ferric sulfate concentration on the leaching rate of chalcopyrite.

of ion strength, I , by using the following equation¹³:

$$\log K_a = \log(0.0102) + \frac{2.036\sqrt{I}}{1 + 0.4\sqrt{I}} \quad (4-3)$$

Moreover, the mass balances on iron, hydrogen and sulfur give

$$C_T(\text{Fe}) = C(\text{Fe}^{3+}) + C(\text{FeSO}_4^+) + C(\text{FeHSO}_4^{2+}) \quad (4-4)$$

$$C_T(\text{H}) = C(\text{H}^+) + C(\text{HSO}_4^-) + C(\text{FeHSO}_4^{2+}) \quad (4-5)$$

$$C_T(\text{S}) = C(\text{FeSO}_4^+) + C(\text{FeHSO}_4^{2+}) + C(\text{HSO}_4^-) + C(\text{SO}_4^{2-}) \quad (4-6)$$

where $C_T(\text{Fe})$, $C_T(\text{H})$ and $C_T(\text{S})$ are the total concentrations of iron, hydrogen and sulfur in the solution, respectively.

By using these relations as well as the equilibrium relations, the concentrations of Fe(III) species in $0.2 \text{ mol dm}^{-3} \text{ H}_2\text{SO}_4$ solutions containing various amounts of ferric sulfate were calculated (Fig. 4-5). As shown in Fig. 4-5, the concentrations of Fe^{3+} as well as that of FeHSO_4^{2+} increased with the increase in $\text{Fe}(\text{SO}_4)_{1.5}$ concentration up to 0.1 mol dm^{-3} with a first order dependency and tended to decline at higher concentration. On the other hand, the FeSO_4^+ concentration simply increased. Compared to FeHSO_4^{2+} , Fe^{3+} is a more principal species. The distribution of Fe^{3+} concentration corresponds to that of the leaching rate. This finding may suggest that the free Fe^{3+} ion plays an important part in the leaching of chalcopyrite with ferric sulfate.

(b) Mixed Potential

The effect of ferric sulfate concentration on the mixed potential of chalcopyrite was examined at 343 K in $0.2 \text{ mol dm}^{-3} \text{ H}_2\text{SO}_4$ solutions containing $\text{Fe}(\text{SO}_4)_{1.5}$ whose concentrations ranged from 0.01 to 1 mol dm^{-3} . A linear relationship was obtained

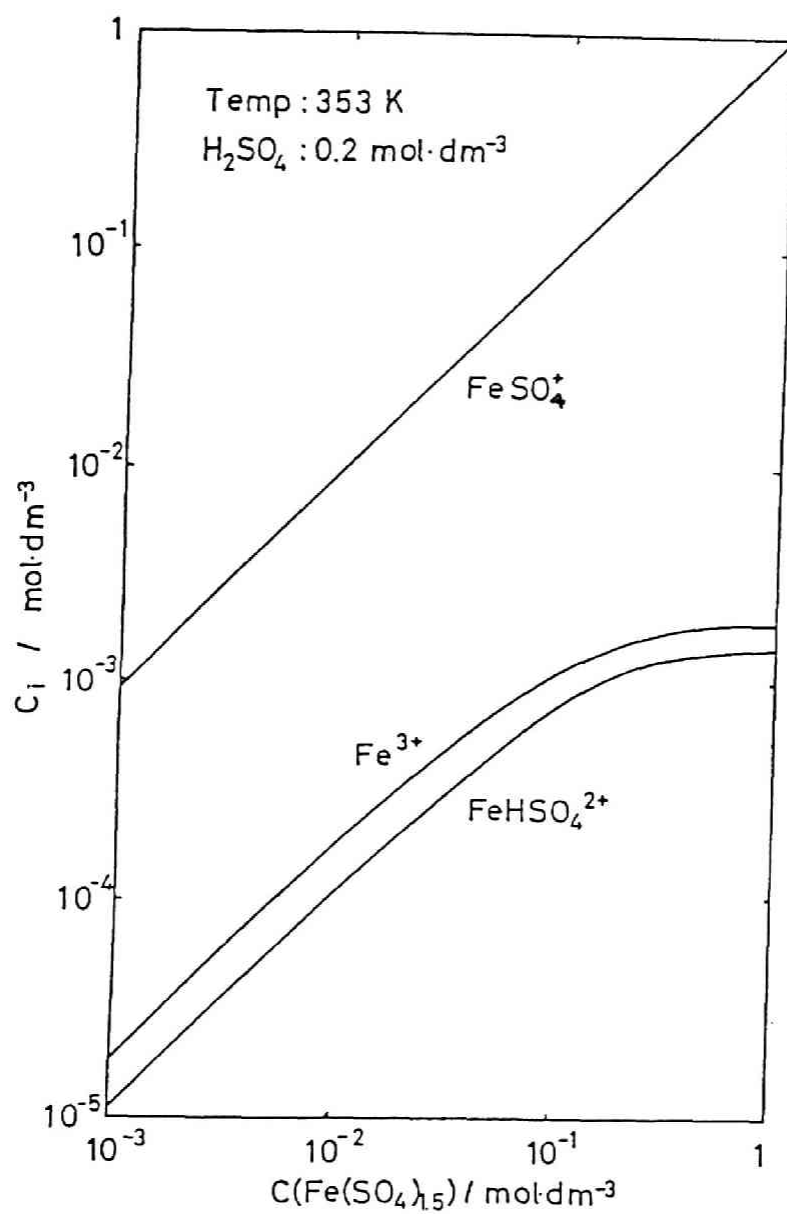


Fig. 4-5 Concentrations of Fe(III)-sulfato and -bisulfato complexes in $0.2 \text{ mol dm}^{-3} \text{H}_2\text{SO}_4$ solutions having different ferric chloride concentrations.

between the mixed potential and the logarithm of the concentration of $\text{Fe}(\text{SO}_4)_{1.5}$, with a slope of $79 \text{ mV decade}^{-1}$ (Fig. 4-6). Jones and Peters⁸ reported a similar relationship with a slope of $62 \text{ mV decade}^{-1}$. The mixed potential change does not exactly correspond to the ferric sulfate concentration dependency of the leaching rate. Therefore, it may be necessary to consider a mechanism other than an electrochemical one at the $\text{Fe}(\text{III})$ concentration above 0.1 mol dm^{-3} .

The leaching rate of sample 15 chalcopyrite in 1 mol dm^{-3} $\text{Fe}(\text{SO}_4)_{1.5}$ solution, which is shown in Fig. 4-4, is smaller by one order of magnitude than that of the same sample in 1 mol dm^{-3} FeCl_3 at the same temperature. However, the mixed potentials of chalcopyrite in these leaching experiments were found to be 707 mV vs SHE in 1 mol dm^{-3} $\text{Fe}(\text{SO}_4)_{1.5}$ and 730 mV in 1 mol dm^{-3} FeCl_3 . The difference of these potentials is not large enough to explain such a large difference in the leaching rate. These findings suggest that the layer of elemental sulfur formed on the chalcopyrite surface affects the leaching of chalcopyrite in an ferric sulfate solution at the second stage which is characterized by linear kinetics. The dense layer of elemental sulfur formed on the surface of the chalcopyrite in the ferric sulfate solution peels off at random on the surface in the second stage of leaching. As a result, the effective reacting surface area is kept almost constant, and the leaching exhibits a linear kinetics.

Based on this assumption, the effect of ferric sulfate on the leaching rate in the second stage of chalcopyrite leaching in

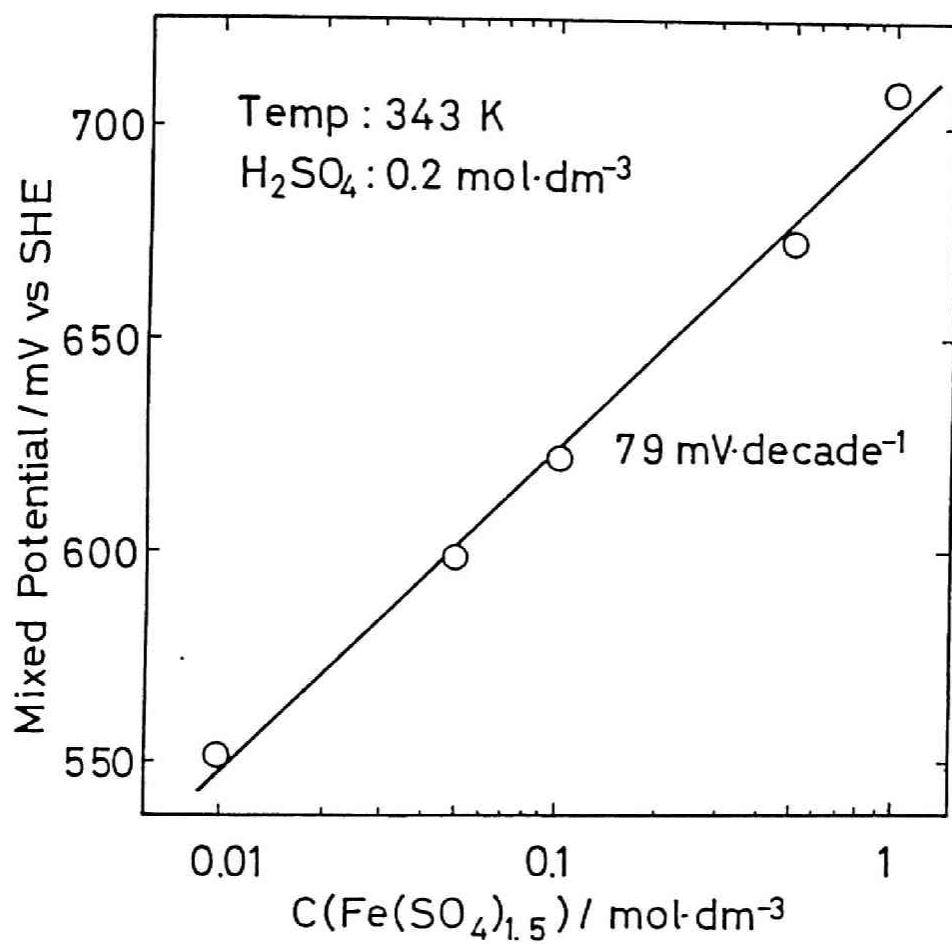


Fig. 4-6 Effect of ferric sulfate concentration on the mixed potential of chalcopyrite.

ferric sulfate solution was examined. At a ferric sulfate concentration of lower than $0.1 \text{ mol dm}^{-3} \text{ Fe}(\text{SO}_4)_{1.5}$, the effect of ferric sulfate concentration was larger than that of the decrease in the effective reacting surface area, and thus the leaching rate increased with the increase in the ferric sulfate concentration. By contrast, at a ferric sulfate concentration higher than $0.1 \text{ mol dm}^{-3} \text{ Fe}(\text{SO}_4)_{1.5}$, the effect of the above two factors balanced each other, and thus the leaching rate become apparently independent of ferric sulfate concentration. Therefore, this analysis shows that the mixed potential of chalcopyrite, which is an intensity factor, is independent of the reacting surface area but increases with the increase in the ferric sulfate concentration.

On the other hand, Munoz et al.⁶ proposed a model in which the electron transfer in an elemental sulfur formed on the surface of chalcopyrite in an aqueous solution of ferric sulfate controls the overall reaction rate. According to their model, the leaching rate can be explained to be independent of ferric sulfate concentration by assuming a constant effective thickness of elemental sulfur layer in the second stage of chalcopyrite leaching, which is repeatedly peeled-off and regenerated, but the dependency of the leaching rate on the ferric sulfate concentration at a low ferric sulfate concentration range can not be explained. Further studies on the morphology of elemental sulfur formed on the chalcopyrite surface are necessary to obtain a fuller understanding on the dependency of the leaching rate of chalcopyrite upon ferric sulfate concentration observed in the

second stage of the leaching reaction.

4.3.5 Effect of the Concentration of Ferrous Sulfate

(a) Leaching Rate

When chalcopyrite is leached in the $\text{Fe}(\text{SO}_4)_{1.5} - \text{H}_2\text{SO}_4$ solutions, $\text{Fe}(\text{II})$ is produced as one of the reaction products. Therefore it is important to know the effect of ferrous sulfate on the leaching rate of chalcopyrite as it will be present in a substantial amount in the actual leaching process.

A series of experiments to confirm the effect of ferrous sulfate were conducted at 343 K in an aqueous solution containing $0.1 \text{ mol dm}^{-3} \text{Fe}(\text{SO}_4)_{1.5}$ and $0.2 \text{ mol dm}^{-3} \text{H}_2\text{SO}_4$, in which the ferrous sulfate concentration was varied from 0 to 1 mol dm^{-3} . The leaching results illustrated in Fig. 4-7 indicate that the leaching rate decreases with an increase in the ferrous sulfate concentration. The addition of $1 \text{ mol dm}^{-3} \text{FeSO}_4$ reduced the leaching rate to 30 % of that observed in the ferrous-free medium.

The present findings are similar to those for the first stage of chalcopyrite leaching which follow a parabolic kinetics reported by Dutrizac et al.^{2,4} and Jones and Peters⁸.

(b) Mixed Potential

The effect of ferrous sulfate concentration on the mixed potential of chalcopyrite was investigated at 343 K in $0.1 \text{ mol dm}^{-3} \text{Fe}(\text{SO}_4)_{1.5} - 0.2 \text{ mol dm}^{-3} \text{H}_2\text{SO}_4$ solutions. As is shown in Fig. 4-8, the addition of ferrous sulfate up to 0.1 mol dm^{-3} had little effect, but thereafter a substantial drop in potential was

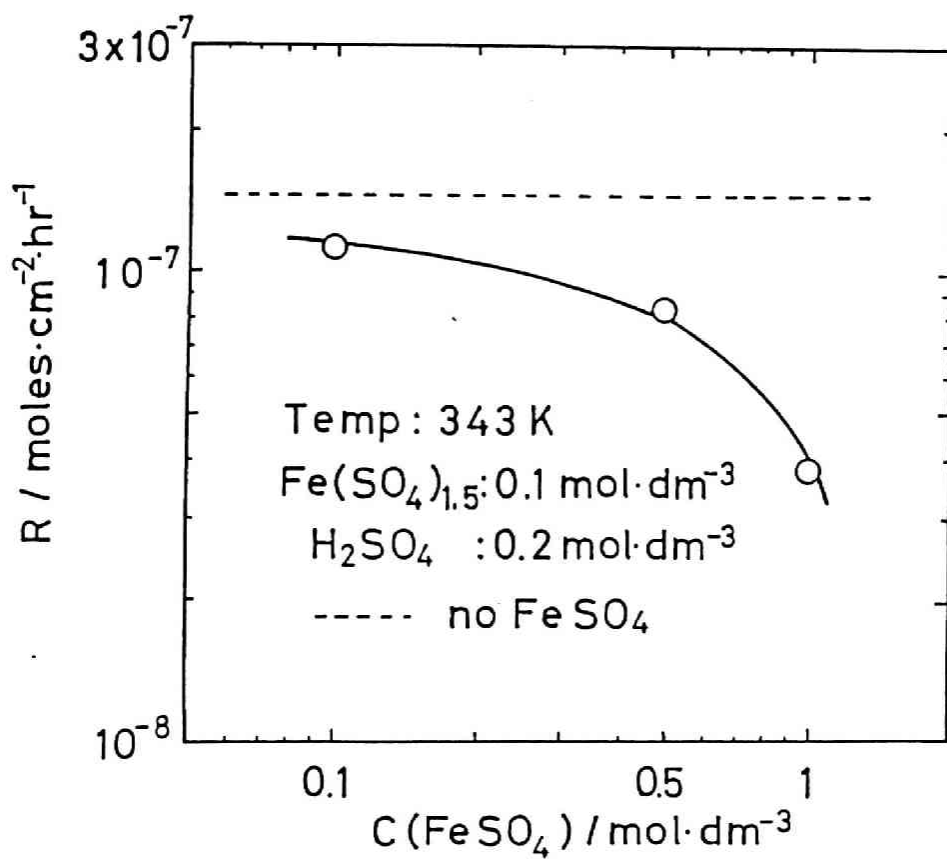


Fig. 4-7 Effect of ferrous sulfate concentration on the leaching rate of chalcopyrite.

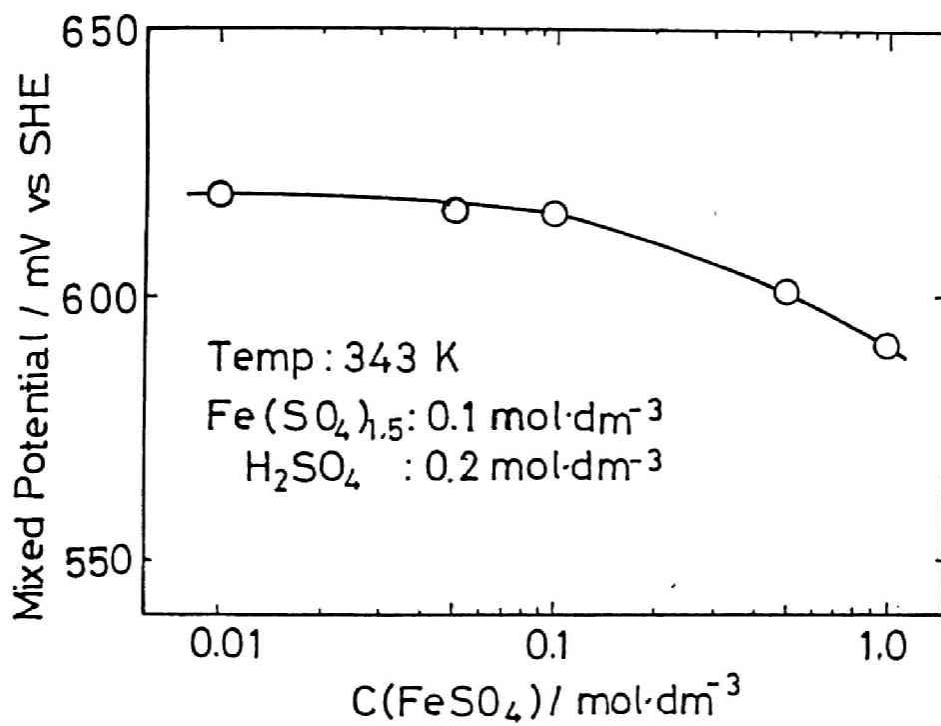


Fig. 4-8 Effect of ferrous sulfate concentration on the mixed potential of chalcopyrite.

observed. A total drop of 28 mV was obtained between 0.01 mol dm^{-3} to 1 mol dm^{-3} FeSO_4 . Jones and Peters¹¹ reported a similar finding. This finding well corresponds to that of the ferrous sulfate concentration dependency of the leaching rate.

(c) Oxidation of Ferrous Sulfate on the Surface of Chalcopyrite Electrode

Judging from the results shown in Fig. 4-8, the oxidation of ferrous sulfate may proceed rapidly on the surface of chalcopyrite. To verify such a speculation, the electrochemical oxidation of ferrous sulfate on the surface of the chalcopyrite electrode was studied. The solid line in Fig. 4-9 depicts the electric current densities measured at 343 K at the constant electrode potential of 656 mV vs SHE in 0.2 mol dm^{-3} H_2SO_4 containing ferrous sulfate whose concentration was adjusted between 0 and 1.0 mol dm^{-3} . As can be seen in this figure, the current densities increased immediately after each addition of ferrous sulfate to the solution, followed by almost a steady state.

The results shown in Fig. 4-9 indicate that a considerably large discharge can occur on the surface of chalcopyrite, and at the same time, that ferrous sulfate is readily oxidized. Rapid oxidation of Fe(II) on the surface of chalcopyrite in the sulfate media may affect the leaching rate and the mixed potential of chalcopyrite. This finding is quite different from that observed for the oxidation of Fe(II) on the surface of chalcopyrite electrode in chloride media. The broken line in Fig. 4-9 shows the electric current densities measured at a

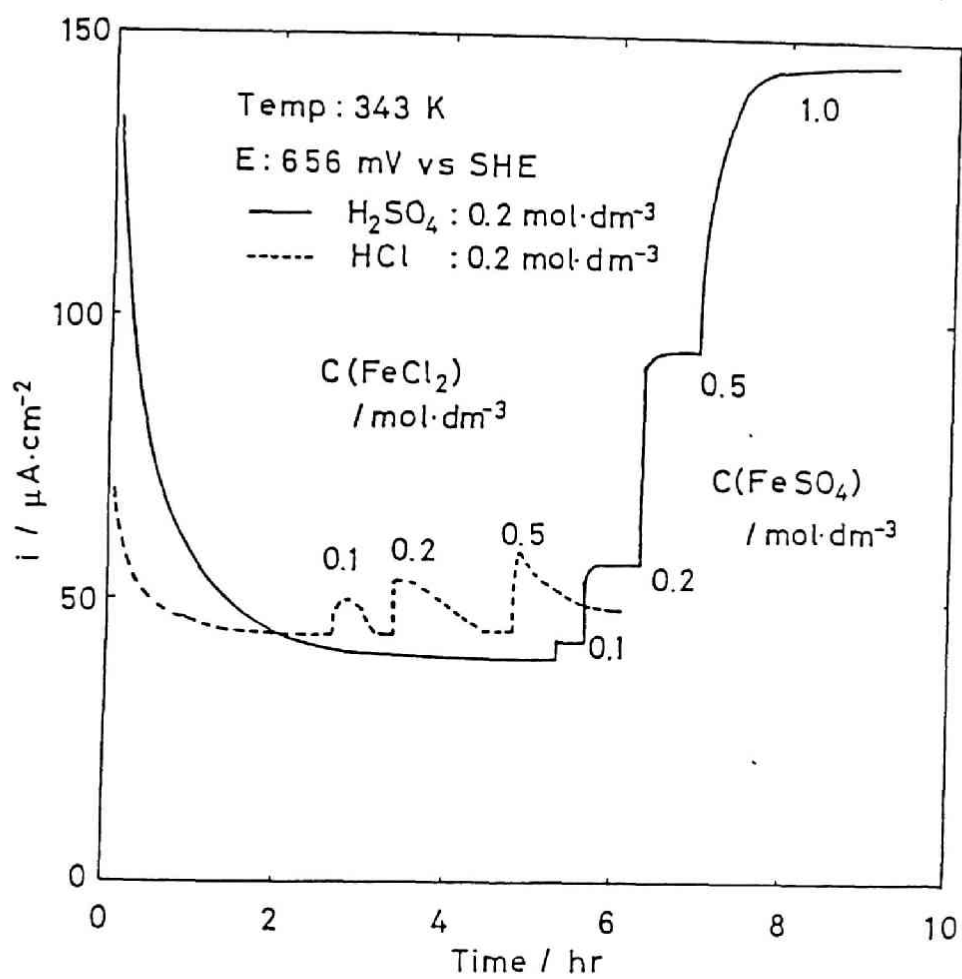


Fig. 4-9 Effect of the addition of ferrous sulfate and ferrous chloride on the stable current densities of anodic polarization of chalcopyrite at 656 mV vs SHE.

constant electrode potential of 656 mV vs SHE in the 0.2 mol dm^{-3} HCl solution containing ferrous chloride whose concentration was adjusted between 0.1 and 0.5 mol dm^{-3} . Although the current density increased immediately after the addition of ferrous chloride to the solution, the current density gradually decreased to that without ferrous chloride, as can be seen in this figure. This indicates that the oxidation of ferrous ions on a chalcopyrite electrode is extremely slow in a chloride medium. As mentioned in Chapter 2, the concentration of ferrous chloride does not affect either the leaching rate or the mixed potential of chalcopyrite.

From these observation, the oxidation rate of Fe(II) on a chalcopyrite surface can be explained by the effects of Fe(II) concentration on the leaching rate and on the mixed potential in both sulfate and chloride solutions. Therefore the effect of Fe(II) on the leaching of chalcopyrite may occur electrochemically.

Dutrizac⁴ reported that the presence of ferrous sulfate causes the leaching rate copper leaching of the chalcopyrite to fall more sharply than that of an equivalent molarity of neutral sulfate such as Li_2SO_4 or MgSO_4 and suggested that this was due to the effect of Fe^{2+} itself. The result obtained in the present work support his suggestion.

4.4 Conclusions

The leaching of natural chalcopyrite crystals with ferric sulfate was studied kinetically. The morphology of the leached

chalcopyrite and the electrochemical properties of the chalcopyrite electrode were also investigated. The principal conclusions obtained are as follows:

1. The leaching of chalcopyrite obeyed a parabolic rate law at the initial stage, then a linear kinetics over the extended period.
2. At the initial stage, a dense sulfur layer was formed on the chalcopyrite surface. The growth of the layer caused it to peel off from the surface, leaving a roughened surface. At the linear stage, no thick sulfur layer was observed.
3. The apparent activation energy for chalcopyrite leaching in a ferric sulfate solution was found to be 76.8 to 87.7 kJ mol⁻¹. The amount of activation energy determined suggests that the leaching of chalcopyrite in a ferric sulfate solution is chemically controlled.
4. The leaching rate of chalcopyrite increased with the increase in Fe(SO₄)_{1.5} concentration up to 0.1 mol dm⁻³, but at a higher ferric sulfate concentration, the leaching rate was only marginally dependent on the concentration of ferric sulfate.
5. The dependency of the mixed potential upon ferric sulfate concentration was found to be 79 mV decade⁻¹ from 0.01 mol dm⁻³ to 1 mol dm⁻³ Fe(SO₄)_{1.5} at 343 K.
6. Both the leaching rate and the mixed potential decreased with the increase in the ferrous sulfate concentration.
7. The anodic current of Fe(II) oxidation on the chalcopyrite surface in a sulfate medium was larger than that in a chloride medium.

References

1. T. Hirato, H. Majima and Y. Awakura: paper submitted to Metall. Trans.
2. J.E. Dutrizac, R.J.C. MacDonald and T.R. Ingraham: Trans. TMS-AIME, 1969, vol. 245, p. 955.
3. J.E. Dutrizac: Metall. Trans. B, 1978, vol. 9B, p. 431.
4. J.E. Dutrizac: Metall. Trans. B, 1981, vol. 12B, p. 371.
5. J.E. Dutrizac: Metall. Trans. B, 1982, vol. 13B, p. 303.
6. L.W. Beckstead, P.B. Munoz, J.L. Sepulveda, J.A. Herbst, J.D. Miller, F.A. Olson and M.E. Wadsworth: "Extractive Metallurgy of Copper", J.C. Yannopoulos and J.C. Agarwal eds., AIME, New York, NY, 1976, vol. 2, p. 611.
7. P.B. Munoz, J.D. Miller and M.E. Wadsworth: Metall. Trans. B, 1979, vol. 10B, p. 149.
8. D.L. Jones and E. Peters: "Extractive Metallurgy of Copper", J.C. Yannopoulos and J.C. Agarwal eds., AIME, New York, NY, 1976, vol. 2, p. 633.
9. J.D. Sullivan: Trans. AIME, 1933, vol. 515, p. 106.
10. D.F. Lowe: Ph.D. Thesis, University of Arizona, 1970.
11. J.P. Baur, H.L. Gibbs and M.E. Wadsworth: USBM RI-7823, 1974.
12. R.S. Sapiieszko, R.C. Patel and E. Matijević: J. Phys. Chem., 1977, vol. 81, p. 1061.
13. C.F. Baes: J. Am. Chem. Soc., 1957, vol. 79, p. 5611.

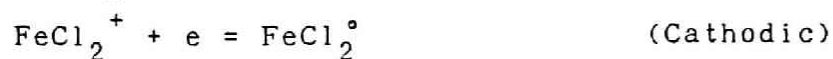
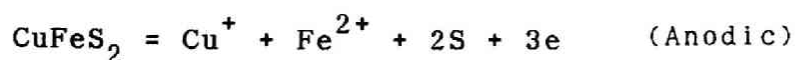
Chapter 5

Conclusions

The present work was undertaken to obtain a fuller understanding of the mechanism of the oxidative leaching of chalcopyrite with ferric chloride, ferric sulfate or cupric chloride. The leaching was investigated chemically, electrochemically and morphologically, by using a massive chalcopyrite crystal of museum grade. Also, the correlation between the chemical leaching and the electrochemical leaching of chalcopyrite was examined.

In Chapter 2, the leaching of natural chalcopyrite crystal with ferric chloride was studied kinetically. The morphology of the leached chalcopyrite was also investigated. The elemental sulfur layer formed on the chalcopyrite surface after leaching in a ferric chloride solution was porous and not a barrier to further leaching. The leaching rate of chalcopyrite in a ferric sulfate solution was approximately one order smaller than that in a ferric chloride solution. This suggests that ferric chloride is a more reactive leachant for chalcopyrite. The leaching rate of several chalcopyrite specimens varied significantly, even though the chalcopyrite crystals originated from the same deposit of the same mine. The leaching rate could not be reproduced in repeat leaching tests utilizing the same specimen polished by Emery paper prior to each experiment. To obtain reliable kinetic data, the following method was developed; the specimen

was subjected to wet polishing with Emery paper before only first leaching and the same specimen without further polishing was used in successive leaching. Using this technique, the effect of several factors on the leaching was investigated. The leaching rate of chalcopyrite was of a half order with respect to the ferric chloride concentration. The effect of ferrous chloride on the leaching of chalcopyrite in a ferric chloride solution was found to be almost insignificant. The leaching rate of chalcopyrite increased with an increase in sodium chloride concentration. The apparent activation energy for chalcopyrite leaching in a ferric chloride solution was found to be 69.0 kJ mol^{-1} . This amount of activation energy suggests that the leaching of chalcopyrite in a ferric chloride solution should be chemically controlled. Also a comparative study of electrochemical leaching and chemical leaching of chalcopyrite was done to elucidate the leaching mechanism of chalcopyrite in ferric chloride media. The mixed potential of chalcopyrite in a ferric chloride solution is determined by a combination of the following anodic and cathodic reactions:

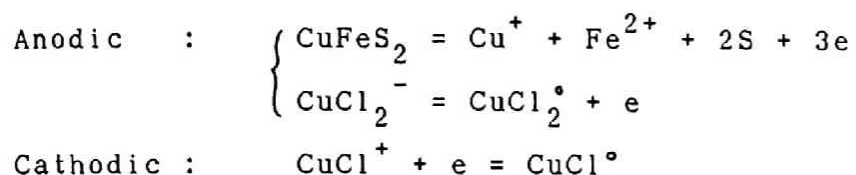


The dependency of the mixed potential upon the ferric chloride concentration was found to be $72 \text{ mV decade}^{-1}$ at 343 K , which is in good agreement with the theoretical value. By displaying the leaching rates of chalcopyrite in ferric chloride on a Tafel plot, a straight line, whose slope was $140 \text{ mV decade}^{-1}$ was obtained. This finding suggests that the leaching kinetics are

controlled by a one electron transfer mechanism. The dependency of E upon $\log i$ for chemical leaching of chalcopyrite in ferric chloride is in good agreement with that for electrochemical leaching. This finding strongly supports the electrochemical mechanism of ferric chloride leaching of chalcopyrite. Cupric chloride, the resultant product of leaching, may play an important role in the later stages of leaching as an oxidizing agent, since cupric chloride is considered to be a more reactive reagent than ferric chloride.

In Chapter 3, the electrochemical leaching and chemical leaching of chalcopyrite were compared to elucidate the leaching mechanism of chalcopyrite with cupric chloride. Also the morphology of the surface of leached chalcopyrite was studied using a single chalcopyrite crystal. The elemental sulfur layer formed on the chalcopyrite surface during the leaching in acidic cupric chloride solutions was porous and not a barrier to further leaching. The leaching of chalcopyrite with cupric chloride showed linear kinetics and its leaching rate was of a half order with respect to the cupric chloride concentration, whereas it was an inverse half order with respect to the cuprous chloride concentration. The mixed potential of chalcopyrite exhibits a $66 \text{ mV decade}^{-1}$ dependency upon cupric chloride concentration, and $-69 \text{ mV decade}^{-1}$ upon cuprous chloride concentration. These dependencies are in good agreement with the theoretical values expected from the mixed potential determined by a combination of the following anodic and cathodic reactions on the chalcopyrite

surface:



Furthermore, the dependencies of leaching rate upon the concentrations of cupric chloride and cuprous chloride were explained by the application of a Butler-Volmer equation to each anodic or cathodic reaction. The plots of mixed potential against the logarithm of the current density calculated from the leaching rate of chalcopyrite in acidic cupric chloride solutions and in acidic cuprous chloride solutions containing $0.1 \text{ mol dm}^{-3} \text{ CuCl}_2$ and $3 \text{ mol dm}^{-3} \text{ NaCl}$ both gave straight lines, whose slopes were $121 \text{ mV decade}^{-1}$ and $135 \text{ mV decade}^{-1}$, respectively. These findings suggest the validity of the leaching kinetics controlled by a one electron transfer mechanism. The dependency of $121 \text{ mV decade}^{-1}$ and $135 \text{ mV decade}^{-1}$ mentioned above for the chemical leaching of chalcopyrite both agree fairly well with the dependency of $130 \text{ mV decade}^{-1}$ for the electrochemical leaching. This strongly supports the electrochemical mechanism of chalcopyrite leaching with cupric chloride. The activation energy obtained for the chemical leaching was fairly close to that obtained for electrochemical leaching, this again supports an electrochemical mechanism.

In Chapter 4, the leaching of natural chalcopyrite crystals with ferric sulfate was studied kinetically. The morphology of the leached chalcopyrite and the electrochemical properties of

the chalcopyrite electrode were also investigated. It was found that the leaching of chalcopyrite obeyed a parabolic rate law at the initial stage, then a linear kinetics over the extended period. At the initial stage, a dense sulfur layer was formed on the chalcopyrite surface. The growth of the layer caused it to peel off from the surface, leaving a roughened surface. At the linear stage, no thick sulfur layer was observed. The apparent activation energy for chalcopyrite leaching in a ferric sulfate solution was found to be 76.8 to 87.7 kJ mol⁻¹. The amount of activation energy determined suggests that the leaching of chalcopyrite in a ferric sulfate solution is chemically controlled. The leaching rate of chalcopyrite increased with the increase in ferric sulfate concentration up to 0.1 mol dm⁻³, but at a higher ferric sulfate concentration, the leaching rate was only marginally dependent on the concentration of ferric sulfate. The dependency of the mixed potential upon ferric sulfate concentration was found to be 79 mV decade⁻¹ from 0.01 mol dm⁻³ to 1 mol dm⁻³ Fe(SO₄)_{1.5} at 343 K. Both the leaching rate and the mixed potential decreased with the increase in the concentration of ferrous sulfate. The anodic current of Fe(II) oxidation on the chalcopyrite surface in a sulfate medium was larger than that in a chloride medium.

Although many features have been clarified through the present study, several problems still remain to be solved. Suggestions for future work are as follows:

1. The leaching rate of several chalcopyrite specimens varied

significantly, even though the chalcopyrite crystals originated from the same deposit of the same mine. This may be attributed to the orientation of the chalcopyrite crystals. The dependency of the leaching rate on the orientation of chalcopyrite crystal must be studied. By so doing, a better understanding of the leaching of chalcopyrite should be obtained.

2. The leaching rate of chalcopyrite in the chloride media was larger than that in the sulfate media and the addition of NaCl increased the leaching rate in the chloride media. Thus it is important to know how anions such as Cl^- or SO_4^{2-} affect the leaching rate. For the complete understanding of the mechanism of chalcopyrite leaching, it is necessary to elucidate the role the anions play in the leaching reaction.

3. It is important to extend kinetic studies to the oxidative leaching of other sulfides, where the experimental techniques developed in this study may be useful.

4. Application of the oxidative leaching of chalcopyrite must be studied to develop new hydrometallurgical processes for recovery of copper from sulfide ores.

